PHOTOVOLTAIC-POWERED WIRELESS COMMUNICATION SYSTEM FOR RURAL SCHOOLS OUTSIDE NATIONAL UTILITY GRID

RICHMORE KASEKE

Submitted in fulfillment of the
requirements for the degree of

MAGISTER SCIENTIAE

In the Faculty of Science and Agriculture
at the University of Fort Hare

Supervisor: Professor E L Meyer February 2007

This work is dedicated to my late father Watson Mutandwa Kaseke.

ACKNOWLEDGEMENTS

My sincere thanks to:

My supervisor, Professor E.L. Meyer for his unmatched guidance and motivation, wisdom and assistance throughout the entire project.

Telkom CoE at the University of Fort Hare, especially Professor H.N. Muyingi, for assistance in providing materials for the project.

GMRDC at the University of Fort Hare for financial support.

FHIT for financial support.

Science Workshop for assistance with construction of an outdoor module rack.

NMMU PV research group for allowing use of indoor testing facilities.

Mr. M. Simon and Mr. X.T Fadana for help with module indoor tests.

Mr. A. Teru for assistance with Open Source Software and network configurations.

Mr. S. Mamphweli and Mr. G. Makaka for their guidance and help in revising this work.

My brother, T.N. Kaseke for his love, support (financially and morally), guidance and help with electronics.

The Almighty God for making this project a success and for all wisdom and blessings that He has given me.

SUMMARY

Access to global information is inarguably one of the key ways of bringing development to any community. In developing worlds, many rural schools lie outside both the Internet Service Provider's (ISP) cable network and the national utility grid. Rapid developments in information and communication technology (ICT) continue to widen the digital divide between urban and rural schools. In South Africa, although these rural areas are outside the ISP's cable network, they enjoy excellent mobile (cellular) communications network coverage. Fortunately, leading mobile operators in the country (MTN and Vodacom) have incorporated mobile data packet services into their cellular communication networks since 2002.

A stand-alone photovoltaic (PV) system for powering ICT equipment in off grid rural schools was designed and installed; and its performance monitored. Performance of the system was considered in two categories, which are; cost and service performance. In cost performance, return on investment (ROI) and payback period (PB) are the two critical considerations. The PV system designed in this study gave an impressive ROI and PB of 286% and 5 years, respectively.

In order to monitor and evaluate the service performance a data acquisition system (DAS) was designed and installed. Besides proving the potential of PV in powering ICT equipment, results from the DAS also suggested a more efficient way of employing PV as a power source for powering equipment that is based on Switched-Mode Power Supply Units. Concurrent and continuous change in irradiance and temperature result in a four-segment pattern of rising and falling module efficiency throughout the day. Generally, modules produce more energy on cooler sunny days than hotter sunny days. Infrared (IR) Thermography was also used as part of both indoor and outdoor module tests. During indoor tests at pre-deployment stage, IR Thermography showed development of hot spots in mismatched cells of reverse-biased modules. On the outdoors, IR Thermography reiterated the effect of bird droppings on module surfaces by showing hot spots forming on areas covered by the droppings.

For internet connectivity, a customized Mobile Internet Device (MIDevice) was designed, built and tested. The device allows remote computer systems to be connected to the Internet via the already existing mobile communication network using General Packet Radio Services (GPRS). An entire rural school local area network (LAN) can be connected to the Internet via a single MIDevice.

An experimental setup was designed in order to monitor and evaluate performance of GPRS in specific and mobile Internet solutions in general. Results obtained proved that GPRS can indeed be a solution for remote Internet connectivity in rural schools. In order to improve performance of GPRS or mobile Internet connections, caching, pop-up blocking and proxy filtering are necessary.

Keywords: Photovoltaic System, Irradiance, Temperature, Hot Spots, Infrared Thermography, Cost Performance, Service Performance, Switched-Mode Power Supply Units, Mobile Internet Device, Mobile Packet Data Services, General Packet Radio Services, Local area network.

CONTENTS

CHAPTER 1

INTRODUCTION

1.1 RATIONALE BEHIND THIS STUDY

Most rural schools in South Africa and Africa at large are lagging behind their urban counterparts in terms of technology. The technological gap between rural and urban schools is referred to as the digital divide. Essentially the divide is measured in terms of the access to information and communication services, especially the Global Information Superhighway (Internet). Information and Communication Technology (ICT) is presently advancing at an extremely fast pace and the divide continues to widen at an equally fast pace. As a result the widening divide continues to erode the quality of education delivered in rural schools while slowing down several rural development initiatives especially those that rely mostly on effective pre-implementation information dissemination and awareness campaigns. Connecting rural schools to the Internet is equivalent to linking these often isolated and almost neglected schools to the rest of the world (Global Village). This will come with enormous benefits, which among others include; improvement of quality of education through provision of access to vast online educational resources, bridging of the divide as rural schools synchronize their curriculum as well as extra curricula activities with the rest of schools worldwide, enhancement of children as well as other community development initiatives and generally keeping rural communities abreast with latest developments in technology. A huge and urgent need to address the lack of ICT solutions in rural communities therefore exists. Although the Internet Service Provider (ISP) cable network does not stretch into these remote and inaccessible areas, these rural communities continue to enjoy good mobile telecommunication coverage. Mobile data services in South Africa have been around for the past four years starting as General Packet Radio Services (GPRS) in 2002, thanks to the country's two leading mobile operators MTN and Vodacom [MTN, 2006 and Vodacom, 2006].

Photovoltaic (PV) power systems have been deployed for powering purposes in their varying scales in different spheres. Fields of application include domestic, commercial or industrial, military and space systems. In all these cases PV power systems always gain competitive edge over other power sources, owing this to their environmental friendliness, easy system scalability and tendency to become cheaper in the long run (lucrative return on investment). The world at the moment is on high alert with regards to environmental issues. The general consensus throughout the globe is a transition towards more and more use of renewable energy sources (RES) as opposed to fossil fuels whose byproducts impart negatively on the environment. Some of the undesirable consequences of the use of fossil fuels include air pollution as well as contribution towards global warming [Meyer, 2002; 5]. PV power sources can therefore be identified as an attractive option world wide since in most parts of the world solar irradiation is an abundant free resource. Success of PV power systems depends on carefulness and resourcefulness of the design approach used. In that regard, system performance is regarded in two parts which are; cost and service performance.

Since most of these rural schools lie outside both the ISP's cable network and the national utility grid, the need for alternative power sources (in this case PV) and connectivity solutions (in this case through existing mobile communication networks) culminated in the undertaking of this research.

1.2 OBJECTIVES OF THIS STUDY

In general the objective of this study was to develop and implement PV-powered ICT solutions to rural schools. Such work was to involve the development, implementation and evaluation of mobile Internet connectivity solutions.

Specifically, a customized and network-independent GPRS-enabled mobile Internet device (MIDevice) that universally allows computer systems to be connected to the Internet via the existing mobile networks was to be developed. Installation and monitoring of the device was to be done in order to ascertain performance of mobile data services in solving Internet connectivity quagmire. Also a PV power system specifically for powering ICT equipment (personal computers and the MIDevice) was to be sized, installed and monitored.

1.3 RESEARCH DESIGN

This study approaches energy resource in general and photovoltaic systems in particular as a source to power ICT equipment for Internet access at remote rural schools. Initially, the dissertation presents the design, implementation and performance monitoring of a PV power system. Finally, a mobile Internet device, designed and built at the University of Fort Hare is presented and its performance discussed.

Chapter 2 presents energy sources presently under exploitation in the world. Various applications of solar energy are discussed in detail. Also discussed in this chapter is the concept of the greenhouse effect and how the use of fossil energy sources (FES) contribute to the global warming.

Chapter 3 discusses PV power system sizing in detail. Mathematical expressions for sizing the various components of a PV system are derived and presented. A method evaluating performance of a PV system is also presented and discussed in detail in this chapter.

In chapter 4 a small scale PV power system, designed and installed at the University of Fort Hare (UFH) as part of this study, is presented. Its performance evaluation, based on the methodology presented in chapter 3 is also given in chapter 4.

Chapter 5 deals with outdoor performance of the modules used in the UFH PV system. Particular emphasis is placed on the net effect of concurrently and continuously changing ambient temperature and irradiance on module efficiency as well as energy production.

Chapter 6 introduces the fundamentals of Global System for Mobile Communication (GSM) and GPRS networks. In the same chapter, migration of GSM networks to GPRS is discussed in detail. Communication procedures, protocol suites, mobile resource management schemes and the available quality of service (QoS) classes in GPRS are presented. Also discussed in this chapter are the network structures that allow packet data exchange between mobile devices and external Internet protocol (IP) networks.

The design and testing of the MIDevice is presented in chapter 7. Its various design features are also discussed. Also presented is an outline of the procedure that an end user can follow when installing the device on a Windows-based machine and when setting up a dial up connection that will allow his/her mobile host to exchange IP packets with the Internet via the mobile operator's network.

For chapter 8, a client-server local area network (LAN) consisting of four clients connected to a single Linux proxy server was set up. The proxy server was then connected to a Windows gateway on which the MIDevice was installed and configured. LAN clients were allowed to freely access the Internet while client-server and server-gateway traffic data was being captured. This traffic data was used to evaluate performance of GPRS as an Internet connectivity solution in a multi-user environment and this evaluation is presented in detail in chapter 8. Also presented in chapter 8 are suggestions on improving performance of GPRS in multi-user mobile Internet applications.

Conclusions are drawn in chapter 9 for all observations after which two appendices are presented. Appendix A explains the energy consumption of the PV load observed in chapter 4. Lastly, Appendix B gives the research outputs associated with this study.

1.4 REFERENCES

MTN South Africa (2006); Accessible from www.mtn.co.za, last viewed on 15/12/2006.

Vodacom South Africa (2006); Accessible from www.vodacom.co.za, last viewed on 15/12/2006.

Meyer E. L. (2002), *On the Reliability, Degradation and Failure of Photovoltaic Modules*, PhD-thesis, University of Port Elizabeth.

CHAPTER 2

WORLD ENERGY SOURCES

2.1 INTRODUCTION

The issue of energy is such an important subject that it takes centre stage in all planning and policy formulation of world governments today. A number of policies and legal frameworks are put in place in every nation to govern energy exploitation and trade. The reason for all this attention is that energy is a vital source of life and development on earth. Life and development are certainly the two key drivers for any nation to want to invest huge sums of money and endless effort in order to secure them.

All sources of energy are categorized into two groups, viz. renewable and non-renewable energy. Each of these two has its own advantages and disadvantages but on the whole the former turns out as the more desirable choice. The major problem with the use of non-renewable energy sources, specifically fossil energy sources (FES), is the negative impact that their byproducts have on the environment. Global warming as one of such undesirable impacts is directly a result of carbon and other gasses collectively termed greenhouse gasses that are emitted as byproducts from the use of FES. The importance and severity of the global warming can clearly be seen by the alertness it has caused world wide leading to world governments joining hands in efforts to reduce greenhouse emissions. Such concerted effort by world governments has seen the adoption of the Kyoto Protocol to the United Nations Framework Convention of Climate Change (UNFCCC) which was signed on March 16, 1998 but only coming into force on February

16, 2005 [Kyoto Protocol, 2006]. In fact the recent UN climate change conference held in Nairobi, Kenya, from the 6th to 17th of November 2006 was attended by six thousand participants from one hundred and eighty nine (189) parties to the UNCCC [UNCCC, 2006].

Irrespective of their negative impact on environment, the use of FES has continued to increase over the years mainly due to two reasons which are cost and technological advancements. FES are relatively inexpensive [Meyer, 2002; 5] as compared to renewable energy sources (RES) and as such it makes economic sense to rely more on FES than RES. Growth of world economies and population places an equally growing demand on energy, which can readily be tapped from FES, thanks to advancements in fossil energy mining and processing technology.

This chapter highlights world energy resources giving also the South African energy resources and future trends. It also discusses the natural greenhouse effect and enhanced greenhouse effect (greenhouse effect that results from human interference). In its concluding remarks, the chapter highlights drawbacks currently affecting global efforts towards the advancements of RES and suggests ideas to aid the development of RES thus contributing to reduction of greenhouse gas emissions.

2.2 GLOBAL ENERGY SOURCES

The world at present has quite a considerable pool of energy sources to tap from. All these sources are broadly categorized either renewable or non-renewable energy sources based on sustainability considerations.

2.2.1 Renewable Energy Sources (RES)

These energy sources generally can be replenished (rejuvenated) on more frequent bases. The rejuvenation can occur either naturally as with wind, geothermal, water (hydro) and solar or artificially as with biomass and to a lesser extent water through cloud seeding and other rainfall improving practices.

The power of naturally blowing wind is directly transferred to mechanical power for turning huge turbines. Attached to these turbines is a transducer commonly known as generator for converting mechanical energy of the turbine into the more efficient electrical energy, which can then be sent through transmission and distribution lines to homes, businesses, schools and so on [NREL, 2006]. Small wind generating plants also exist and are normally suited for localized small scale purposes like water pumping and home power.

Geothermal energy is derived from heat reserves in the earth. These reserves are proposed to be formed by the radioactive decay inside the core of the earth, which heats the earth from the inside out [Wikipedia, 2006]. The tapped heat energy has three forms of applications, which are geothermal electricity, heating through deep earth pipes and direct geothermal heat pumping for heating and cooling buildings. However geothermal energy is not a well developed source world wide since its occurrence favors certain geologically unstable parts of the world. By the end of 2004 about 43 geothermal plants existed throughout the USA [DOE-1, 2006] for instance.

Biomass energy is derived from organic materials from plants and animals also known as biomatter. Three forms of bio fuel are produced. Solid biofuel like wood and combustible crop remains can be burnt directly for energy. Liquid biofuel includes ethanol and bio-diesel that are derived from plants. Ethanol is blended with gasoline and used as blended fuel in petrol engines while bio-diesel is simply used in diesel engines. Biogases include gases like methane released during anaerobic digestion or fermentation of organic matter by bacteria. Biogases can also be produced through a more efficient process called gasification. The gasses produced can then be used in gas engines and turbines for electricity production.

A more popular application of water energy is in hydro electricity generation whereby mechanical energy of flowing water is used to turn turbines for generating electricity. Such hydro power stations are vital as they contribute a major part of the electricity supply throughout the world to date. Some of the famous hydro stations in Africa include Inga hydro station in the Democratic Republic of Congo and Cabora Bassa hydro station in Mozambique. Cabora Bassa station currently supplies to Mozambique, South Africa and even Zimbabwe. On the other hand, developments at the Inga station promises up to 35000 Megawatt of electric power [SADC, 2006] through the Western Power Corridor (Wescor) Project. Apart from hydroelectricity there are other forms of energy derived from water and these include tidal power, tidal stream power, wave power, ocean thermal energy conversion (OTEC), deep lake water cooling and blue energy [Wikipedia-2, 2006]

Solar energy is tapped in two forms either as heat derived from thermal radiation from the sun that reaches the earth or as electrical energy derived from photon energy in sunlight. Figures 2.1 to 2.5 discuss the five common applications of solar energy at present.

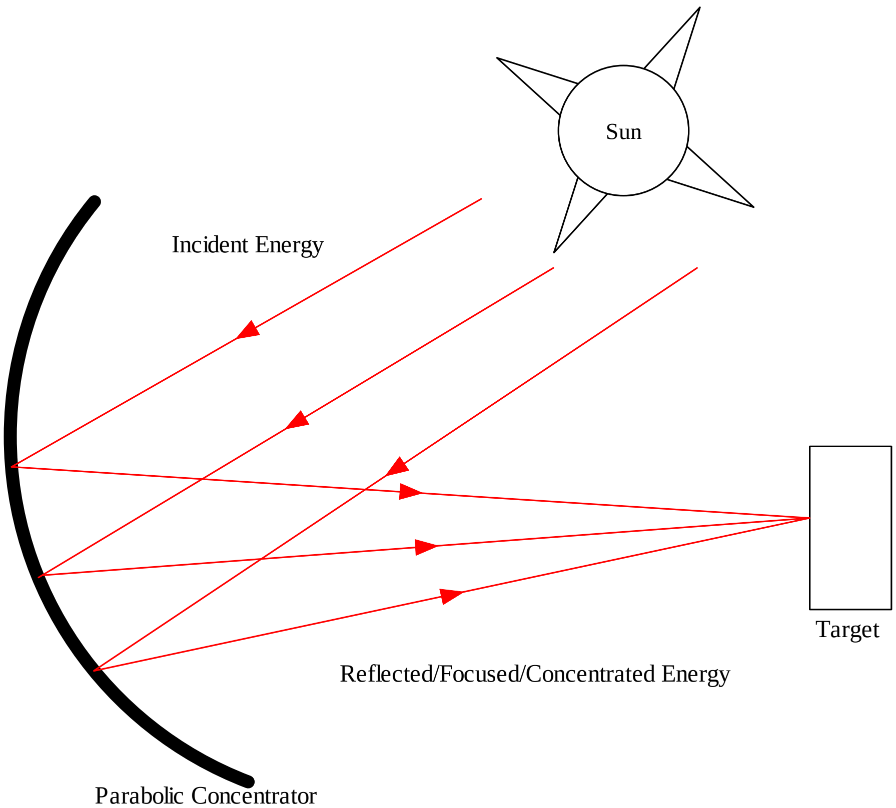

Figure 2.1: Concentrating solar power systems

A parabolic trough collector has a linear parabolic-shaped reflector that focuses the sun's radiation on a linear receiver (target) located at the focus of the parabola. Due to its parabolic shape the trough can focus the sun at 30 to 100 times its normal intensity (concentration ratio), thus achieving temperature above 400°C [DoE-1, 2006]. Another type of solar concentrator systems uses solar dishes/engines that track the sun on two axes hence giving typical concentration ratio of over 2000 and working fluid temperature over 750°C [DoE-1, 2006]. If such system is used to heat-up water, superheated steam can be collected and channeled into steam turbines for electricity generation. The generated heat can also be used as a heat source in solar thermal plants employing stirling engines.

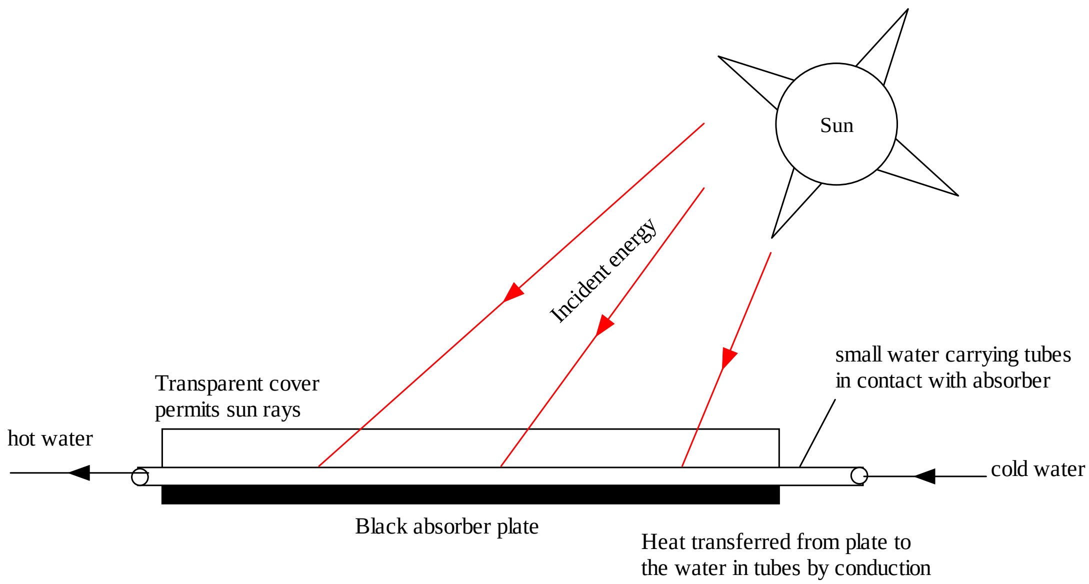

Figure 2.2: Solar hot water systems

The main applications of solar water systems are in heating water for domestic purposes (replacing or adding to the conventional electrical geyser systems) and heating swimming pools. The solar collector system is either flat-plate type or evacuated tube type. Figure 2.2 shows a liquid flat-plate collector in which cold water enters from one side and exits on the other as warm water after exchanging heat by conduction with the black absorber plate. Air flat-plate collectors use air instead of water. Cool air enters through one end by natural convection or with the aid of a fan and leaves on the other as warm air after exchanging heat with the absorber plate. Since conduction is slower in air than in liquids, air flat-plate collectors are less efficient than liquid flat-plate collectors. In general, flat plate collectors can reach temperatures up to 200°F (300°C) [EERE, 2006]. On the other hand evacuated-tube collectors are more efficient than flat-plate collectors and can reach temperatures up to 350°F (600°C) [EERE, 2006].

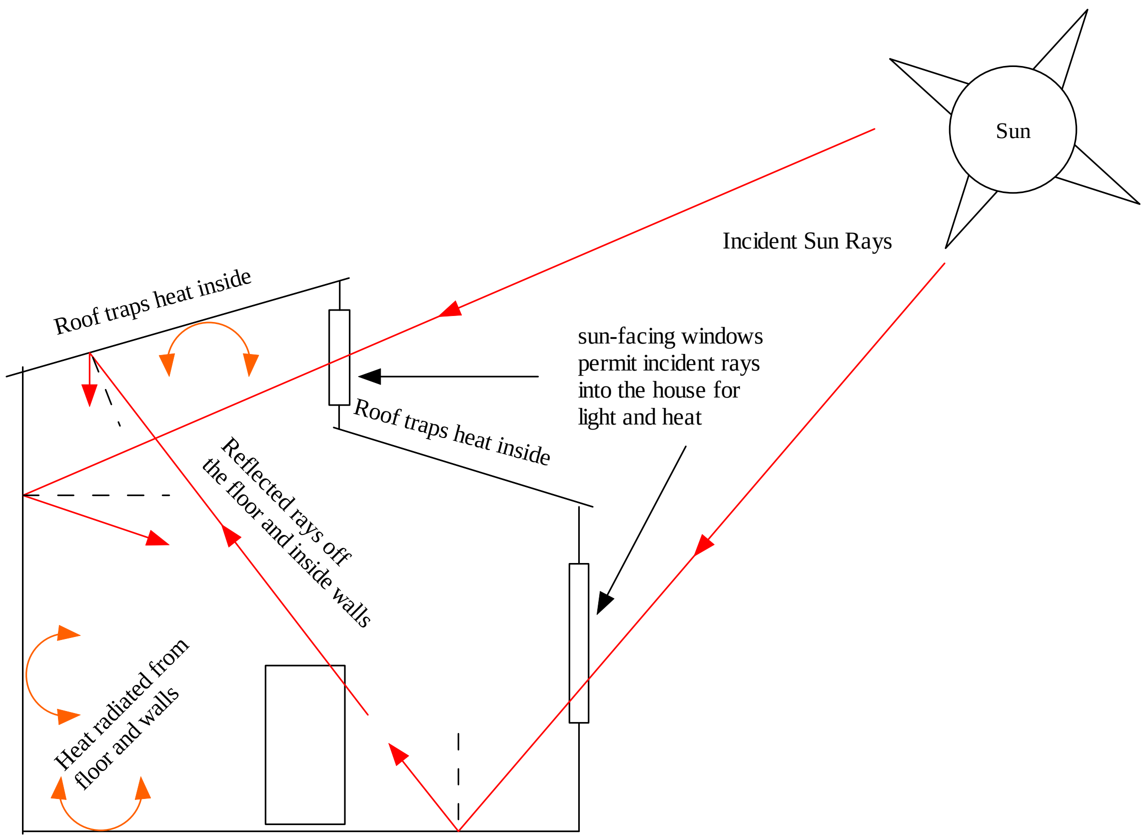

Figure 2.3: Passive solar heating and daylighting in residential structures

In passive solar heating and daylighting, residential buildings/structures are carefully designed to utilize heat and light directly from the sun. Large transparent window surfaces are placed on the sun-facing walls in order to allow sun's rays into the house for heating and daylighting. Internal floors and walls absorb and later radiate the heat thus keeping the indoor temperatures within the comfort zone (18°C - 25°C) in winter without the need for electrical heating systems. Light that enters through the windows will maintain adequate indoor lux levels also without the need for electrical lighting. In summer, passive solar residential structures require adequate ventilation to indoor temperatures within the comfort zone. Adequate ventilation can be achieved by strategically locating and operating features like windows and doors in order to allow free air exchange between the cooler outside environment and inside of the residential structure in summer.

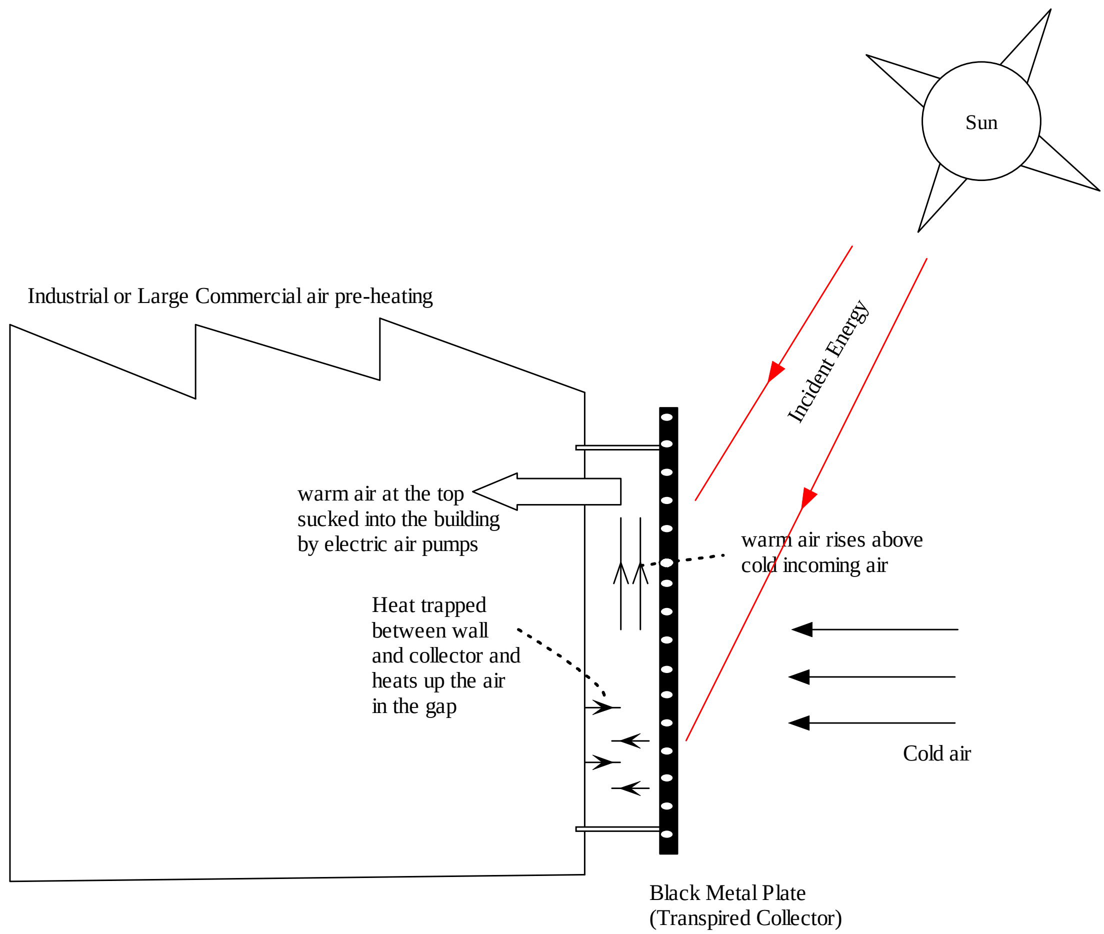

Figure 2.4: Solar process heat and space heating and cooling

In figure 2.4, the black metal plate absorbs solar heat energy and radiates part of it. The plate is also perforated to allow cooler air flow through it, warming this air once in the gap between the plate and building wall. A large portion of the radiated heat is trapped in the space between the plate and the wall and is used to heat up the inflowing cool air. As the air gets warmer, it becomes lighter and will rise above the cooler air. Electric air pumps are installed at the top as shown in the figure to suck the warm air into the building.

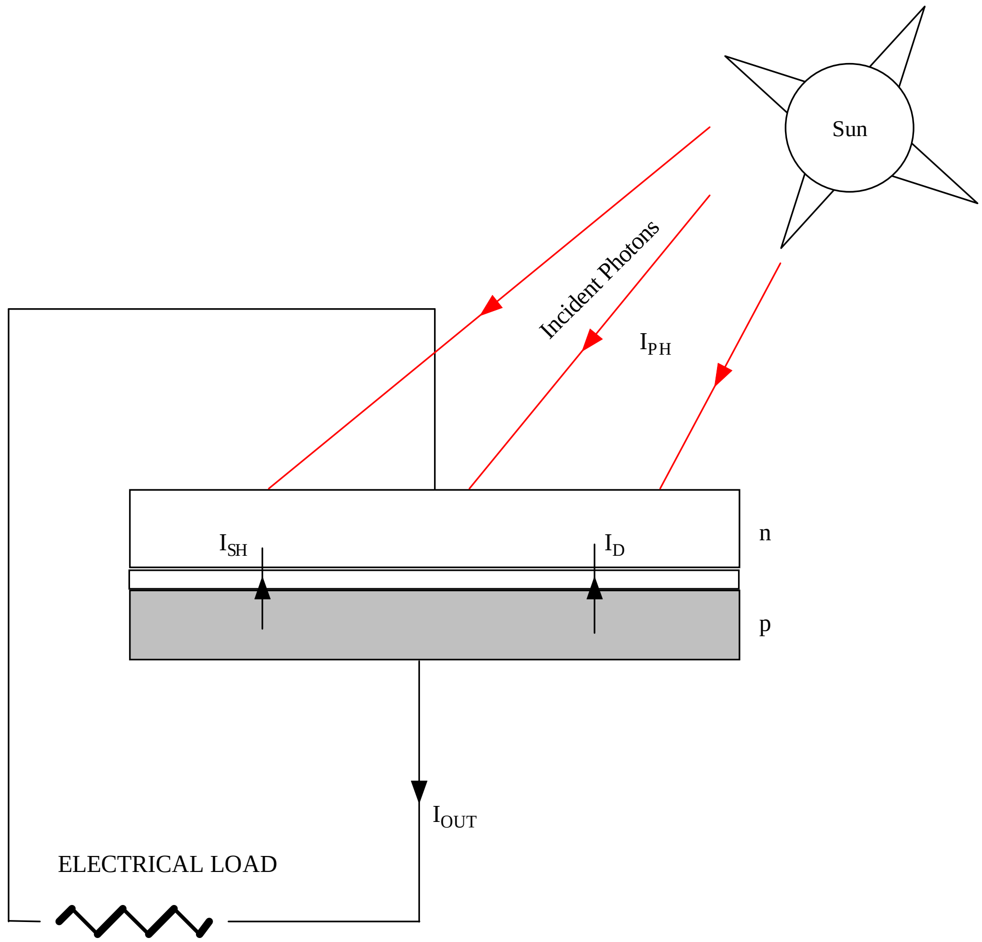

Figure 2.5: Photovoltaic (solar cell) systems

Photovoltaic systems depend on certain semiconductor materials like silicon to convert photon energy in light to electrical energy at the atomic level. A technique called doping is used to introduce excess positive charges (holes) or negative charges (electrons) in pure semiconductor materials. A solar cell is formed by combining p-type layer (with excess holes) and n-type layer (with excess electrons) to form a diode as shown in figure 2.5. A junction referred to as p-n junction is developed by the short-lived majority charge diffusion across the boundary between the two opposite layers. Once fully developed the p-n junction prohibits further majority charge diffusion. As the cell gets illuminated by the sun, photons are absorbed by atoms. After absorbing the photon energy, valence electrons of atoms become excited to the conduction band of the semiconductor where they become free conduction electrons. Every semiconductor material has a certain band gap energy which defines the minimum energy required to knock off an electron from the shells of its atoms. For the generation of free electrons to take place, the lights photons should contain energy greater or equal to the band gap energy of the solar cell material. These free electrons find it difficult to cross the p-n junction to recombine with holes in the p-type layer. An external path with an electrical load allows electron current to flow from the n-type to the p-type layer. However I_{OUT} in figure 2.5 shows the flow of conventional current. Ideally, I_{OUT} should be equal to the photon current (I_{PH}) from the sun, however, unwanted currents due to electro-hole recombination (I_D) and shunt resistance (I_{SH}) reduce the output current from the solar cell [Meyer, 2002; 21-22 and Messenger and Ventre , 2000; 309-310].

2.2.2 Non-Renewable Energy Sources (NRES)

These are energy sources that cannot be replenished as they are used. NRES can either be simple, for instance, uranium or fossil energy sources (FES) like coal, crude oil and natural gas.

Uranium is used as a source of radioactive atoms for nuclear energy production in nuclear reactor chambers. Through the process of fission, neutrons bombard uranium atoms resulting in a nuclear reaction that releases huge amount of energy as heat and radiation. Apart from the energy, more neutrons are released as uranium atoms split into lighter elements. A chain of similar reactions occur as the released neutrons bombard other uranium atoms. Even though uranium is a hundred times more common than silver, only a rare isotope of uranium, U_{-235}, is used for nuclear energy production since its atoms are easily split [DOE-2, 2006].

Fossil fuels are primarily compounds of carbon and hydrogen formed on a carbon backbone. Such resources contain huge amounts of potential energy, which can only be released when burning them in proper furnaces or engines. During ideal combustion, carbon combines with enough oxygen to form a less harmful gas called carbon dioxide (CO_2) while hydrogen reacts with oxygen to produce water. However if combustion is incomplete, carbon reacts with oxygen to form a more harmful gas known as carbon monoxide (CO).

2.3 THE GREENHOUSE EFFECT

Greenhouse effect formally refers to the natural air conditioning system that keeps the earth's temperatures within bearable levels. In order for such air conditioning to happen an energy balance [Tsai and Chou, 2005] must be maintained on earth. The greenhouse effect depends on the existence of certain atmospheric gasses known as greenhouse gasses (GHGs). These GHGs absorb infrared heat from primarily three sources, incident sunlight, reflection from the earth, and radiation from the warm earth surfaces during day, and re-emit it to space and back towards the earth at night. If the energy balance depicted in figure 2.6 is sustained then the greenhouse effect is at the most desirable level of operation.

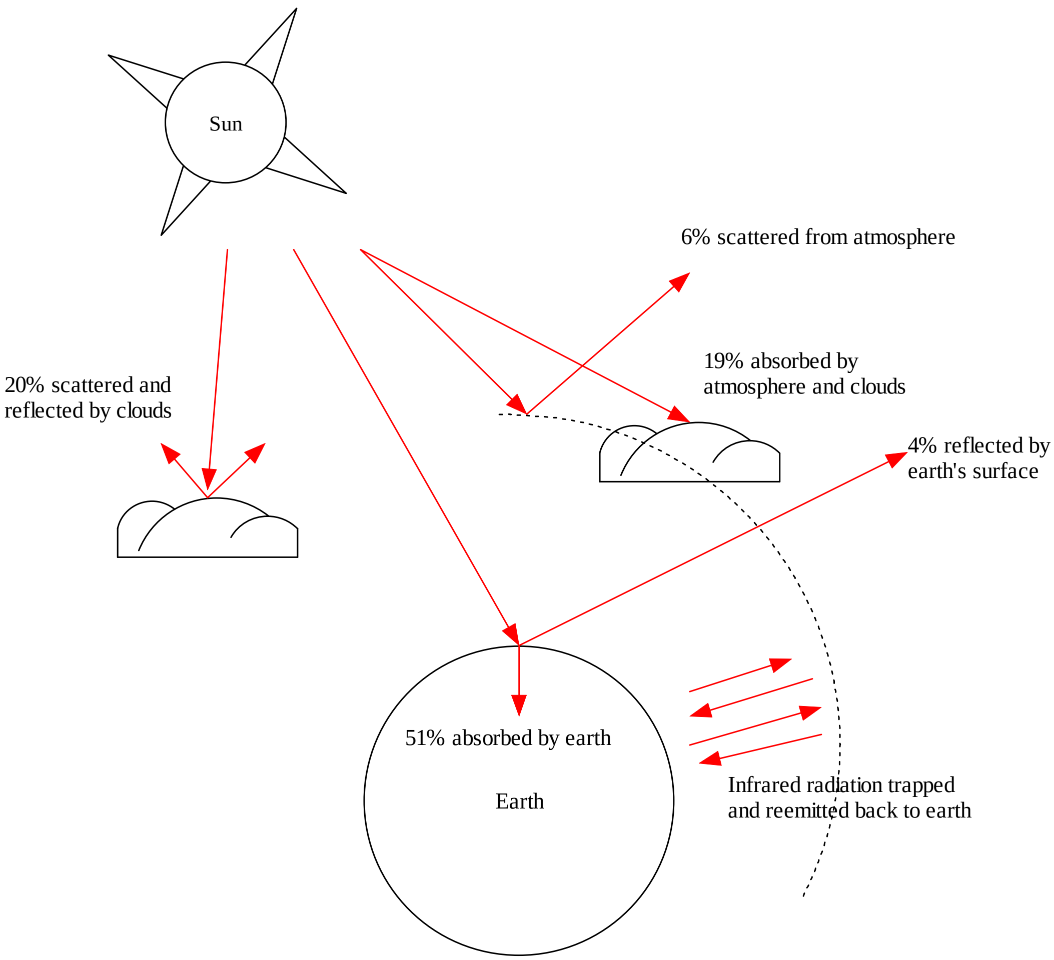

Figure 2.6: Energy Balance [Adapted from UCAR, 2006]

Unfortunately due to mainly human activities, for instance burning of fossil fuel for energy, excess amounts of GHGs were released and are still being released into the atmosphere leading to what can be termed as enhanced greenhouse effect. Such level of greenhouse effect totally offsets the energy balance and has undesirable impact on global climates. With more GHGs in the atmosphere, more heat energy than necessary is trapped and re-emitted back to the earth causing a phenomenon known as global warming. Global warming results in glacier melting, floods and droughts that have traumatized communities and frustrated development efforts of governments around the world in recent past and the present era.

2.4 SOUTH AFRICA AND ENERGY

South Africa has a thriving energy industry supported by large reserves of coal and uranium [Cooper and Prinsloo, 2005]. Natural gas and crude oil also exist but in very limited quantities hence the country relies more on imports. Fossil fuel is currently providing approximately 90% of energy in South Africa, with coal providing 75% of the fossil fuel based energy supply [DME-3, 1999]. South Africa mines about 270 million tons of coal per year of which 70 million is exported, 150 million is used locally and an estimated 50 million is discarded [DME-2, 2002]. In addition, 91% of the total amount of electricity generated in 1999 was derived from coal [NER, 2000]. This very high percentage of coal combustion results in excessive carbon dioxide emissions. Indeed amongst developing nations, South Africa has one of the highest levels of carbon dioxide emissions per capita as can be seen from figure 2.7 [IEA, 2001].

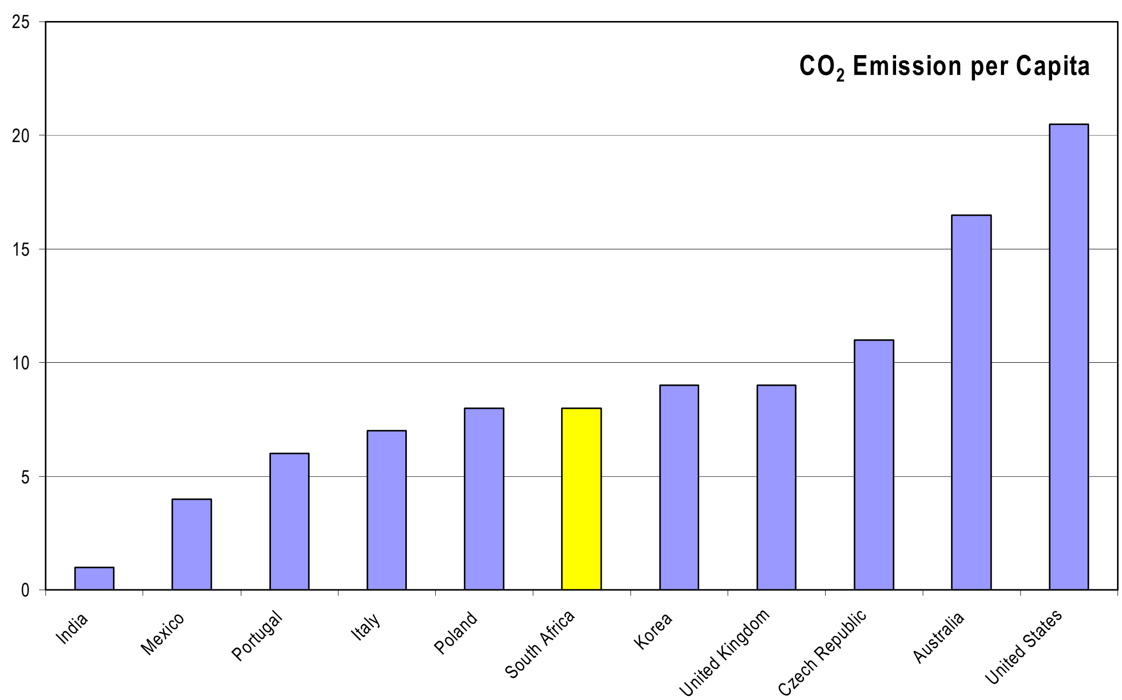

Figure 2.7: Carbon Dioxide emissions per capita [Adapted from IEA, 2001]

A wide range of RES are found in South Africa and they include hydro, solar, wind, wave energy, ocean currents and biomass. Renewable energy resources provide approximately 10% of South Africa's primary energy of which biomass accounts for close to 10% of net energy consumption at the national level. Other renewable energy resources account for a small but rapidly increasing percentage of net energy.

2.4.1 The Future of RES

The year 2003 saw the country set a 10-year target for renewable energy. The target entails up to 10 000 GW/h (0.8Mtoe) renewable energy contribution to final energy consumption by 2013 [DME-1, 2003]. However such a target is by no means an easy one and will require huge human and capital investment. At present, renewable energy development lags behind conventional energy sources due to their high costs. Figure 2.8 gives an overview of energy supply for South Africa for the year 2002. In the figure, hydro power source was stated independent from the renewables just to emphasize its contribution, otherwise it falls under renewables.

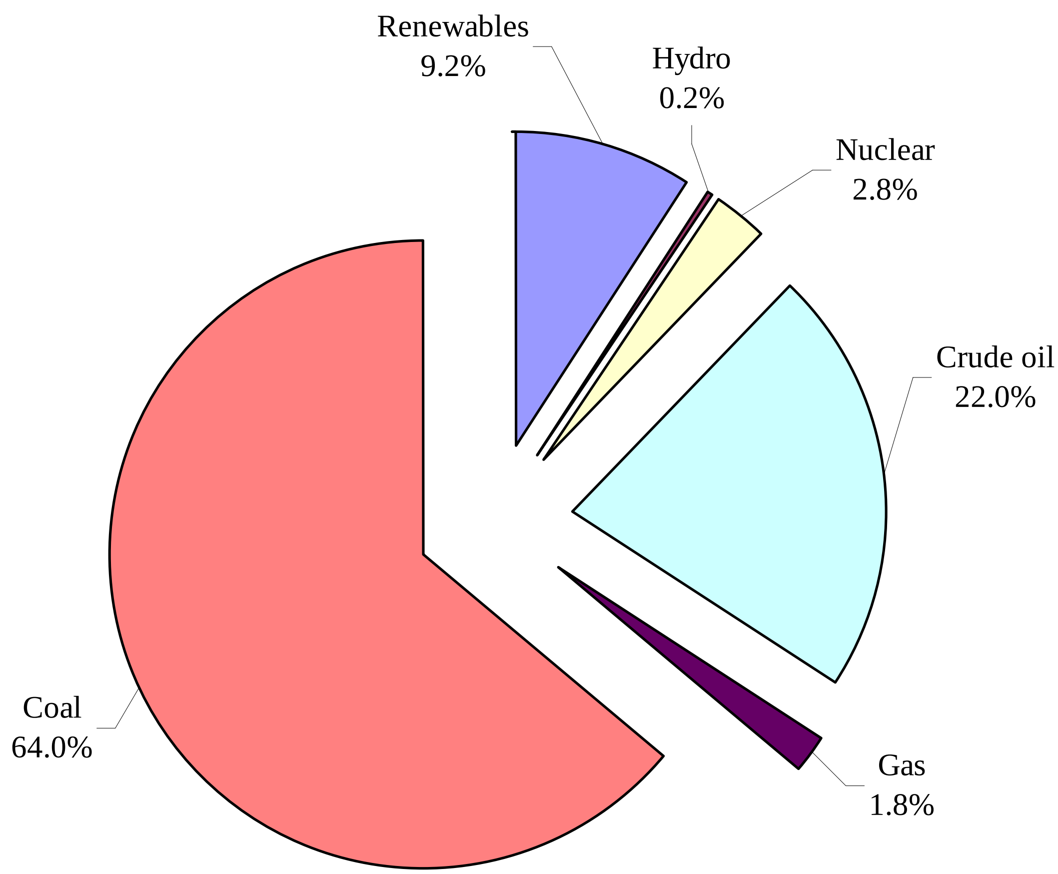

Figure 2.8: South Africa's primary energy supply in 2002 [Adapted from Cooper and Prinsloo, 2005]

2.5 SUMMARY AND CONCLUSIONS

This chapter succeeded in highlighting energy options that are available to the world. It is clear from the discussions that use of NRES especially FES is detrimental to the environment and that RES presents a lasting solution to the dreadful consequences of global warming and climate change. Treaties like the Kyoto protocol play a key role in sensitizing the issues of greenhouse effect, global warming and subsequent climate change. The idea of restricting member states to certain limits of emissions can only be viewed as a way of buying time as GHGs will continue to build in the atmosphere though at a rate slower than what it could have been in an unrestricted scenario. At present renewable energy technologies suffer mainly due to their associated high capital costs. However, it is important to stress that in order to effectively address the issue of high capital costs, world governments and organizations should take advantage of the already existent agreements of cooperation, for instance the mentioned Kyoto Protocol, and invest sufficient human and financial resources in the development of RES. In fact financial resources need to be made readily available for research and other noble activities that seek to promote renewable energy technologies. Through such activities, cheaper, more efficient and sustainable ways of exploiting RES can be developed hence making RES more competent in terms of both cost and performance amongst other cheaper energy sources like coal.

2.6 REFERENCES

Cooper C. and J. Prinsloo (2005), "Digest of South African Energy Statistics", Department of Minerals and Energy, South Africa; p. 7, 61; accessible from http://www.dme.gov.za/, last viewed 28/11/2006.

DME-1, Department of Minerals and Energy, South Africa (2003), "White Paper on Renewable Energy"; accessible from http://www.dme.gov.za/, last viewed 28/11/2006.

DME-2 (2002),Energy Outlook for South Africa, Department of Minerals and Energy, Pretoria, South Africa.

DME-3 (1999), Digest of South African Energy Statistics, compiled by CJ Cooper, Department of Minerals and Energy, Pretoria.

DoE-1, Department of Energy, United States of America (2006), Geothermal Energy; http://www.eia.doe.gov/kids/energyfacts/sources/renewable/geothermal.html, last viewed 25/11/2006.

DoE-2, Department of Energy, United States of America(2006), Nuclear Energy; accessible from http://www.ne.doe.gov/public_Informatio/nePIPublications2.html, last viewed 28/11/2006.

IEA (2001), Analysis of Reports and Discussions with various sources from Industry, Government and the Department of Energy National Laboratories. Office of Integrated Analysis and Forecasting, US DOE.

Kyoto Protocol (2006); accessible from http://en.wikipedia.org/wiki/Kyoto_Protocol, last viewed on 26/11/2006.

Messenger R., J. Ventre (2000), "Photovoltaic system engineering", CRC Press, London.

Meyer E. L. (2002), *On the Reliability, Degradation and Failure of Photovoltaic Modules*, PhD-thesis, University of Port Elizabeth.

NER 2000), Electricity Supply Statistics for 1999, National Electricity Regulator, Pretoria.

NREL, National Renewable Energy Laboratory (2006), National Wind Technology Center; accessible from http://www.nrel.gov/wind/animation.html, last viewed 26/11/2006.

SADC, Southern Africa Development Community (2006), SADC Today; accessible from http://sardc.net/editorial/sadctoday/view.asp?vol=155&pubno=v8n2, last viewed 26/11/2006.

Tsai W. T. and Y .H. Chou (2005), "Overview of environmental impacts, prospects and polices for renewable energy in Taiwan", Renewable & Sustainable Energy Reviews, **9**, p.119-147.

UCAR, University Corporation for Climatic Research (2006); accessible from http://www.ucar.edu/learn/1_3_1.htm, last viewed 28/11/2006.

UNCCC-1, United Nations Convention on Climate Change (2006), *United Nations Climate Change Conference Press Release*, Nairobi, Kenya; accessible from http://unfccc.int/2860.php, last viewed on 26/11/2006.

Wikipedia (2006), Renewable Energy; accessible from http://en.wikipedia.org/wiki/Renewable_energy, last viewed 26/11/2006.

CHAPTER 3

DESIGN AND PERFORMANCE EVALUATION OF A STAND-ALONE PHOTOVOLTAIC POWER SYSTEM

3.1 INTRODUCTION

Photovoltaic (PV) power system design involves determining the appropriate sizes of the various system components that include battery storage, PV array and balance of system (BOS) components [Messenger and Ventre, 2000; p97]. This exercise of establishing the sizes of the components is usually referred to as system sizing. In as much as system sizing determines the component sizes and hence the overall size of the PV system, it also determines the total cost (installation cost) of the system. During system sizing care should be taken in order to achieve quality PV power systems at minimum cost. In lieu of the just mentioned fact, overall PV system performance can be regarded under two categories, viz. service performance and cost performance.

Any PV system, in economic terms, represents capital investment and therefore the two critical issues as in any investment are the payback period and the return on investment. In that sense, PV power systems with the optimal performance in terms of cost would offer the shortest possible payback time as well as highest return on investment over its entire life period. On the other hand, service performance is measured in terms of quality of service (QoS) delivery of the power system. QoS factors to be considered include the ability of the PV system to generate and supply power efficiently, adequately and reliably. Neither cost nor service performance of the system should be improved at the expense of the other as this is detrimental to the overall system performance. For instance, under-sizing components will improve system cost performance at the expense of the QoS of the system and as such, the system is bound to fail. Likewise, over-sizing is an extravagant approach and can easily blow PV system's installation cost out of proportion and beyond reach of an average potential investor.

This chapter introduces the set of mathematical equations that can be used for the optimal sizing of the main PV system components namely; Load, Battery Bank and PV Array. From the sizes of these main components and the subsequent system currents and voltages, sizes of the various BOS components can be established. A method of evaluating cost performance of PV systems is also presented and discussed in this chapter.

3.2 SYSTEM SIZING

3.2.1 Load

The load of the system presents a business case for the design of the system. The demand of every load device needs to be measured and the total energy requirement (in kVAh for AC power or kWh when dealing with DC power) of the entire load should be determined as follows:

$$kVA_n = \sqrt{kW_n^{\,2} + kVAR_n^{\,2}} = kV_{n(rms)} \times I_{n(rms)} \tag{3.1}$$

$$E_{AC} = \sum_{all\ \mathrm{n}} kVA_n \times t_n \tag{3.2}$$

$$E_{DC} = \sum_{all\ i} kVA_{i(DC)} \times t_i \tag{3.3}$$

$$E_{Load} = 1.3\left(\frac{E_{AC}}{\eta_{AC}} + \frac{E_{DC}}{\eta_{DC}}\right) \tag{3.4}$$

where: $kV_{n(rms)}$ is the root mean square voltage for the n^{th} AC device in kilo-Volts;

$I_{n(rms)}$ is the root mean square current for the n^{th} AC device in Amperes;

kW_n is the true power for the n^{th} AC device;

$kVAR_n$ is the reactive power for the n^{th} AC device;

t_n are the daily operational hours for the n^{th} AC load device;

t_i are the daily operational hours for the i^{th} DC load device;

E_{AC} represents total daily energy consumption for the AC load;

E_{DC} represents total daily energy consumption for the DC load.

η_{AC} and η_{DC} as the efficiencies of DC-AC and DC-DC conversion processes, respectively.

E_{Load} gives the total daily energy consumption for the entire system load including the DC-AC and DC-DC converters. In order to cater for any instantaneous or short lived upsurge in demand that normally occurs during device operation and to guarantee adequate supply, the load is deliberately oversized by 30% (hence the factor 1.3) [Kaseke and Meyer, 2006].

3.2.2 Battery bank

We consider the battery bank as consisting of series connected columns each in turn consisting of parallel connected batteries as figure 3.1 shows.

Thus the size of the storage facility is obtained as follows:

$$B_s = \frac{V_o}{V_{NB}} \tag{3.5}$$

$$B_p = \frac{E_{load} \times DoA}{\eta_b \times V_o \times C_{NB} \times DoD} \quad (3.6)$$

$$B = B_s \times B_p \quad (3.7)$$

where: V_0 is the DC operating voltage;

V_{NB} is the nominal battery voltage;

η_b is battery efficiency;

DoD is depth of discharge;

C_{NB} is nominal (rated) battery capacity in kAh;

DoA is the days of autonomy;

B_s is the total number of series connected columns;

B_p represents the total number of batteries in parallel per column;

B is the total number of batteries in the battery bank.

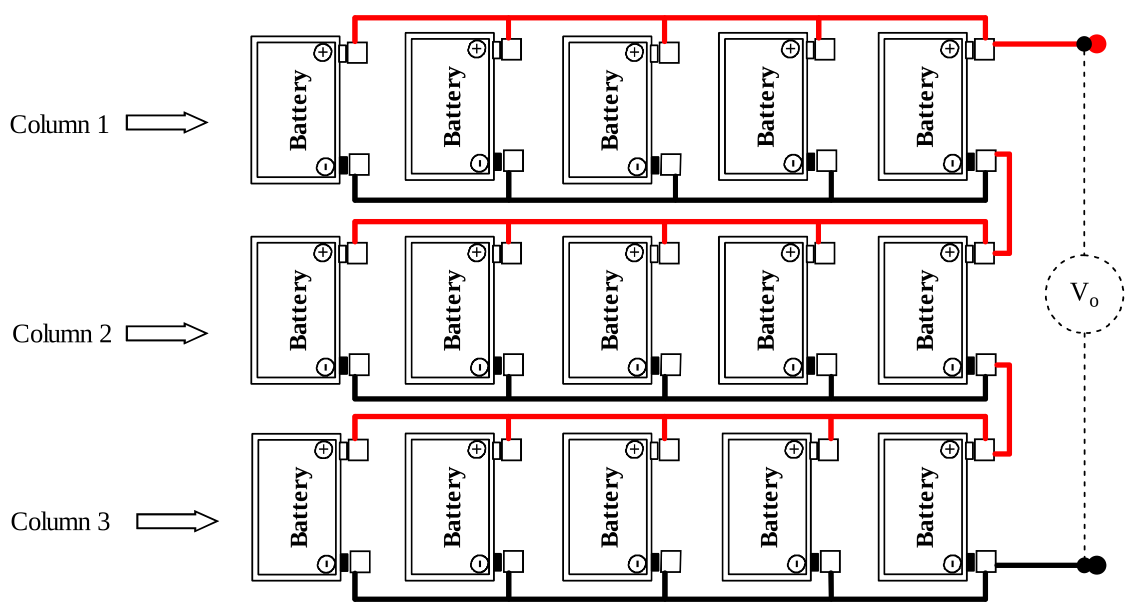

Figure 3.1: Layout of a PV system storage showing series and parallel configuration of batteries to form a battery bank

3.3.3 PV array

In stand-alone PV systems, the array is the only component with the ability to generate power and therefore acts as the source input to the system. On the other extreme, the load only consumes energy from the system thus represent output. It therefore follows that under ideal operating conditions total daily input should always be greater or equal to the total daily output. If this condition is satisfied, it will ensure that the storage facility is not continuously discharged. Similar to the battery bank, the PV array is considered as series connected columns each in turn connected as shown in figure 3.2. The appropriate size of such an array is obtained as follows;

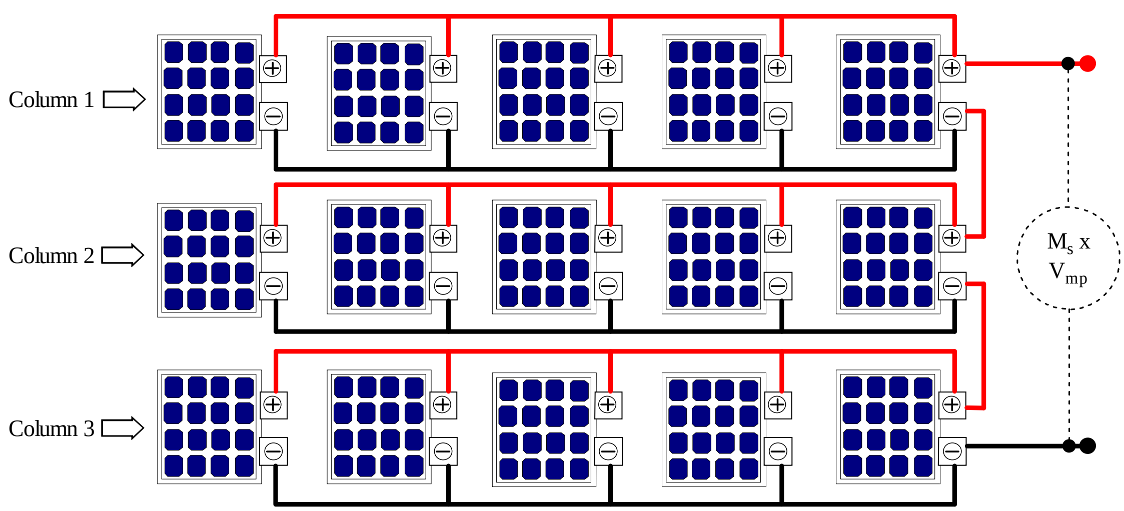

Figure 3.2: Layout of a PV system generator showing series and parallel configuration of modules to form a PV array

$$M = M_s \times M_p \tag{3.8}$$

$$M_s \geq \frac{V_{NB} \times B_s}{V_{mp}} \tag{3.9}$$

$$M_p \geq \frac{E_{Load}}{\eta_b \times M_s \times P_{mp} \times H_{sun}} \qquad (3.10)$$

where: M represents the total number of PV modules in the array;

M_s is the number of series connected columns;

M_p is the number of parallel connected PV modules in each column;

V_{mp} is the module voltage at peak power point;

P_{mp} is the rated peak power of the module array in kW.

H_{sun} represents the average minimum sun hours for the location. A sun hour is equivalent to 1000 Wh/m^2 of solar irradiation. In order to calculate the total sun hours per day, a time integral of the solar irradiance over the entire day is used. Historical site weather data is useful in calculating the characteristic minimum sun hours (average low peak sun hours) for that particular site. Figure 3.3 shows a contour map giving the minimum sun hours for various sites on the African continent. The site for this study, that is, University of Fort Hare (UFH) is highlighted by a blue circle on the map. It is clear from the map that minimum sun hours for our site are between 4 and 5 kWh/m^2.

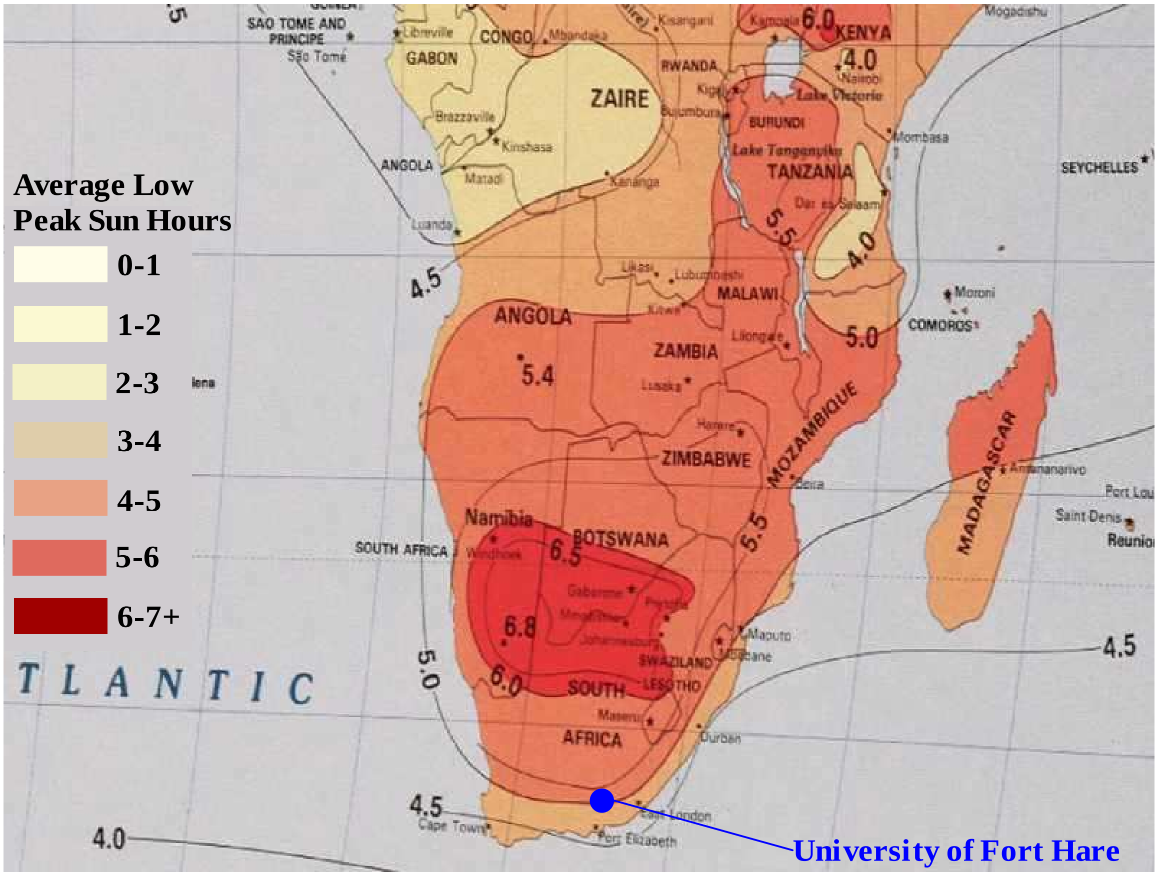

Figure 3.3: Average minimum sun hours for African sites [adapted from Advanced Energy Group, 2006]

However, 4.0 kWh/m^2 of irradiation (equivalent to 4 sun hours) were used as the design sun hours for our location.

3.3 EVALUATION OF PV SYSTEM PERFORMANCE

3.3.1 Cost performance

PV power system represents a capital investment and as such it is important to ascertain the payback time (period) and the return on investment. In simple terms, payback period (*PB*) can be defined as the maximum number of years it will take before the investors start to realize profit on their investment. Commonly PV power systems are evaluated against the national utility grid. Capital cost would therefore be the total cost of building the entire stand-alone PV system. However, there is also capital cost for the grid connection, which is the connection fee [Eskom, 2006]. It therefore follows that the actual capital is the difference between PV capital cost and grid connection fee. Annual cash flow is the total monthly savings over a period of twelve months. Monthly savings are equivalent to the amount that the PV system owner would have paid as monthly electricity bill, if they were using the utility grid.

Return on investment (*ROI*) is sometimes known as the marginal efficiency of capital (investment) of simply expected rate of profit [Slavin, 1996; 115] and is expressed as a percentage. The higher the *ROI*, the better the investment.

Here the analysis was done with the assumption that inflation rates are minimal and stable over time such that risks are negligible. The payback period in years is calculated as follows:

$$PB = \frac{Capital\ Cost}{Annual\ Cash\ Flow} \qquad (3.11)$$

$$ROI = \frac{\Pr ofit}{Capital\ Cost} \qquad (3.12)$$

$$\Pr ofit = (SL - PB) \times ACF - AdC \quad (3.13)$$

SL is system life (in years) and *ACF* is annual cash saving/flow. *AdC* represents the total additional costs over the life time of the system, for instance, cost to replace batteries on 5-year intervals. The *ROI* given by equation (3.12) is the total overall return on investment calculated over the entire life time of the system.

3.3.2 Service performance

The fundamental aim of designing and installing PV power systems is to power a given electrical load. It is therefore tempting and exceedingly easy for one to evaluate performance of the PV system by merely looking at total daily production (by the PV array) and consumption (by the system load) of electrical energy. However this kind of approach is not entirely incorrect, it is merely incomplete as it leaves out other factors that could affect both array production and the supply to the load. Such factors include regulation as well as the ability of the storage batteries to retain charge.

As shown in equations (3.8 -3.10), PV array is sized based on rated module parameters at peak production which in the ideal case is the same as module performance at standard test conditions (STC: 1000 W/m^2, 25°C cell temperature and AM1.5 global spectrum). Outdoor conditions greatly differ from STC with irradiance levels normally lower than 1000 W/m^2 and cell temperatures above 25°C. At ambient temperatures above 25°C PV modules will be operating at temperatures well above ambient and can lose up to 14% of their potential energy production [van Dyk *et al.*, 2000]. Other factors besides environmental conditions that can greatly reduce outdoor module output are the inherent module defects. Such defects include mismatched cells [Meyer, 2002; 41-43] and module shunt paths [Meyer, 1999; 16-20].

Modules connected in a regulated system operate at lower power (P_{op}) than the rated peak power [Meyer and Mapuranga, 2005]. This is due to the operation of the regulator, which prevents the charging voltage (module voltage) from exceeding a threshold voltage referred to as regulated voltage (V_{reg}). Also, the regulator should be able to properly control battery charging and discharging in order to prevent excessive discharge and over charging. Discharging the battery to deeper levels than recommended as well as high discharge rates will reduce battery life as well as its ability to retain charge [Crompton, 1990; 31/3-4 and Linden, 1984; 13-15, 13-19]. Similarly, overcharging results in excessive heating and energy loss due to gassing [Lesnier and Ang, 1990; 130].

The battery bank's size is based on manufacturer's ratings of nominal battery voltage and ampere-hour capacity. Of greater importance is the ability of the battery to retain charge. It is known that battery terminal voltage is related to its state of charge during both charging and discharging. It therefore follows that, if a battery has a poor ability to retain charge, then during discharge battery voltage will rapidly collapse.

3.4 SUMMARY AND CONCLUSIONS

This chapter has identified two key performance issues with regard to PV power system design and installation. The two issues are cost and service. The idea is to entice any PV system design and installation to try and strike a balance between the two issues as this will help curb the usually high installation costs that have characterized the PV industry and acted as the major deterrent for average potential investors over the years. A set of standard sizing equations was also presented with a promise to determine optimal sizes of the various PV system components. These equations were used in this study to size the system at UFH. This chapter has also managed to identify key service performance analysis parameters for the three components of the PV system viz. PV array, regulator and battery bank. Of particular importance pertaining to PV array service performance is the ability of the modules to meet the daily energy requirement of the load. With the regulator, effective control of charging and discharging as well as its effect on module production should be ascertained. The ability of the battery storage to retain charge should also be ascertained.

3.5 REFERENCES

Advanced Energy Group, (2006), http://www.solar4power.com/map10-global-solar-power.html; last viewed May 10, 2006.

Crompton T. R. (1990), "Battery Reference Book", Butterworths and Co.

Eskom (2006) South Africa's National Utility Company, "Eskom Tariffs and Charges 2006/7", accessible at: www.eskom.co.za , last viewed: August 20, 2006.

Kaseke R. and E. L. Meyer (2006), "PV power system sizing for information and communication devices in schools outside the national utility grid", *Proceedings of the World Renewable Energy Congress IX*; Elsevier, Flourence, Italy; PV93.

Lasnier F. and T. G. Ang (1990), "Photovoltaic Engineering Handbook", Adam Hilger.

Linden D. (1984), " Handbook of Batteries and Fuel Cells", McGraw-Hill.

Messenger R. and J. Ventry (2000), "Photovoltaic Systems Engineering", CRC Press.

Meyer E. L. (2002), *On the Reliability, Degradation and Failure of Photovoltaic Modules*, PhD-thesis, University of Port Elizabeth.

Meyer E. L. and B Mapuranga (2005), "The Effect of Temperature on the Performance of Photovoltaic Modules at Regulated Voltage", *Proceedings of the 15th PVSE conference*; Shanghai, China.

Meyer, E. L. (1999), *Investigation of Properties and Energy Rating of Photovoltaic Modules*, MSc-dissertation, University of Port Elizabeth.

Slavin S. L. (1996), “Economics”, Irwin/McGraw-Hill.

van Dyk E. E. et al (2000), “Temperature dependence of output parameters of crystalline silicon photovoltaic modules”, South African Journal of Science, **96**; 198-200.

CHAPTER 4

DESIGN, INSTALLATION AND PERFORMANCE ASSSESMENT OF THE PHOTOVOLTAIC SYSTEM

For all figures except 4.1, 4.3 and 4.4, the following line convention is used

		Module	***Battery***	***Load***
Line Colour		*Blue*	*Red*	*Green*
Marker Type	*Power*	*Diamond*	*Diamond*	*Diamond*
	Voltage	*Circle*	*Circle*	*Circle*
	Current	*Triangle*	*Triangle*	*Triangle*

4.1 INTRODUCTION

Chapter three laid the foundation for the design and performance evaluation of stand-alone systems in general. A number of issues pertaining to proper system designing were discussed along with a set of mathematical equations for use in effective system sizing. Based on the equations presented in chapter three, a small-scale stand-alone system was sized, installed and monitored. This chapter outlines the size and performance of various system components of the system at the University of Fort Hare (UFH).

4.2 LOAD DESCRIPTION AND DEMAND MEASUREMENTS

Figure 4.1 shows the separate demand profiles of the three load devices measured over a period of two hours. In order to determine total demand and daily consumption for each of the three load devices, their AC current and voltage requirements were measured using a Fluke 177 true rms multimeter and verified with a Hewlett Packard 971 Multimeter. The characteristic load consisted of one Pentium 4 desktop Central Processing Unit

(CPU), a 15 inch Cathode Ray Tube (CRT) monitor and a single Mobile Internet Device (MIDevice) that was designed as part of this study. As figure 4.1 indicates, consumption profile for each device is characterized by a peak referred to as start-up peak. The reason for this is that, at star-up each device executes a self test procedure, which entails running all its internal circuitry and sub-systems as well as scan its drivers. An example is the CPU which runs all its fans and checks all ports and peripherals like mouse and keyboards that might be attached to it at start-up. As a result of this self test sequence all three devices registered peak demand at start-up, which lasts for less than 5 minutes.

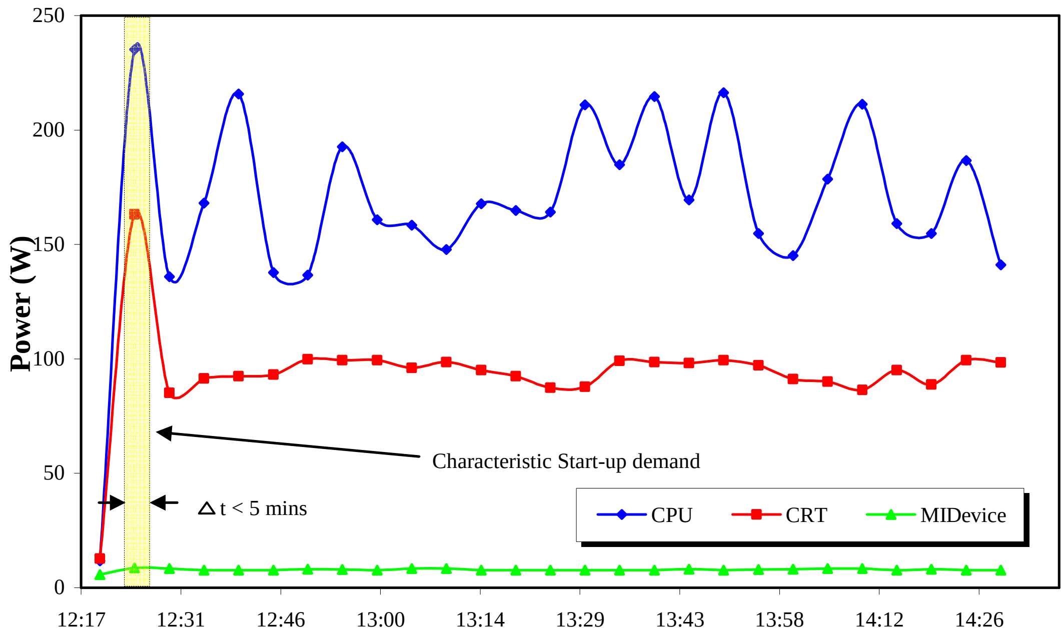

Figure 4.1: Demand profiles for the system load devices

4.3 UFH SYSTEM CAPACITY

Table 4.1 summarizes the size of the UFH system used in this study. After an analysis based on the relationship between battery life and depth of discharge [Kaseke and Meyer, 2006], the number of batteries required was reduced to only 9. The aim of this analysis is to reduce cost of battery storage facility and hence the overall installation costs for the photovoltaic (PV) system. The norm in the design of the storage facility requires the storage capacity to be large enough to sustain operations during days of little or no generation from the PV array (days of autonomy, *DoA*). Since the installed battery capacity far exceeds the daily requirement of the load, the effective depth of discharge (DoD) per battery is very little. This subsequently improves battery life. Reducing the storage facility to only nine contributes to a more significant saving on installation cost. The increase in the effective DoD per battery due to the reduction in the size of the battery bank is so small that it only results in an insignificant change in battery life. In that sense, nine batteries could still surface with even less battery maintenance cost over the entire life of the PV system.

Table 4.1: Initial System Sizing of the UFH system

Load			**Battery Bank**		**PV Array**	
		t_n (hrs)	V_o	12 V	V_{mp}	16.5 V
kVA_1	0.168	2	V_{NB}	12 V		
kVA_2	0.094	2	*DoD*	20%	P_{mp}	0.70 kW
kVA_3	0.008	2	*DoA*	3		
η_{AC}	0.8		C_{NB}	0.100 kAh	H_{sun}	4
E_{AC}	0.54 kVAh		η_b	0.9		
E_{DC}	0		B_s	1	M_s	1
$\boldsymbol{E_{Load}}$	**0.8775 kWh**		B_p	12	M_p	4
			B	**12**	***M***	**4**

In the table kVA_1, kVA_2 and kVA_3 represent the measured apparent power demand for the CPU, CRT monitor and the MIDevice, respectively. The battery efficiency, η_b, for lead acid batteries is roughly 90% [Messenger and Ventre, 2002; 53]. There were no direct current (DC) loads in the system hence E_{DC} is zero. Equations (3.2) – (3.10) introduced in chapter 3 were used in order to obtain the total daily energy consumption (E_{AC}) for the alternate current (AC) loads and for the entire load (E_{Load}) for the system as well as the total battery and PV array sizes.

4.3 EXPERIMENTAL SET-UP

A regulated PV power system consisting of four 70 W monocrystalline modules, nine shallow discharge sealed lead-acid (SLA) batteries and a Tarom 245 Pulse Width Modulation (PMW) Solar Charge Controller were installed at the University of Fort Hare. The Project site is located at 32.8° latitude south of the equator and hence the fixed rack for the PV array was tilted at the same latitude angle facing north. Figure 4.2a shows the outdoor components (four monocrystalline modules and the pyranometer). As expected for any outdoor mounted module, there is evidence of bird droppings on module surfaces. The PV rack carries other module types and a spectroradiometer (black tube next to the pyranometer). However these other components are being used in other PV research areas currently running at the Fort Hare Institute of Technology. Figure 4.2b shows some of the indoor components (CRT monitor and CPU) of the system.

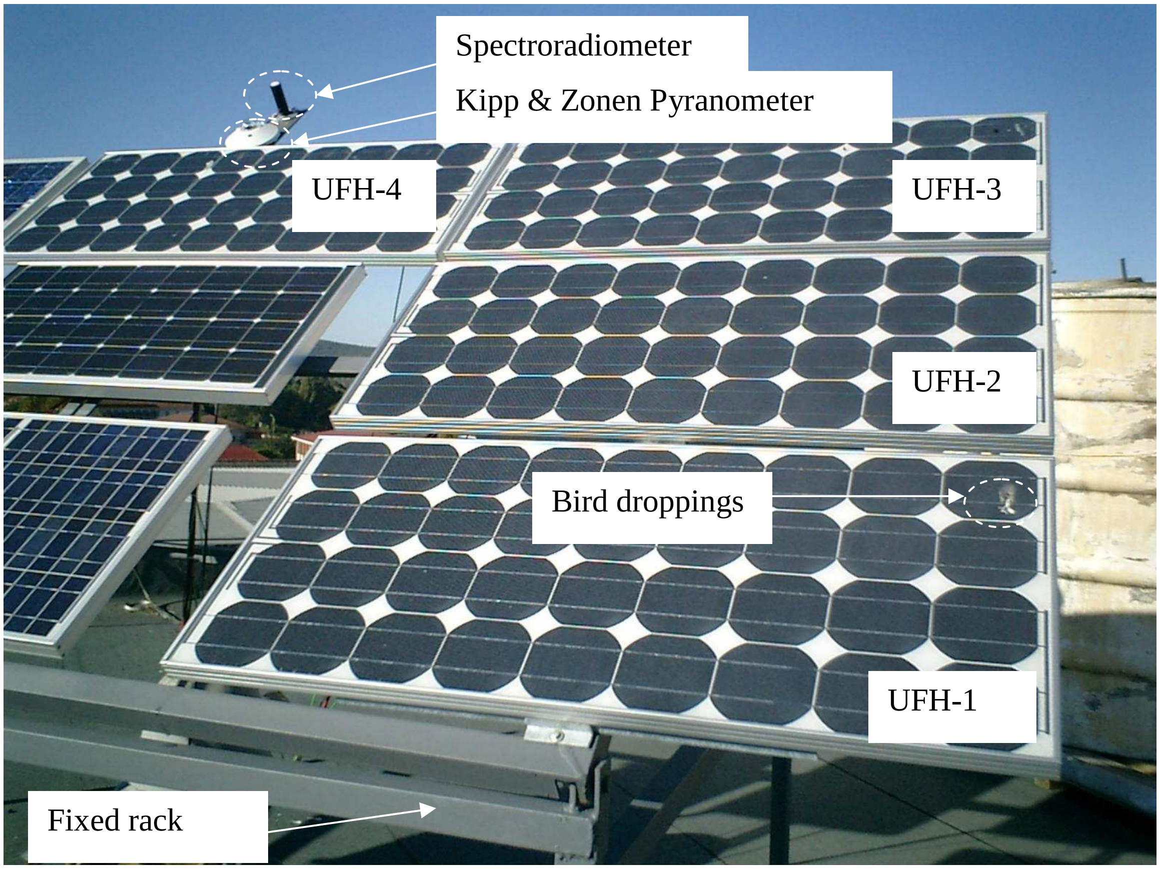

Figure 4.2a: PV array and pyranometer

DC lighting load shown in figure 4.2b was not part of the initially intended load. However, after the PV system was commissioned, it was realized that there was a quite considerable amount of excess energy produced by the array per day. This excess production presented an opportunity for scaling up the load hence the addition of the DC lighting load.

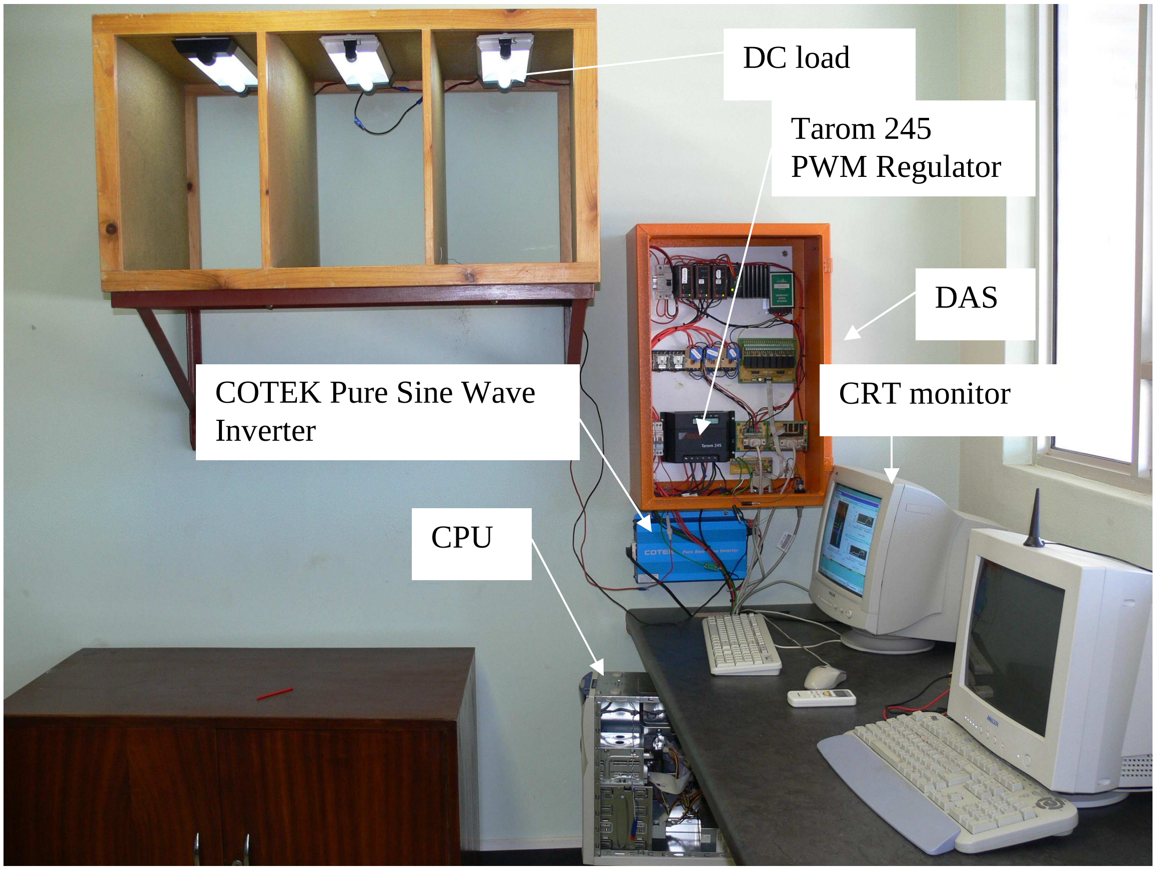

Figure 4.2b: Indoor components of the UFH system

A data acquisition system (DAS) made up of current and voltage transducers and PC boards was installed to continuously monitor current and voltage for the PV array, battery bank and load at 10-minute intervals. Type-K thermocouples were fitted to measure both ambient and cell temperature of the module continuously throughout the day. Figure 4.3 shows a schematic drawing of the DAS. A pyranometer mounted on the module rack was used to measure solar irradiance levels. Temperature and irradiance information was also collected using the DAS.

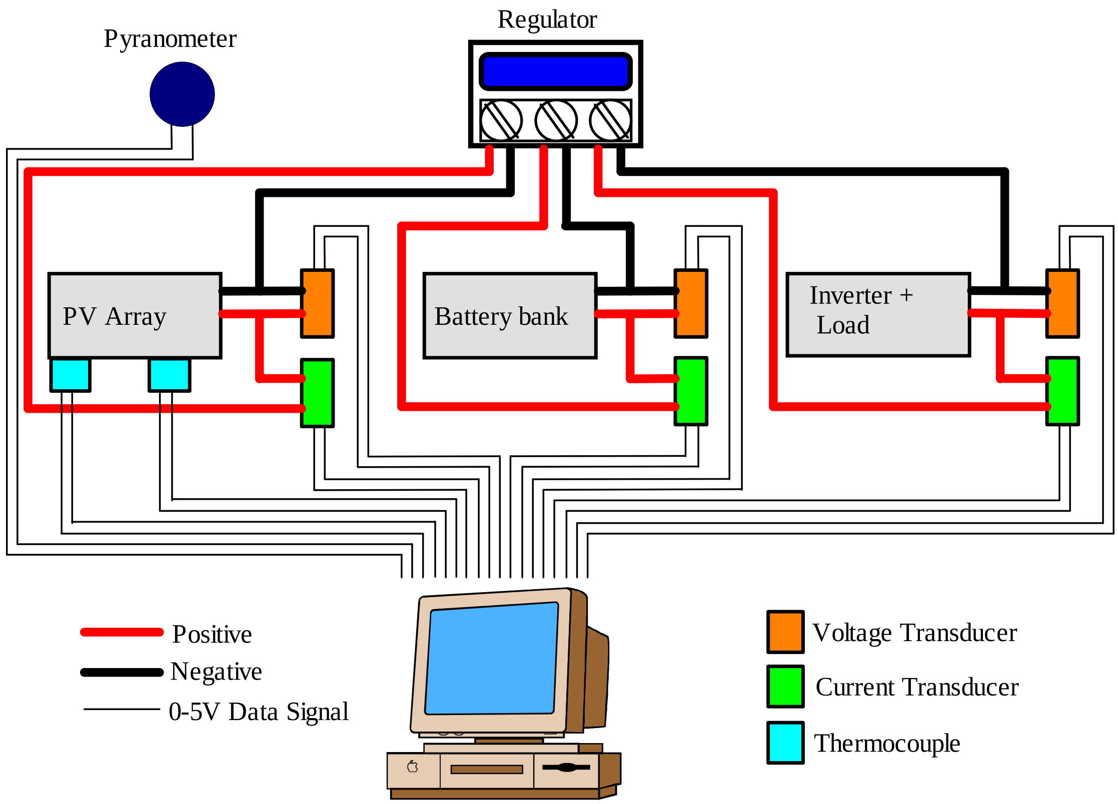

Figure 4.3: Layout of the data acquisition system

4.4 BASELINE DETERMINATION

The performance characteristics of the four single crystalline modules were measured at STC using a Spire-Sun, Xenon pulsed solar simulator (SPIRE 240A). This was done before the modules were deployed outdoors and is used as a baseline for ongoing outdoor monitoring and degradation analysis.

Table 4.2 lists the rated power and power measured under standard test conditions (STC: 1000 W/m², 25°C cell temperature, AM1.5 global spectrum). Also listed are the corresponding efficiencies. From table 4.2, it is evident that all modules performed well within acceptable levels.

Table 4.2: Summary of rated and measured values

Module	Peak Power (W)		Efficiency (%)		
	P_{rated}	P_{STC}	η_{rated}	η_{STC}	% Difference
1	70	69.58	11.54	11.40	1.21
2	70	70.73	11.54	11.59	-0.43
3	70	70.75	11.54	11.76	-1.91
4	70	69.22	11.54	11.34	1.56

Percentage difference in table 4.2 is the percentage difference of η_{STC} from η_{rated}. Figure 4.4(a) shows the corresponding characteristic current-voltage (*I*-*V*) curves of the four modules listed in table 4.2.

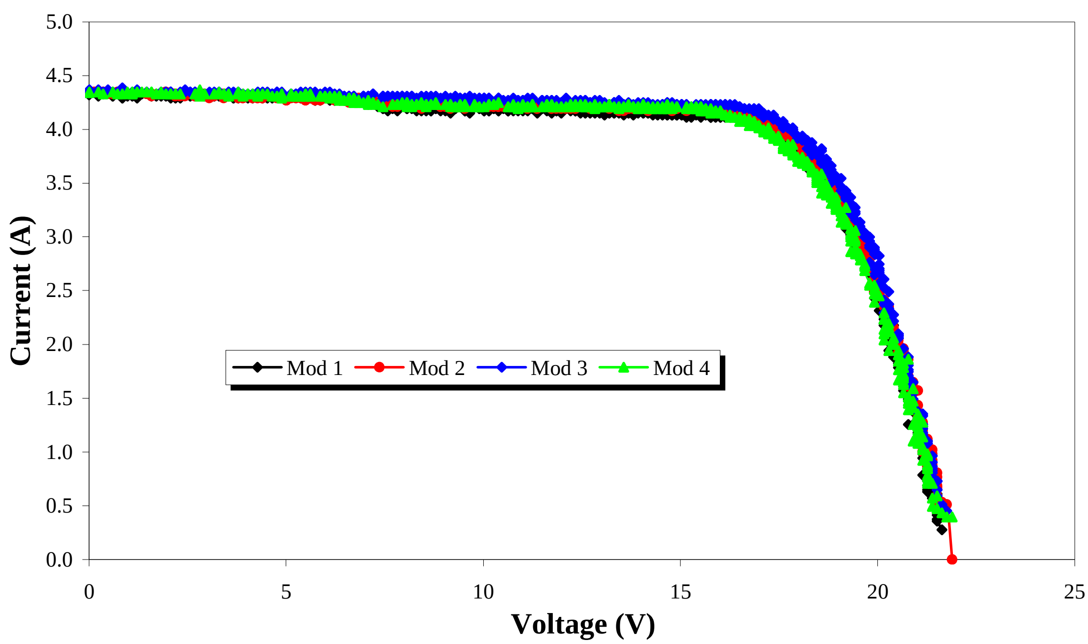

Figure 4.4(a): Module I-V curves at standard test conditions (STC).

Evident from the characteristic curves in figure 4.4(a) is a slight break in the horizontal part of the *I-V* curves of modules 1 and 4. This is attributed to a slight mismatch in the performance of individual cells in the module. Clearly all four modules exhibit this behavior. No obvious cracks or cell defects were observed during a comprehensive visual inspection.

Figure 4.4(b) shows the indoor Infrared Thermography of module 4. The module was reverse-biased in the absence of light 25 VDC at 5 A. Ideally, the module should behave like a junction diode. However mismatch cells behave like resistors that dissipate power inside the module and therefore become hot spots represented by bright spots on the image.

When these modules are operating outdoors, mismatched cells may cause power dissipation and consequently the formation of hot spots on cells with lower power producing capabilities. This in turn may result in irreversible damage to the module [van Dyk, 2002]. Although this mismatch seems to be insignificant, it poses a potential degradation mode which may with time significantly reduce power production.

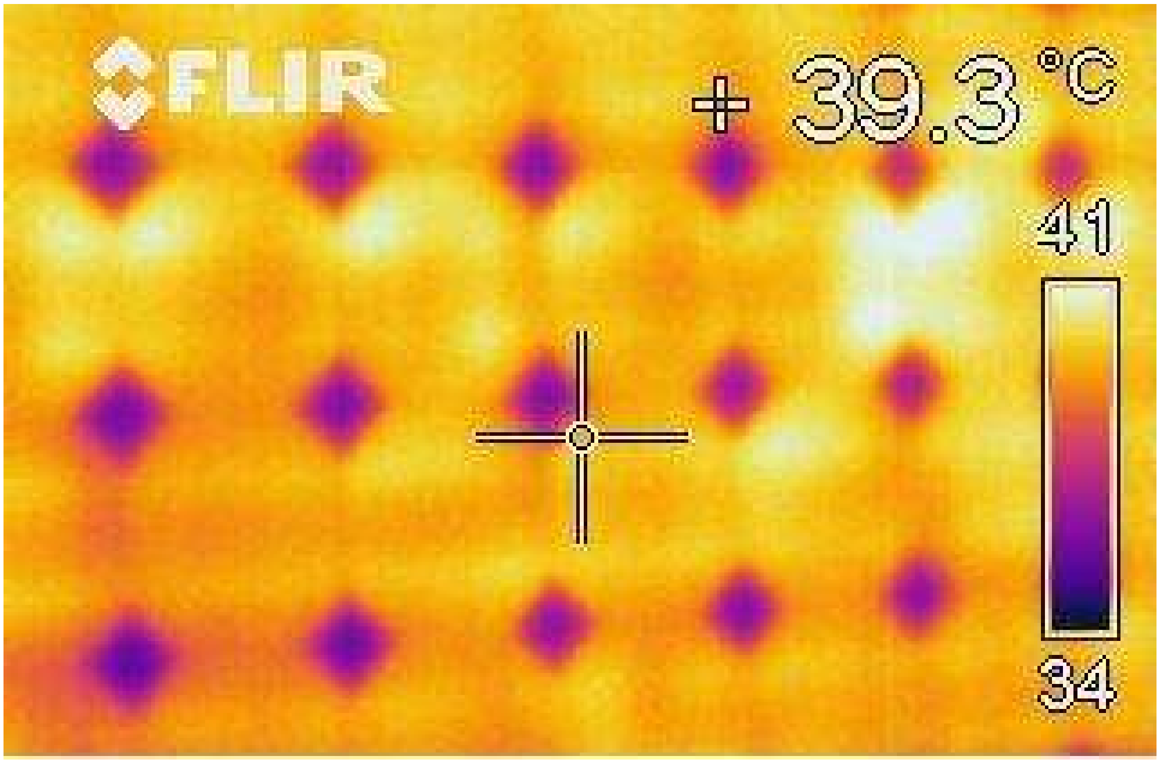

Figure 4.4(b): Infrared Thermography of module 4 when reverse-biased in the dark to 25 VDC at 5 A

4.5 COST PERFORMANCE ANALYSIS

Table 4.3 lists the payback and return on investment for the UFH system. Cost savings on electricity was calculated from equations (3.11) – (3.13) presented in chapter 3 using the national utility (Eskom's) NightSave Rural tariff plan [Eskom, 2006].

Table 4.3: Cost performance of the UFH system

Item Description	Value
Capital Cost	R17 464-00
Annual Cash Flow	R3 467-00
Payback period	5 years
Profit	R49 900-00
Return on investment	286%

The UFH system therefore, promises to return more than double the costs incurred at installation by the end of its guarantee after 25 years.

4.5.1 Risk on investment

It needs to be stressed that the results in table 4.3 were calculated with the assumption that inflation [Hyman, 1997; 12 and Hall, 2005; 633-638] remains relatively stable over the 25 years. This is more unrealistic especially in our (African) developing economies amid eminent threat from all sorts of political interferences and instabilities. However, if inflation causes a proportionate rise in money price while maintaining relative price [Lipsey, 2004; 51] of all goods and services, then the system would still perform quite well. This is derived from the fact that, both running expenses and annual cash flow (calculated from the electricity charge at that time) will increase as inflation rises hence profit will remain almost the same. Inflation becomes a problem when it causes a more significant rise in the relative price of running expenses in comparison to the general price level [Lipsey, 2004; 51].

A more serious risk is posed by module degradation caused by natural or semi-natural factors. Natural causes involve the natural deterioration of module cell constituents due to long periods of outdoor exposure. Semi-natural causes involve hot spots formed when shade is cast on cell by module frames, bird droppings and surrounding objects. Hot spots can also form as a result of mismatched cells as mentioned in section 4.5. Degradation reduces module output and may with time result in a reduction in annual cash flow. Proper maintenance is the only mitigation factor for risks due to semi-natural causes.

4.6 SERVICE PERFORMANCE ANALYSIS

4.6.1 Generation and supply

Figure 4.5 gives PV array, battery bank and load power curves on three consecutive sunny days. Average AC load demand was found to be 0.112 KVA. This demand represents the actual demand and is less than half of the demand used in the system design (see table 4.1). This prompted further investigation. The regulator used in the study allows any loads connected to the system to be powered directly by module output while any excess output from the module is directed towards battery charging. At the time when full load is switched on in the morning, module output will not be adequate to meet such a large demand hence the battery will have come in so as to complement module output. The result is a jump or surge battery power.

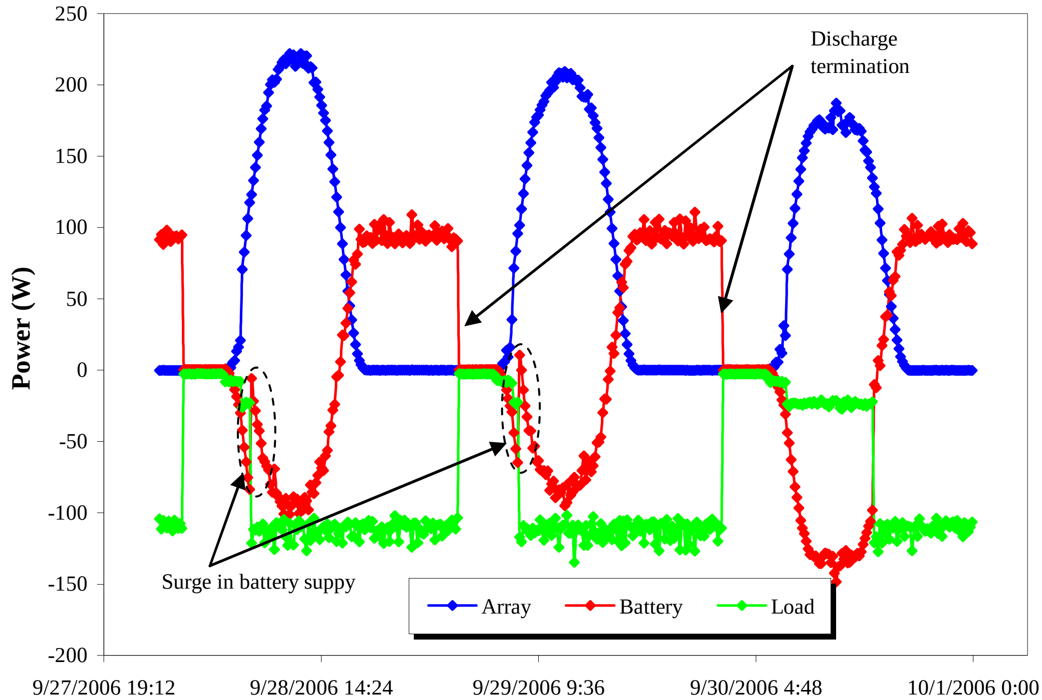

Figure 4.5: Module, battery and load power vs. time of day on August 6, 2006

Oscilloscope measurements of the inverter (Cotek S600-212) output voltage signal revealed a true sine wave of 150 V in amplitude. Current measurements show that the load continued drawing the same current at this new voltage as its current at 240 V (rms). This phenomenon can be well explained in light of the type of devices constituting the load (see Appendix B). All load devices are generally electronic device whose main circuitry is made of numerous micro-electronic circuits and components. These components, unlike constant power devices, have the ability to work on a voltage range while drawing a constant current as a result they can be regarded as voltage operated. It is this property that allowed the load devices to operate at peak voltage of 150V while still drawing the same rms current. Constant power devices would draw more current as the input voltage is lowered so as to maintain a constant power input. Examples of these include pumps, motors and other inductive loads.

Also evident from figure 4.5 is the fact that at night when array output is zero, battery supply is generally less than load demand. This is rather unusual since it is expected that during this time, only the battery bank should supply the entire load meaning, therefore, its output must be greater than or equal to load demand. However the low battery output is attributed to the regulator operation. The regulator uses parallel (shunt) regulation principle [Lasnier and Ang, 1990; 142] in which the regulator is in parallel with both the PV array and the battery bank. Battery terminal voltage is in actual fact higher than the voltage at the terminals of the regulator but because the two are in parallel the voltmeter records the smaller of the two voltages.

Figure 4.6 shows the DC current and voltage profiles for the battery bank and load measured throughout the night. In this figure, load voltage is higher than battery voltage. Current from the battery is almost equivalent to current drawn by the load hence the manipulation of battery voltage by the regulator is the only cause of the unusual discrepancy in supply and demand.

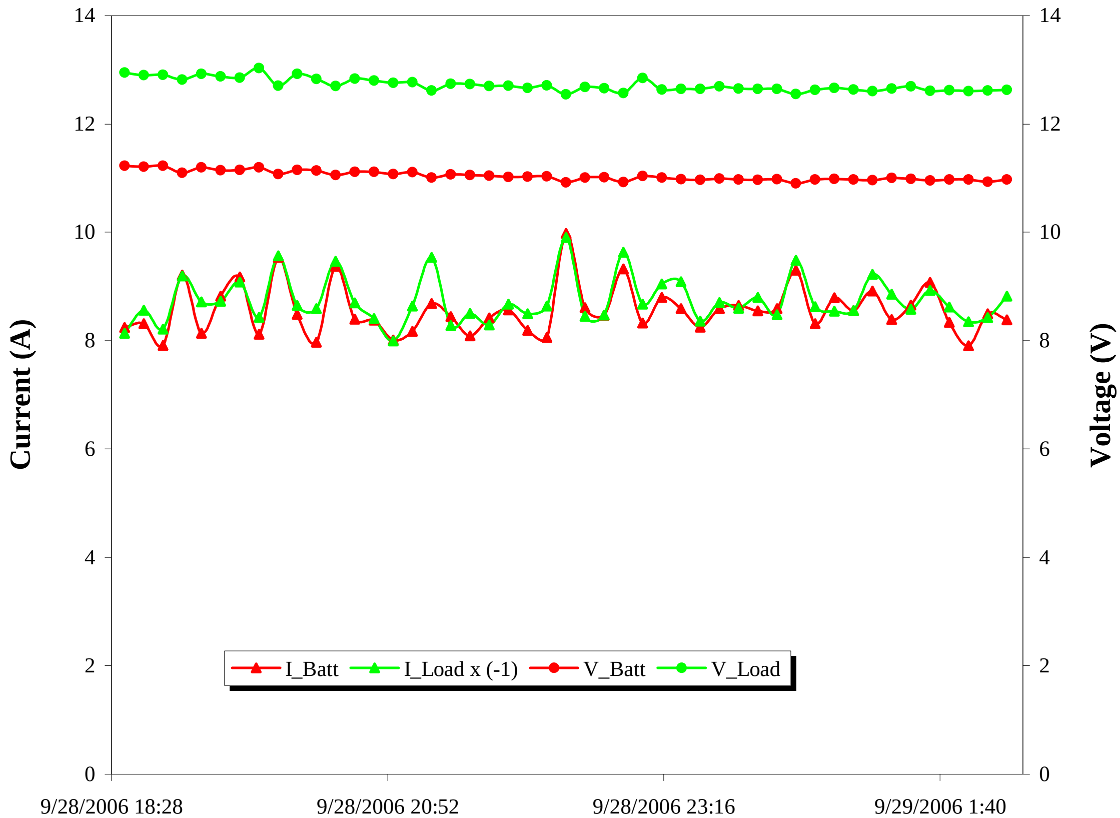

Figure 4.6: Current and Voltage for the battery and load measured at night

4.6.2 Regulation and the Battery Storage

The regulator used in the study uses pulse width modulation (PWM) technique which basically is a constant voltage technique in which charging current tapers according to the charging needs of the battery. As figure 4.7 shows, at end of charge, the charging source in not completely terminated, instead, the battery bank is thrown into standby mode with its voltage clamped to a low level while short current pulses are supplied in order to maintain it at full charge.

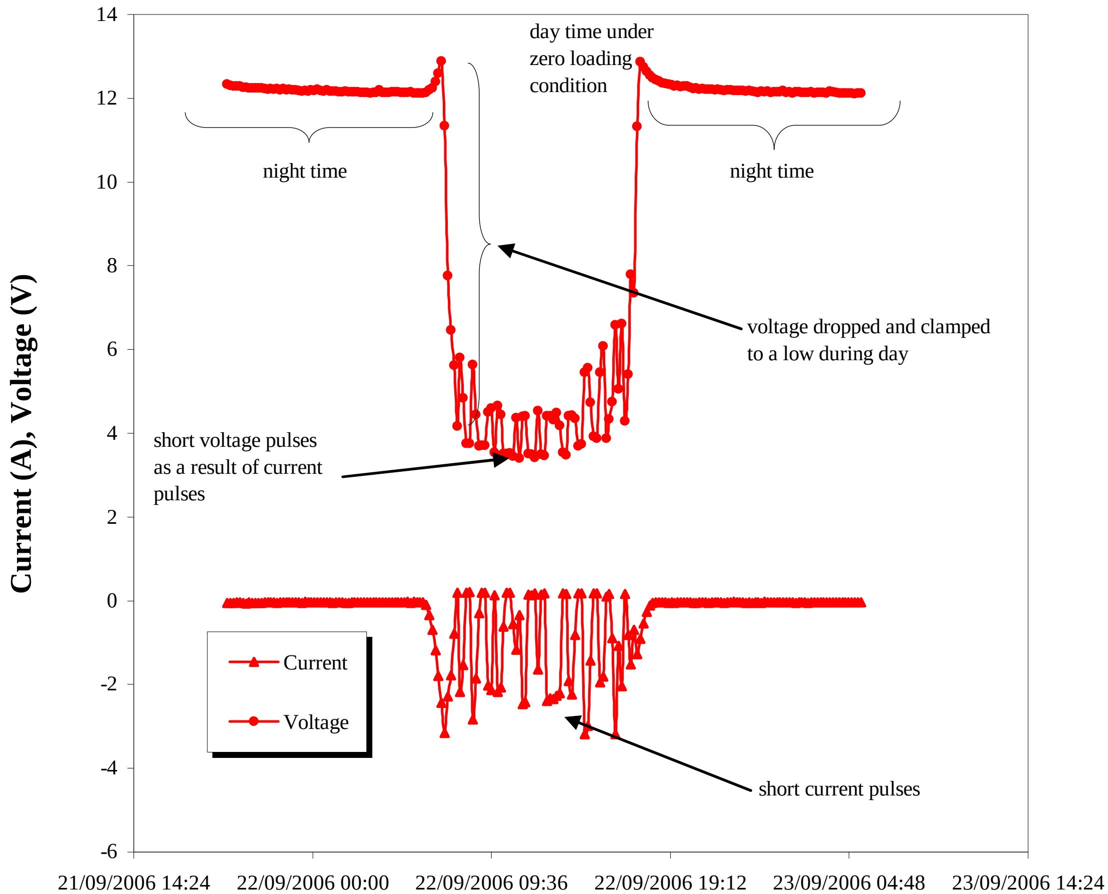

Figure 4.7: Battery current and voltage behaviour at end of charge using PWM regulation technique

The ability of the regulator to control battery discharge is also demonstrated in figure 4.8 where the load is disconnected at end of discharge. The discharge rate is found to be 9 A/h, which translates to an effective 1 A/h for each battery in the battery bank. All of the batteries are rated as 100Ah/10h, which on average means at most each one of them can supply 10 A constantly for 10 hours. However considering 100Ah as the available capacity (C_p) per battery and 10 hours as the discharge time (t), then Peukert's Law (see equation (4.1)) suggests that the maximum discharge current (I) would approximately be 6.9 A. Again by Peukert's Law, if each battery in the bank contributes 1 A towards the total discharge current of 9 A, then its discharge would last for 100h. Under such discharge conditions full capacity is obtainable at higher end point voltage per battery cell [Crompton, 1990; 31/3-4]. The Peukert's constant (*k*) for lead-acid batteries between 1.1 and 1.2 but for our calculations 1.2 was used [Wikipedia, 2006].

$$C_p = I^k t \qquad \textit{Peukert's Law} \qquad (4.1)$$

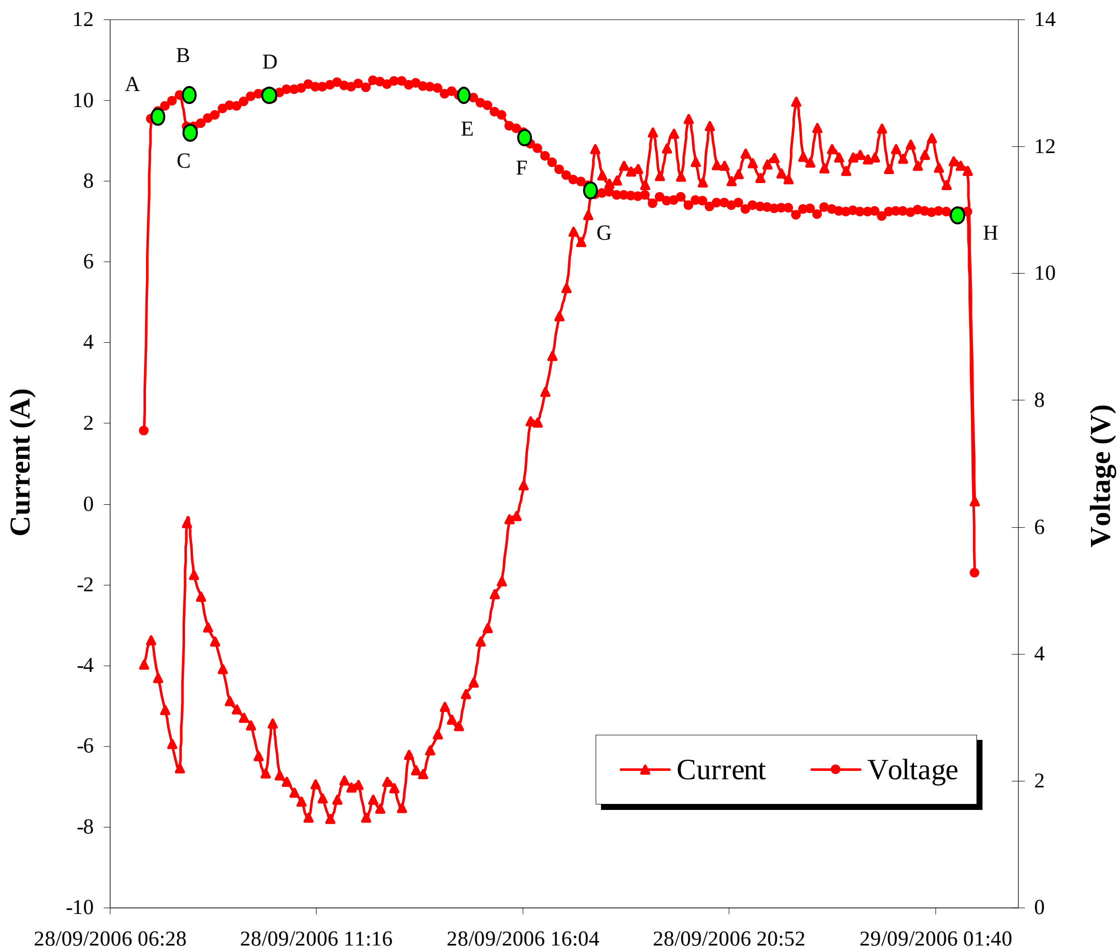

Figure 4.8: Battery current and voltage during regulated charging and discharging

At point A in figure 4.8, the battery begins to charge. Charging voltage rises with the rise in module voltage. Point B represents the load reconnect point where full load is reconnected hence the drop in battery voltage to C. This voltage drop is due to the battery bank being suddenly forced to address the sudden upsurge in demand at a stage when module output is still low. Point C-D shows a gain in charging voltage as module output increases in the day. The regulator maintains a relatively constant charging voltage between D and E while E-F coincides with drop in module output. Point F is like a point of inflexion on the charging voltage curve and signifies beginning of discharge. F-G-H represents discharge with G marking the point when the storage takes over supply to entire load.

4.6.3 Battery Bank

Figure 4.9 shows a full discharge cycle that stretched for roughly 30 hours between October 13 and 15, 2006. Firstly the batteries were fully charge after which full load (CPU, CRT monitor and the MIDevice) was connected. Battery bank voltage during discharge displayed a more gradual decline (approximately 0.015V/h), which suggests that the storage facility is in good order and has very good charge retention ability. A total of 261.37 Ah were drawn from the battery bank in 30.17 hours, which translates to 29.04% depth of discharge and an average discharge current of 8.71 A for the entire battery bank. This translates to an average discharge current of 0.97 A per battery, which is an acceptable rate of discharge since it is less than the manufacture’s 10-A rate.

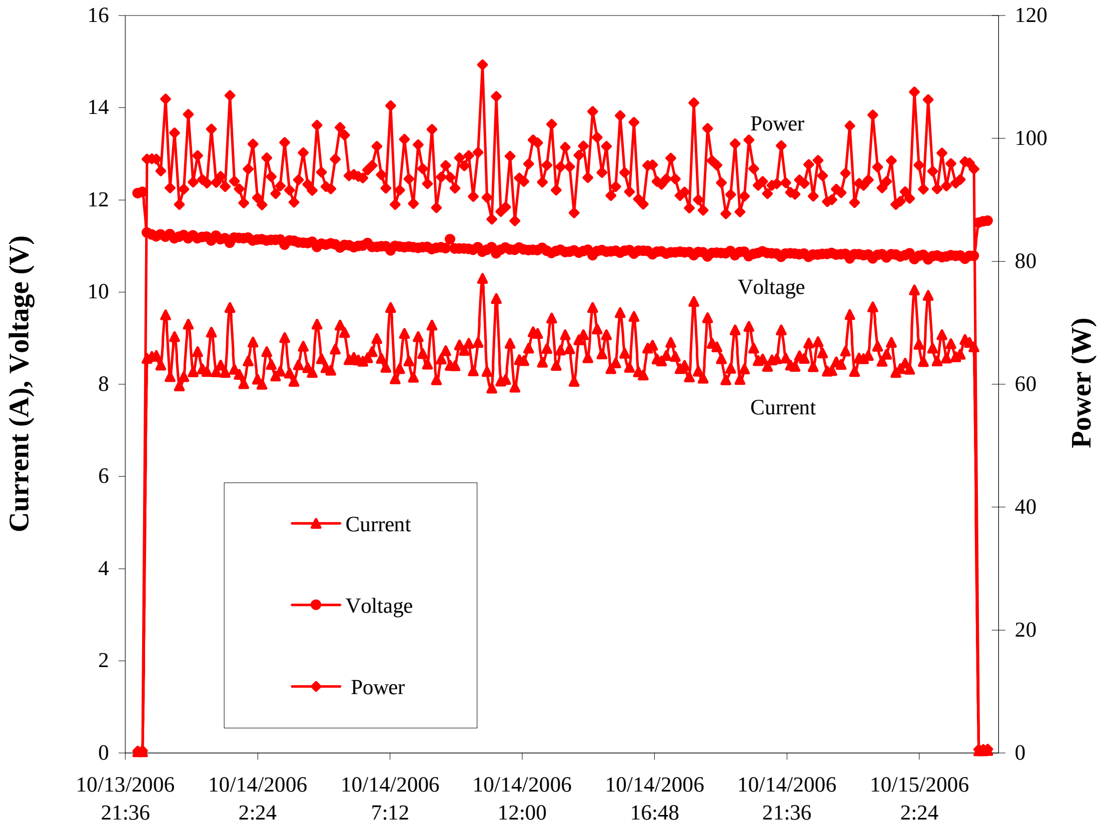

Figure 4.9: Full battery discharge cycle

4.7 SUMMARY AND CONCLUSION

The UFH stand-alone PV system was successfully designed, successfully installed and monitored and the following are some of the conclusions that can be drawn from the results obtained and presented thus far.

PV module design should be regarded as a capital investment from which the investor concerned should realize a profit. In this regard, all PV power system designs need to aim at providing the much needed power at optimized cost. PV modules in stand alone systems sometimes generate more than what the load requires especially on clear sunny days (sun hours ≈ 7-8 kWh/m^2). Normally this excess is just wasted in the regulator (property or requirement of shunt regulation) unlike in grid–connected systems where this can be sold to other users thus making investment into PV more lucrative. However excess production becomes vital in stand-alone systems for assisting the storage facility to recover from extended periods of discharge without necessarily having to completely disconnect system load. An instance would be after the system has gone through the entire days of autonomy.

Sometimes demand budgeted for in the design is not the same as the actual demand after installation. It is therefore imperative for designers to do post-installation measurements in order to ascertain the actual demand as this can present an opportunity for load expansion thereby adding value to the system and improving the system's capacity utilization rate [Slavin, 1996; 113] in cases where post demand is found to be less that the demand catered for in the design. For instance, the UFH system is being run at half load capacity giving 50% capacity utilization system inefficiency. Where possible at pre-installation, modules should be tested at STC to verify rated values and detect any serious inherent defects hence reducing the investment risk. Also post implementation assessment is necessary to ascertain proper functionality of all system components.

4.8 REFERENCES

Crompton T. R. (1990), "Battery Reference Book", Butterworths and Co.

Eskom (2006), South Africa's National Utility Company, "Eskom Tariffs and Charges 2006/7", accessible at: www.eskom.co.za , last viewed: August 20, 2006.

Hall R. E. (2005), "Economics, Principles and Applications", Thompson South-Western.

Hyman D. N. (1997), "Microeconomics", Irwin/McGraw-Hill.

Kaseke R. and E. L. Meyer (2006), "PV power system sizing for information and communication devices in schools outside the national utility grid", *Proceedings of the 6th World Renewable Energy Congress*; Elsevier, Flourence, Italy; PV93.

Lasnier F. and T. G. Ang (1990), "Photovoltaic Engineering Handbook", Adam Hilger.

Lipsey (2004), "Economics", Oxford University Press.

Meyer E. L. (2002), *On the Reliability, Degradation and Failure of Photovoltaic Modules*, PhD-thesis, University of Port Elizabeth.

Simon M. (2005), *Design and Implementation of an Automated Photovoltaic Module Current- Voltage Tester employing a Variable Power Supply*, MSc-dissertation, University of Fort Hare.

Slavin S. L. (1996), "Economics", Irwin/McGraw-Hill.

van Dyk E. E. et al (2000), "Temperature dependence of output parameters of crystalline silicon photovoltaic modules", South African Journal of Science, **96**; 198-200.

Wikipedia, 2006; Accessible from http://en.wikipedia.org/wiki/Peukert's_law, last viewed 15/12/2006.

CHAPTER 5

PHOTOVOLTAIC MODULE EFFICIENCY AND ENERGY PRODUCTION UNDER OUTDOOR CONDITIONS

5.1 INTRODUCTION

Several ambient factors influence performance of Photovoltaic (PV) modules mounted outdoors. These factors include among others, ambient temperature, solar irradiance and spectral distribution. Rating of module performance using solar simulators is done under carefully controlled conditions that are essentially different from outdoor conditions that the same modules will be subjected to. Usually standard test conditions (STC) used to rate modules are defined as 1000 W/m^2 solar irradiance, 25°C cell temperature and air mass 1.5 global spectrum [van Dyk *et al*, 2002]. In fact these STC combine the irradiation of a clear summer day, module temperature of a clear winter day and the spectrum of a clear spring day [Bücher *et al*, 1998]. Clearly such conditions are more theoretical than they ever are realistic. Furthermore, during these indoor tests, the environmental factors are considered in isolation, that is, module response is noted when varying each of the factors in turn, *ceteris paribus*. Again such variation is not continuous; rather it steps through discrete levels. For instance, as way of varying irradiance inside indoor simulators, filters are used that set irradiance to the desired level. However after having said all this, it remains ironic if not unfortunate that PV system design presently rely on module STC ratings.

Outdoor environment factors concurrently change but PV modules are known to have a certain response to change in each of these outdoor environmental factors. This chapter seeks to apply the known relationships between each of outdoor environmental factors (specifically ambient temperature and solar irradiance) and module performance parameters (efficiency and energy production) in explaining the observed outdoor performance of the University of Fort Hare (UFH) PV array. Findings from this chapter can easily be generalized to cater for other outdoor mounted modules of the same technology.

Use of a regulator, though highly recommended in all PV power system applications, has a limiting effect on the modules' maximum energy production. The effect of regulation was also investigated, subsequently quantified and thus will be presented in this chapter.

Module frame shading was noted during outdoor monitoring of the PV modules and therefore will also form part of the discussions in this chapter.

5.2 SOLAR CELL BASICS

5.2.1 Construction

Doping is a process by which tiny but controlled amounts of "impurities" are added to pure (intrinsic) semiconductors in order to improve their electrical conductivity [Duncan, 1983; 75]. The resultant material with improved conductivity is called extrinsic semiconductor and two such semiconductors exist, which are; n-type and p-type. A p-type material has free (unbound) positive charges (holes) while n-type material has free electrons. A solar cell (PV cell) fundamentally consist of two opposite extrinsic semiconductor materials that are joined together to form a p-n junction as figure 5.1 depicts. Holes in the p-type are attracted to electrons in the n-type while electrons in the n-type are attracted to holes in the p-type material. As a result of the bidirectional diffusion of majority charge carriers across the p-n junction, the n-type material near the junction becomes positively charged and the p-type material negatively charged hence forming a barrier/depletion layer also known as the space charge region (SCR) as shown in figure 5.1. When the barrier layer is fully developed, it induces an internal (in-built) electric field that prevents further exchange of majority charge carriers between the p-type and the n-type layers. At this condition, the Fermi-levels (E_F) in both regions are equal and the junction is said to be in thermal equilibrium [Meyer, 2002; 20]. The in-built electric field is directed from the n- side of the junction to the p- side of the same junction as shown in figure 5.1. V_{bi} in the figure represents the barrier potential associated with the in-built electric field (E field).

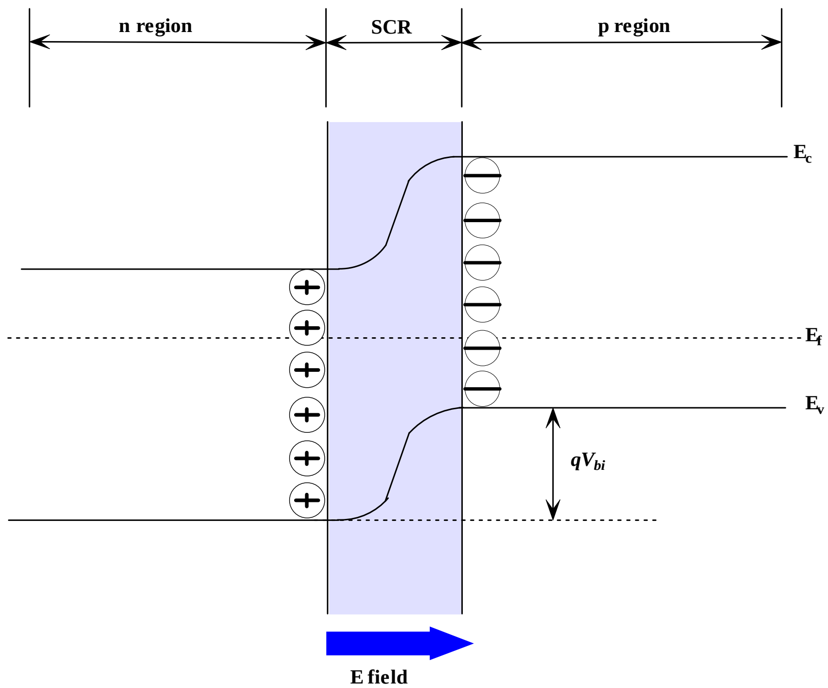

Figure 5.1: Simplified energy band diagram of a p-n junction solar cell in thermal equilibrium. The space charge region (SCR) region is filled with charged donor and acceptor ion cores (not shown) [After Meyer, 2002; 21]

5.2.2 Operation

Every semiconductor material has its own characteristic band gap between the valence band and the conduction band. Valence band represents the allowable energies of valence electrons that are bound to the host atoms while conduction band represents the allowable energies of electrons that have received energy from some mechanisms and are now no longer bound to specific host atoms [Messenger and Ventre, 2000; 298]. It is therefore appropriate to define band gap energy of a semiconductor material as the minimum energy that an electron in the valence band should gain to jump to the conduction band. Likewise an electron in the conduction band should shed energy equal to the band gap energy in order to fall to the valence band.

When a PV cell is illuminated, light photons with energy that is greater or equal to the semiconductor material's band gap are absorbed by the valence electrons. Photon energy is given by:

$$E_{PH} = h\nu = \frac{hc}{\lambda} \tag{5.1}$$

where: h is the Plank's constant;

ν is frequency of the photon;

c is speed of light in a vacuum;

λ is the photon's wavelength.

Once an electron has absorbed a photon with energy higher than the bandgap, it jumps from the valence band to become a free electron in the conduction band leaving behind a vacancy (hole) in the valence band. In effect, absorption of photons leads to the creation of electron-hole pairs (EHPs). The in-build electric field immediately sweeps the generated electrons to the n-side and holes to the p-side. These additional majority charge carriers will cause a current flow in the external circuit or simply result in a voltage at the external terminals of the material in the absence of a complete external circuit. Figure 5.2 shows the operation of an illuminated solar cell. Electrons flow in the external circuit from the n-type material to the p-type material. However, conventionally current is considered as consisting of positive charges (holes) flowing in the opposite direction to the flow of electrons as shown in figure 5.2.

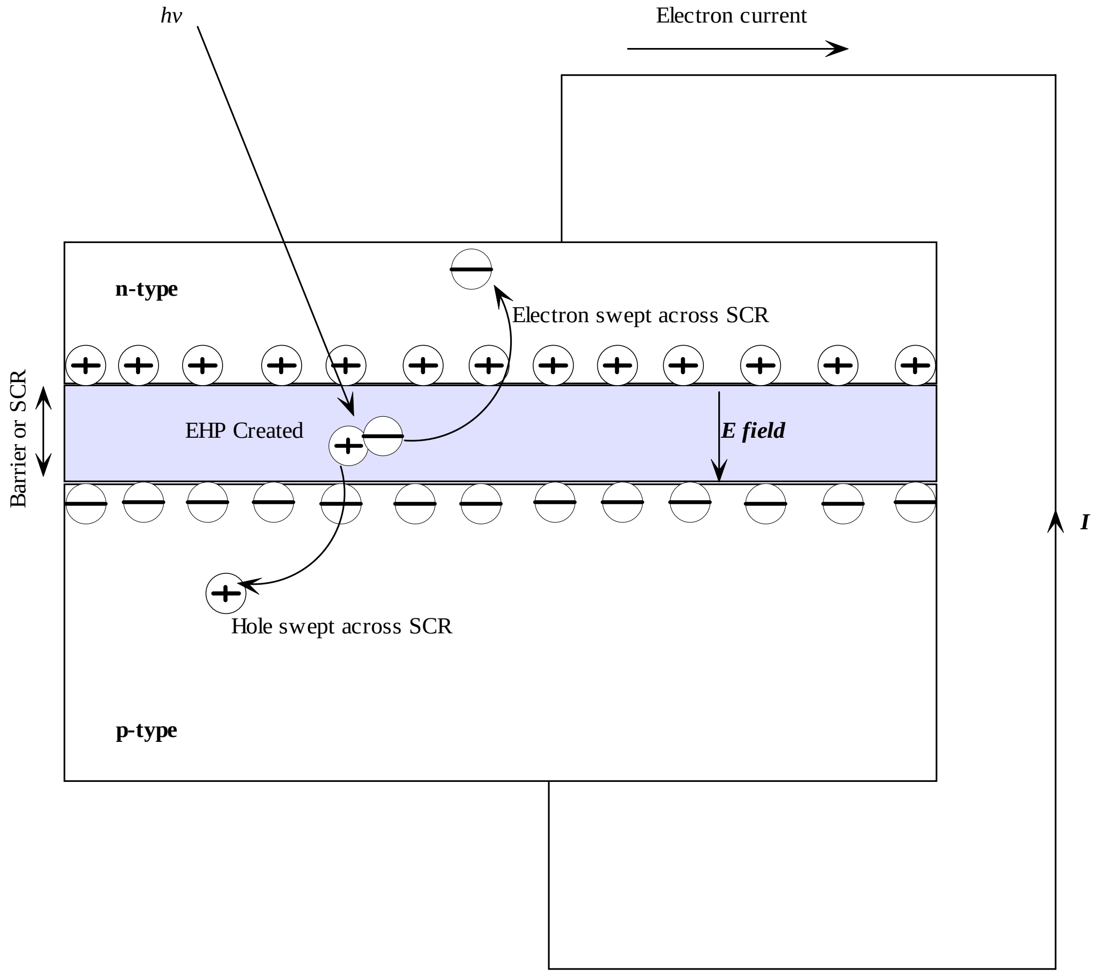

Figure 5.2: Simplified operation of an illuminated solar cell

5.2.3 Electrical characteristics

Clearly, a solar cell is simply a junction diode of large area, forward biased with a photovoltage that is derived from the disassociation of electron hole pairs created by incident photons within the in-built field of the p-n junction barrier [Lasnier and Ang, 1990; 70]. Energy band diagrams for the normal, short-circuit and open-circuit operations of the PV cell are given in figure 5.3 (a), (b) and (c), respectively. Figure 5.3 (d) shows the electrical equivalent circuit for a practical solar cell. R_{sh} and R_s are the shunt and series resistances within the solar cell structure.

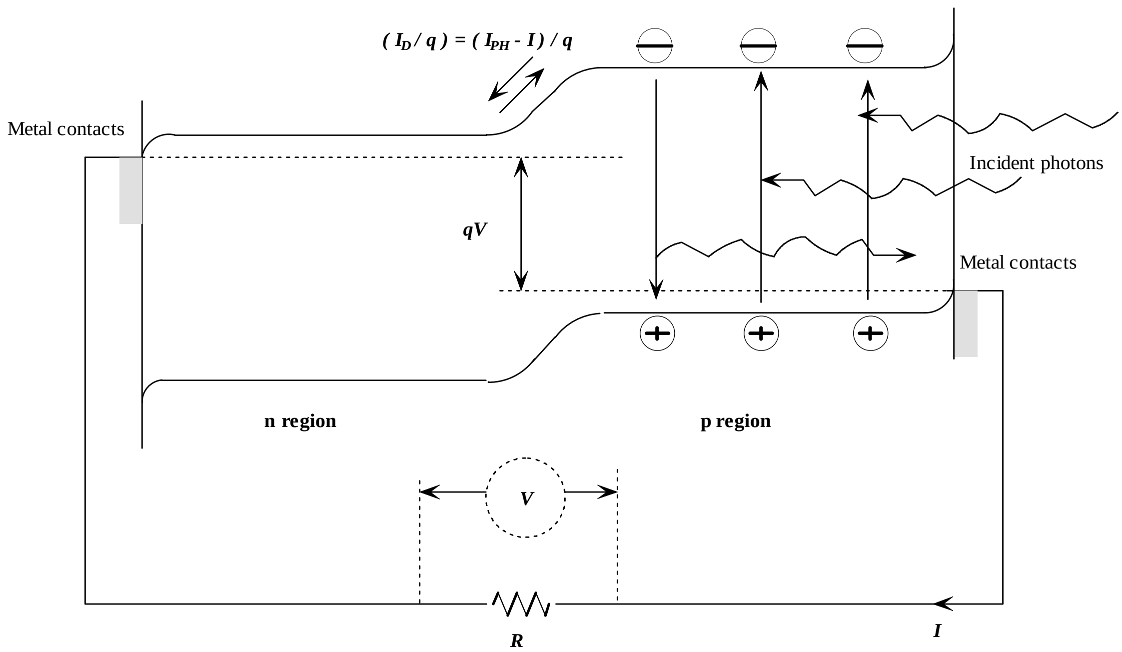
(I_D / q) = (I_PH - I) / q
Metal contacts
Incident photons
qV
Metal contacts
n region
p region
V
R
I

(a)

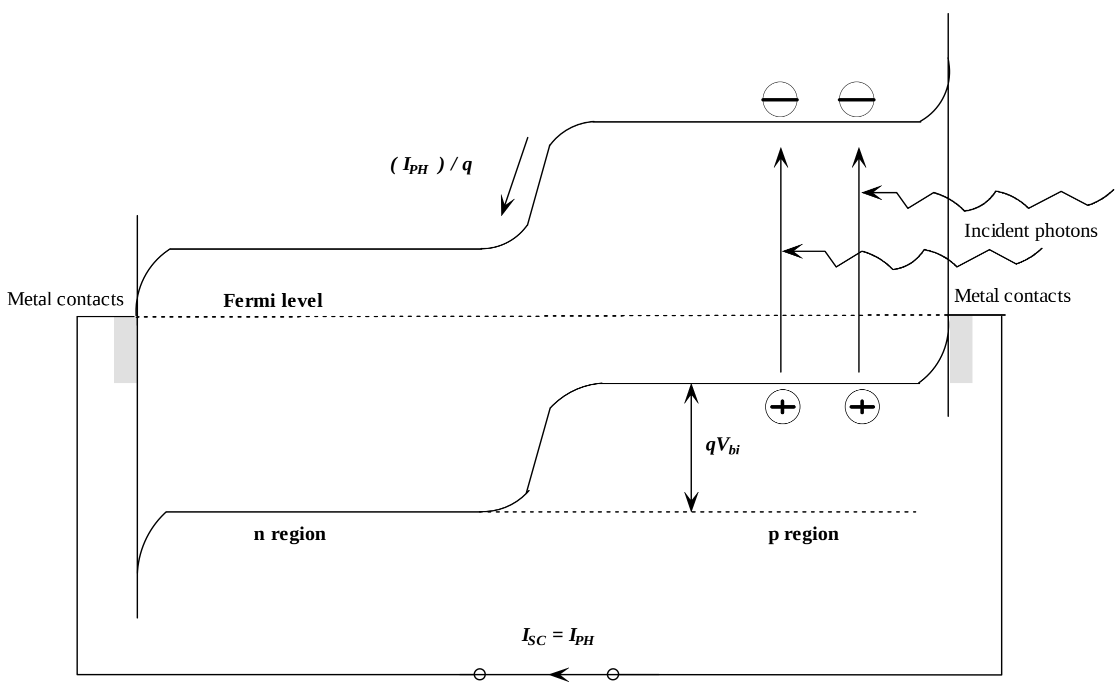
(I_PH) / q
Incident photons
Metal contacts
Fermi level
Metal contacts
qV_bi
n region
p region
I_SC = I_PH

(b)

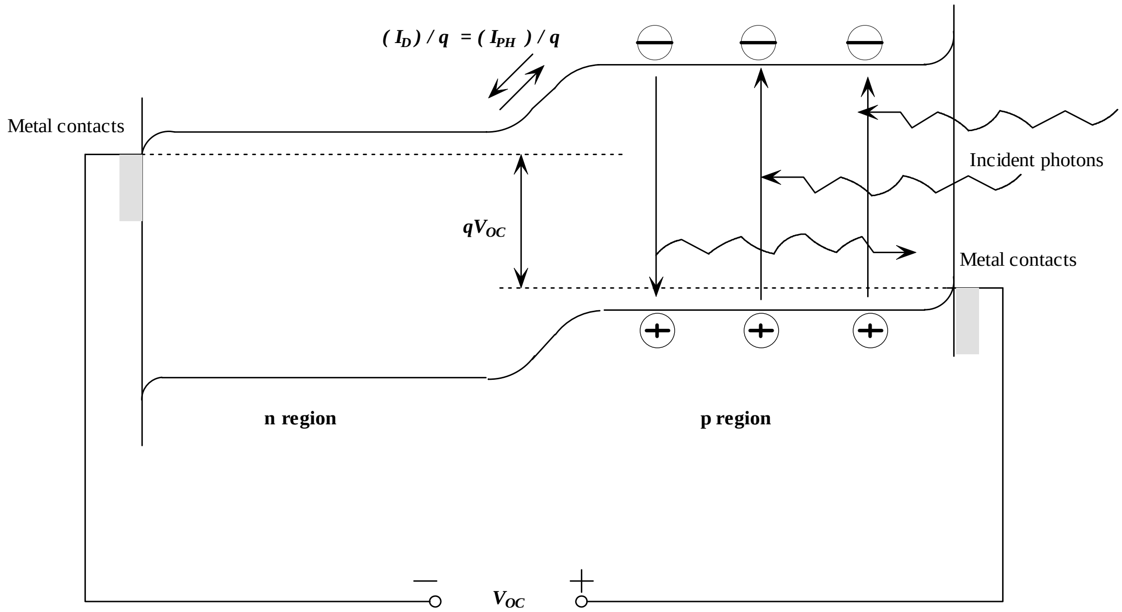

(c)

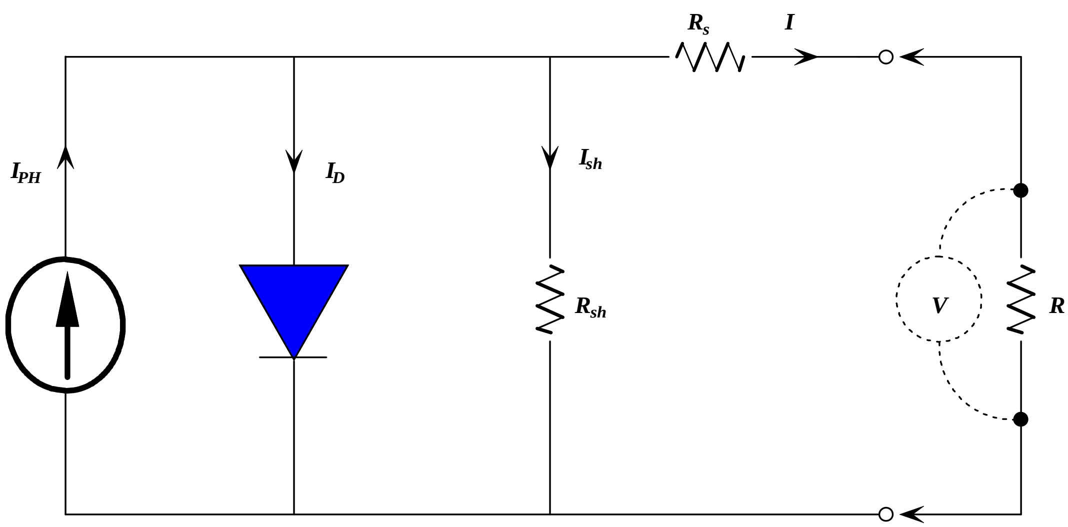

(d)

Figure 5.3: (a) Energy band diagrams of an illuminated p-n junction solar cell in; (a) normal operation (i.e. connected to an external load), (b) short circuit, (c) open circuit condition and (d) equivalent circuit of a practical p-n junction solar cell with parasitic resistances and connected to an external load whose resistance is *R* [Adapted from Meyer, 2002; 22-23]

Shunt resistances provide paths for undesirable current flow and both resistances cause power dissipation within the cell. As a result series and shunt resistances reduce the efficiency of the solar cell.

If, however, the external load resistor is chosen such that the solar cell operates at the maximum attainable voltage and current then the PV cell is said to be at a maximum power operation point since it will deliver the maximum possible power (P_{max}) to the load. Thus:

$$P_{max} = V_{max} \times I_{max} \tag{5.2}$$

and;

$$R_{opt} = \frac{V_{max}}{I_{max}} \tag{5.3}$$

where: V_{max} and I_{max} are the maximum attainable voltage and current, respectively;

R_{opt} is the optimized external load resistance for the maximum power operation of the PV cell.

If the external circuit is simply a conductor connecting the p-type to the n-type material, then the PV cell is operating in the short-circuit mode. Short-circuit current (I_{sc}) can be considered equivalent to the photocurrent, that is, proportional to the irradiance, X (W/m^2) and is given by [Lasnier and Ang, 1990; 71]:

$$I_{sc} = I_{PH} = KX \tag{5.4}$$

where: I_{PH} represents the photocurrent;

K is a constant.

In the absence of a complete external circuit (open-circuit condition), a voltage appears at the external terminals of the PV cell. This voltage, referred to as the open-circuit voltage (V_{oc}), corresponds to the voltage drop across the p-n junction and is given by [Lasnier and Ang, 1990; 72]:

$$V_{oc} = \frac{A k_B T}{q} \ln\left(\frac{I_{PH} - I_0}{I_0}\right) \tag{5.5}$$

where: A is the ideality factor;

k_B is the Boltzmann's constant;

T is the junction temperature;

I_0 is saturation current;

q represents the electronic charge.

Figure 5.4 shows the typical *I-V* curve of a PV module. Also shown in this figure are the maximum voltage (V_{max}) and current (I_{max}), short-circuit current (I_{sc}), open-circuit voltage (V_{oc}) and the maximum power point P_{max}.

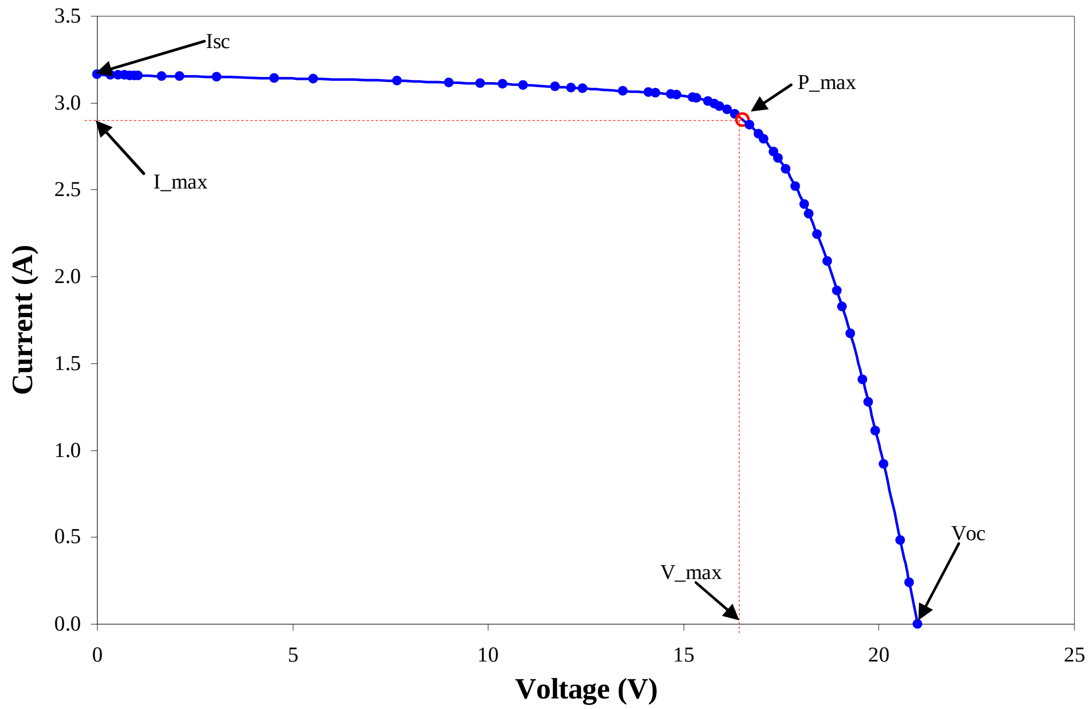

Figure 5.4: Typical I-V curve for a p-n junction solar cell

5.3 EFFECT OF AMBIENT TEMPERATURE

Solar cell efficiency is given by [Fahrenbruch and Bube, 1983; 13];

$$\eta_s = FFI_{sc}V_{oc}/P_{\max} \tag{5.6}$$

where FF represents the cell's fill factor. Ambient temperature and irradiance are related to cell temperature by [Messenger and Ventre, 2000; 48]:

$$T_{cell} = T_{amb} + \left(\frac{NOCT - 20}{0.8}\right)X \tag{5.7}$$

where T_{amb} is the ambient temperature, and $NOCT$ is the Nominal Operating Cell Temperature and X the irradiance. An increase in ambient temperature will therefore, result to an increase in cell temperature.

With irradiance remaining constant as cell temperature increase, minority charge carrier concentration due to thermal excitation [Lesnier and Ang, 1990] increases while the energy band-gap decreases. Open circuit voltage decreases more significantly in response to increase in minority charge carriers than the increase in short circuit current in reply to the decrease in band-gap energy. Consequently maximum available power decreases prompting a decline in efficiency. I_{sc} as a function of temperature, T, is given by [Scott, 1998; 47]:

$$I_{sc}(T) = BT^{\gamma} e^{-E_{G0}/kT} e^{qV_{oc}/kT} \tag{5.8}$$

where: B is a constant independent of temperature;

E_{G0} is the linearly extrapolated zero temperature band gap of the semiconductor;

k is the Boltzmann constant;

T is the semiconductor temperature;

γ includes the temperature dependences of the fundamental parameters determining I_0 and generally has values between 1 and 4 [Green, 1992; 91].

The rate of change of V_{oc} with temperature is given by [Green, 1992; 91]:

$$\frac{dV_{oc}}{dT} = -\frac{V_{G0} - V_{oc} + \gamma(kT/q)}{T} \tag{5.9}$$

where: V_{G0} is the linearly extrapolated zero temperature open-circuit voltage of the semiconductor.

Generally, the decrease in V_{oc} due to temperature is more significant than the increase in I_{sc}, thus P_{max} decreases [Scott, 1998; 47, Meyer and Mapuranga, 2005].

Decrease in efficiency in response to increase in cell temperature at constant irradiance means that the cell will convert less of the energy falling on it. Conversely, increase in efficiency due to a decrease in cell temperature means the module is now converting more of the incident photon energy. It is however not possible to say with certainty whether module power output decreases or increases in response to a given change (a rise or fall) in efficiency since at any instant, module efficiency is simply the ratio of output to input power at that particular time. Surely 11% of 100 W/m^2 is far less than 8% of 1000 W/m^2. This phenomenon is clearly shown in figure 5.5, which is a plot of irradiance (Ps), module output (Pmod) and efficiency (eff.) against time of day. In segment A, module output, irradiance and efficiency are all increasing. However in segment B, module output continues to rise irrespective of the fall in efficiency which shows the presence of other contributing factors. However total energy yield for a given interval shows some relationship with average ambient temperature for the entire interval as will shown in later sections.

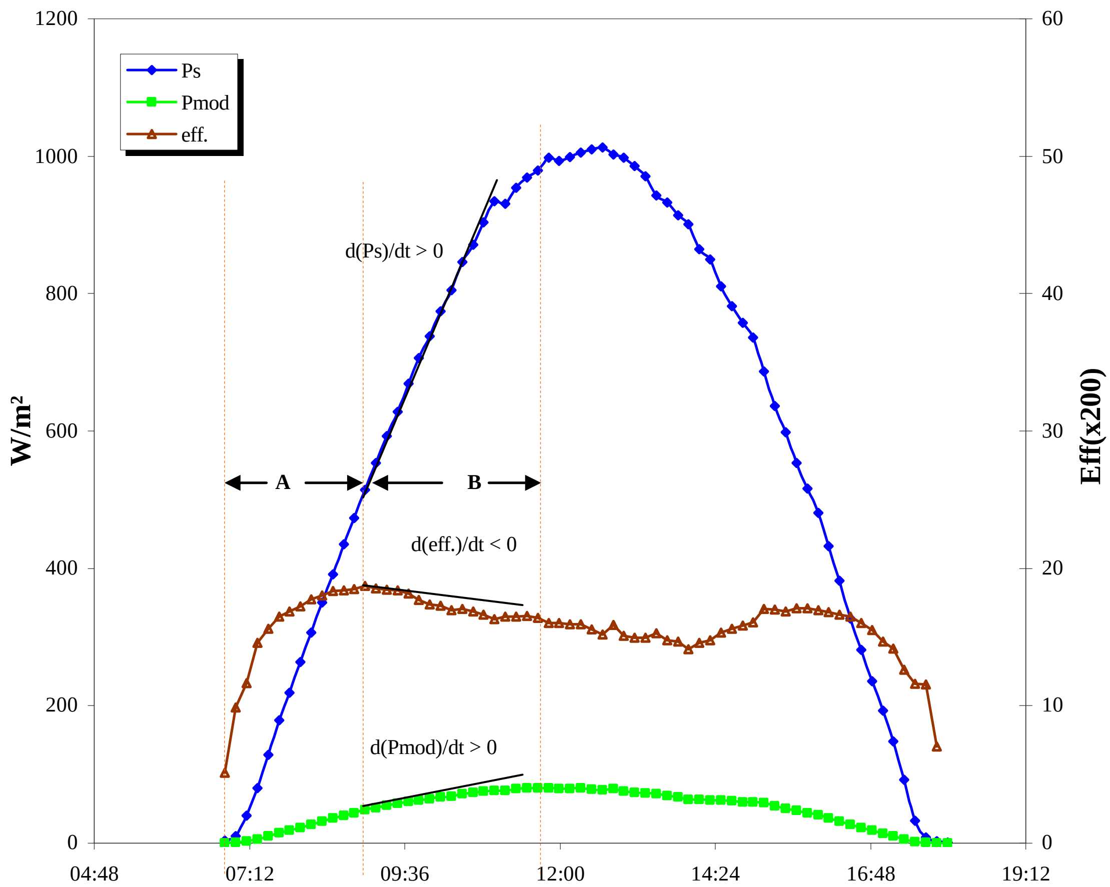

Figure 5.5: Irradiance, module output and efficiency vs. time

5.4 EFFECT OF IRRADIANCE

The effect of irradiance occurs in two contradicting ways. Firstly, increase in irradiance as given by equation (5.7) will increase the cell's operating temperature. Secondly, since the sun imparts energy to the cell in photons, the higher the irradiance the greater the photon flux. Equation (5.10) [van Dyk *et al.*, 2002] relates cell current to level of irradiance. While current increases linearly with irradiance, voltage increases logarithmically as given by equation (5.11) [van Dyk *et al*, 2002].

$$I_{PH} = XI_{PH,1-sun} \tag{5.10}$$

$$V_{oc} = \frac{V_{oc,1-sun}}{1+\delta \ln \frac{1}{X}} \tag{5.11}$$

where δ is a dimensionless coefficient that is solar cell technology specific, $I_{PH,1-sun}$ and $V_{oc,1-sun}$ are the photon current and open-circuit voltage, respectively, at 1000 W/m^2 (1 sun). Equation (5.10) is equivalent to equation (5.4) thus K is equal to $I_{PH,1\text{-}sun}$.

Considering the first case at constant ambient temperature, an increase in cell temperature due to increase in irradiance has exactly the same effect as would an equivalent increase in cell temperature due to increase ambient temperature at constant irradiance. As a result efficiency decreases. Regarding the second case at constant cell temperature, cell output current is given by [Meyer, 2002; 24]:

$$I_{out} = I_{PH} - I_D - I_{sh} \tag{5.12}$$

where I_{PH}, I_D and I_{sh} are the photon current, dark recombination current and shunt current, respectively. Assuming that dark recombination and shunt currents are negligible and equating equation (5.10) to (5.11) we obtain;

$$I_{out} = I_{PH} = I_{sc} \tag{5.13}$$

Substituting equations (5.11) and (5.13) into (5.6) the expression for efficiency is obtained as follows;

$$\eta_s = A^{-1} FFI_{PH,1-sun} \left(\frac{V_{oc,1-sun}}{1-\delta \ln X} \right) \tag{5.14}$$

where A represents the cell aperture area. Clearly from equation (5.14), efficiency, like open circuit voltage has a logarithmic dependence on irradiance at constant cell temperature.

Higher instantaneous irradiance levels usually, but not always, coincide with high module output at that particular instant subject to the instantaneous efficiency. When all else remain constant, total energy production in a given interval is related to irradiation in that entire interval.

5.5 METHODOLOGY

5.5.1 Summary of Modules Evaluated

Spire-Sun, Xenon pulsed solar simulator (SPIRE 240A) was used to test each of the modules under standard test conditions (STC: 1000W/m^2, 25°C cell temperature, AM1.5 global spectrum). Table 5.1 lists the technologies of the four modules used in this study. Also listed are the rated power, STC measured powers and the corresponding STC efficiencies.

Table 5.1: Summary of modules used in the study

Module	Technology	P_{rated} (W)	P_{STC} (W)	η_{STC} (%)
1	Mono-Si	70	69.58	11.40
2	Mono-Si	70	70.73	11.59
3	Mono-Si	70	70.75	11.76
4	Mono-Si	70	69.22	11.34

All four modules performed well within acceptable levels and no obvious cracks or cell defects were observed during a comprehensive visual inspection. The minor differences in STC performances could be attributed to the slight mismatch that was exhibited in the *I-V* curves of these modules.

5.5.2 Experimental Procedure

All four modules were connected into a parallel PV array and mounted on the rack outdoors. The array was connected to the load and battery bank through a 12/24V Tarom 245 pulse width modulation (PWM) Solar Regulator. A data acquisition system (DAS) consisting of voltage and current transducers, computer cards and other accessories was designed and installed.

Type-K thermocouples were used to measure back-of-module temperature (cell temperature) and ambient temperature. For cell temperature measurements, the tip of the thermocouple was placed in contact with the back side of an arbitrary chosen cell on the module. The ambient temperature thermocouple was placed in a well ventilated shaded area to prevent interference from direct sunlight. A pyranometer for measuring irradiance was mounted on the plane-of-array. The pyranometer and thermocouples formed part of the DAS.

The regulator was programmed to operate in voltage regulation mode that allows the user to set end-of-charge voltage. In this case the end-of-charge voltage was set at 14.3 V. This end-of-charge voltage level was optimal since it allowed batteries to be fully charged. Higher voltage levels may easily lead to overcharging and subsequent damage to the batteries. The system was left to run in a “free mode” in which only the regulator was in control. This meant that the load could run and the battery could charge for as long as the regulator could allow.

At every ten-minute intervals the DAS recorded current, voltage, irradiance and temperature data writing it to an external text file in computer memory.

5.5.3 Quantifying effect of regulation

The normal operation of a regulator in a PV power system protects the battery bank by ensuring safe charging and discharging of the battery. Safe charging means; controlled rate of charging and end-of-charge detection upon which charging current is terminated. Likewise, safe discharging implies; controlled discharge rates and end-of-discharge detection upon which the system load is disconnected. Exceedingly deep discharge and over-charging is detrimental to satisfactory battery operation and will ultimately reduce battery life. Notwithstanding the advantages, a regulator tends to prevent modules from reaching maximum power point by clamping the voltage to a level (V_{reg}), in this case 14.3 V, that is lower than rated voltage at maximum power point ($V_{\max}$) [Meyer and Mapuranga, 2005].

A wide range of regulators using different regulation techniques are currently commercially available. Different regulators will affect module power production in different ways. The less advanced the regulator the easier it is to quantify the effect of regulation on power production. The reason for this is that less advanced regulators simply disconnect the modules when end-of-charge point is detected. As such the DAS will record a drop in module power until charging resumes. Figure 5.6 shows this kind of effect. The shaded area in the graph represents power loss due to regulation.

On the other hand, advanced regulators have the capability of dissipating excess module power output using complex internal circuits. This means that such regulators will not disconnect the modules at end-of-charge and therefore the DAS will continue to record normal regulated module output even though this output is being dissipated within the regulator itself. In some instances if the load is connected, the regulator simply throws the batteries into standby mode while the load is powered directly by the module output. Once again in this case the DAS will record normal module output at regulated voltage.

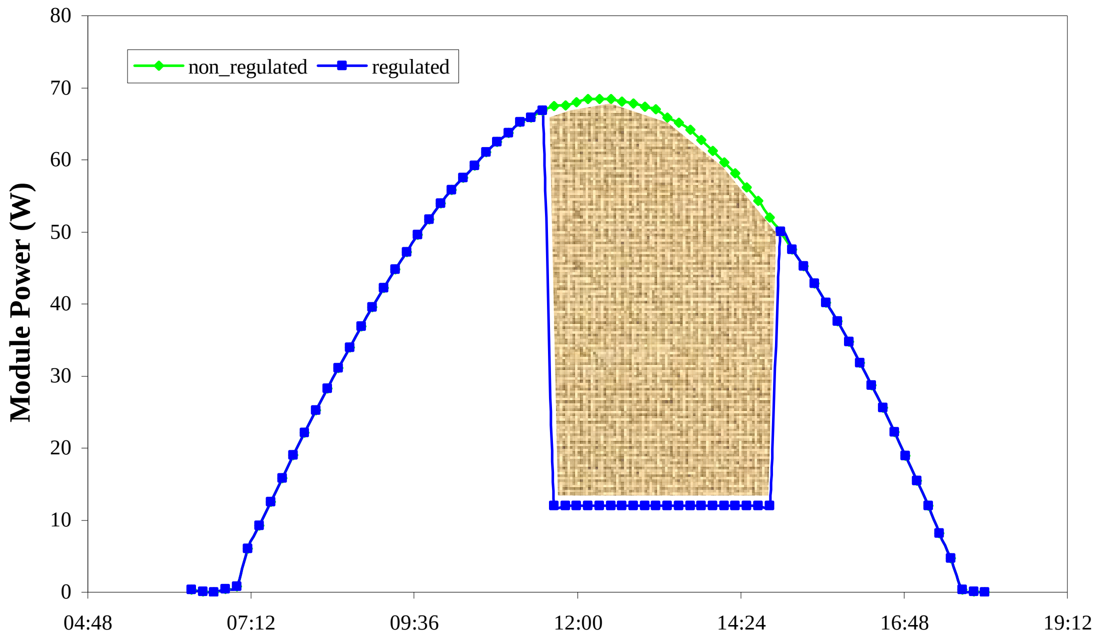

Figure 5.6: Effect of regulation on module due to less advanced regulation techniques

It is therefore clear in these cases that quantifying the effect of a regulator on module power production can not be easily done as in the case of less advanced regulators.

The regulator used for the University of Fort Hare (UFH) system uses the PWM in which charging is done at constant voltage and a tapering charging current that depends on the charging needs of battery. With PWM, charging current is not completely terminated at full charge, instead short current pulses are constantly supplied to the battery in order to retain it at full charge while the load is powered directly from the module output.

Figure 5.7 shows the I-V characteristics for the four PV modules in the array. V_{reg} was the preprogrammed end-of-charge voltage while $V_{\max}$ was the rated voltage at peak production which was the same for all four modules. Clearly from the figure, the impact of regulation on current is far less significant than the impact on voltage. However this analysis was done at a single STC irradiance level. P_{max} is known to vary with irradiance and so do V_{max} and I_{max}.

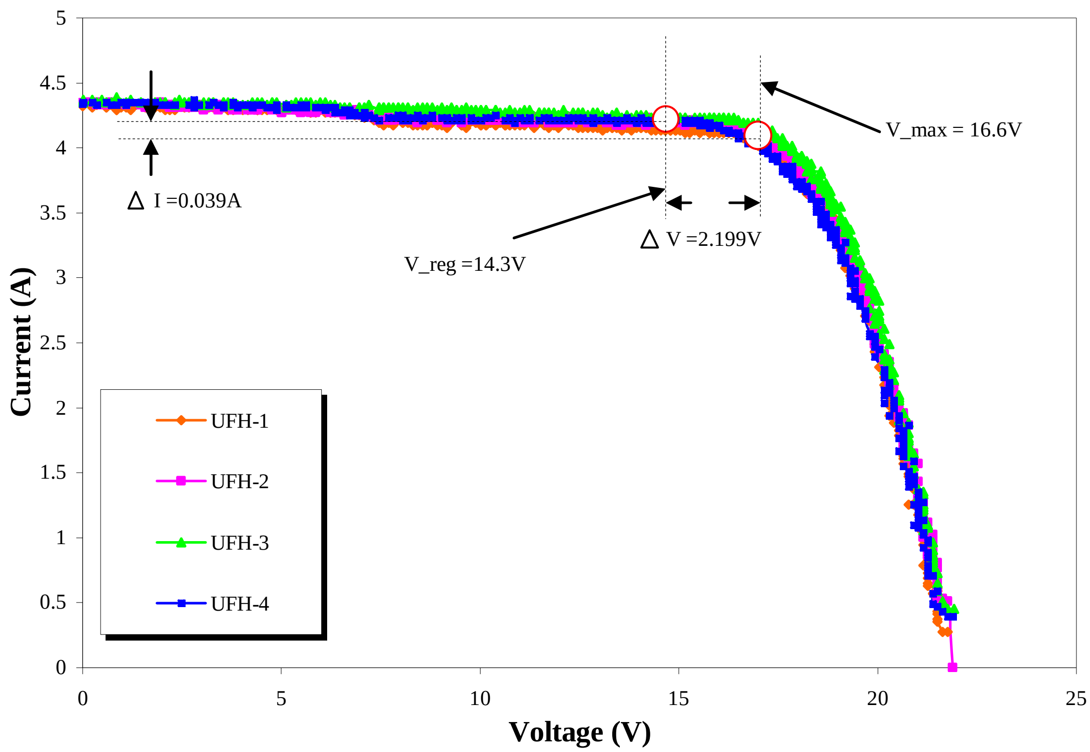

Figure 5.7: Operating power point at regulated voltage compared to P_{max} for the PV array

Figure 5.8 shows simulated *I-V* curves at different irradiance levels. The curves were simulated using PVSIM software. Accordingly, P_{max}, V_{max} and I_{max} are varying with irradiance. Table 5.2 is derived from figure 5.8 and gives the values of P_{max}, V_{max} and I_{max} for every irradiance level. Also given are ΔV_{max} and ΔI_{max} which represent the positive percentage difference between any two successive maximum voltages and currents, respectively. On average, V_{max} changed by 2.4% while current changed by 328% between 250W/m^2 and 1000 W/m^2.

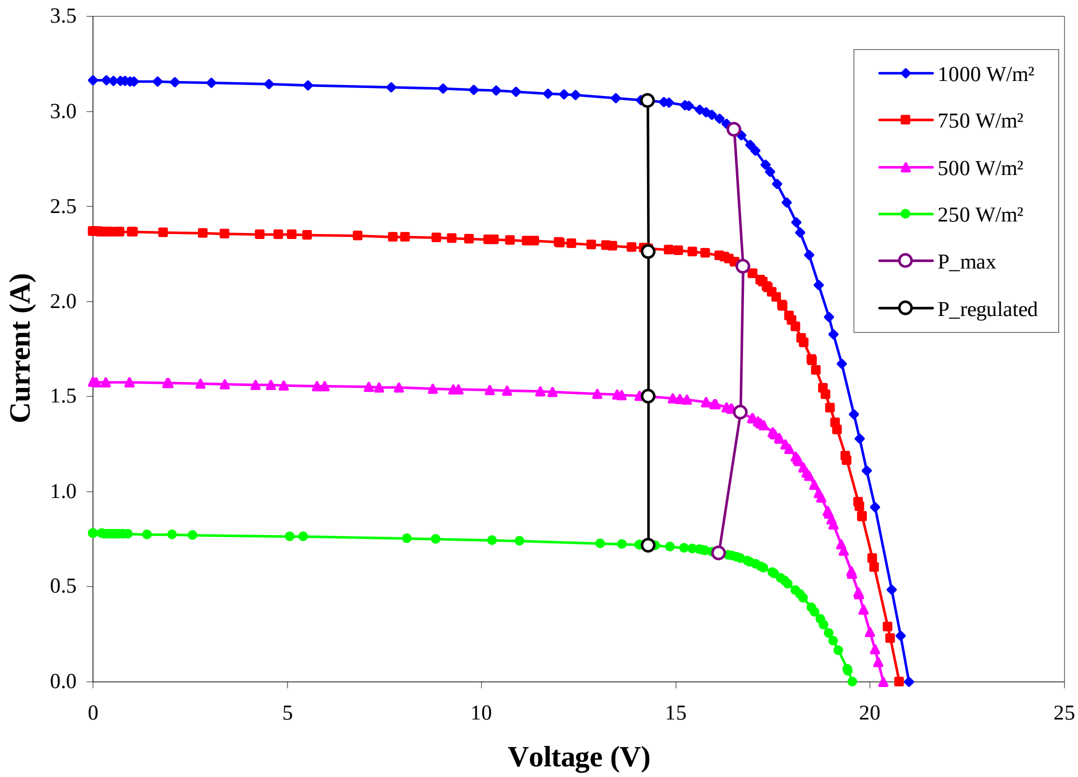

Figure 5.8: Simulated *I-V* curves for varying irradiance levels showing maximum and regulated power points

Table 5.2: Maximum power, voltage and current at varying irradiance levels

Irradiance (W/m^2)	P_{max} (W)	V_{max} (V)	I_{max} (A)	ΔV_{max} (%)	ΔI_{max} (%)
250	10.9191	16.1073	0.6779	-	-
500	23.6275	16.6626	1.4180	3.4	109.2
750	36.5372	16.7249	2.1846	0.3	54.1
1000	47.9339	16.5090	2.9035	1.3	32.9

Table 5.3: Comparison of V_{max} and I_{max} with corresponding V_{reg} and I_{reg}

Irradiance (W/m^2)	V_{max} **(V)**	V_{reg} **(V)**	ΔV **(%)**	I_{max} **(A)**	I_{reg} **(A)**	ΔI **(%)**
250	16.1073	14.2962	13.5	0.6779	0.7180	5.9
500	16.6626	14.2990	14.5	1.4180	1.5001	5.8
750	16.7249	14.2991	14.2	2.1846	2.2617	3.5
1000	16.5090	14.2844	11.2	2.9035	3.0570	5.3

Table 5.3 gives V_{max} and I_{max} and the corresponding regulated voltages (V_{reg}) and currents (I_{reg}) for every irradiance level in figure 5.8. In the table, ΔV represents the positive difference between a given pair of related non-regulated and regulated voltages expressed as a percentage of the non-regulated one. Likewise, ΔI represents the difference between related non-regulated and regulated currents expressed as a percentage of the non-regulated one. Clearly from the table, regulation has a greater effect on voltage than current.

In order to quantify, with relative ease, the effect of the regulator on module power production, three important assumptions are in order. Two of the three assumptions are based on the two tables (5.2 and 5.3). Firstly, it is assumed that the system load is optimal and thus will allow modules to operate at P_{max} throughout the day. Secondly, from table 5.2, it is assumed that the daily variation of irradiance from sunrise to sunset has negligible effect on V_{max}, thus, modules are considered to be operating at almost the rated V_{max} throughout the day. It is clear from table 5.3 that regulation results in a 5% average increase in output current accompanied by 13% average decrease in operating voltage. However, it is this decrease in voltage that results in an overall decrease in module power output when operating in regulated systems.

In order to arrive at the non-regulated profile, the three assumptions explained earlier were used. In summary, the assumption is that modules could have produced the same current profile while operating at almost the rated maximum voltage if it were not for the regulator. Figure 5.9 shows the approximate profile for the non-regulated case as well as the actual recorded profile, which is the regulated profile. The shaded area in the graph represents the energy loss due to regulation.

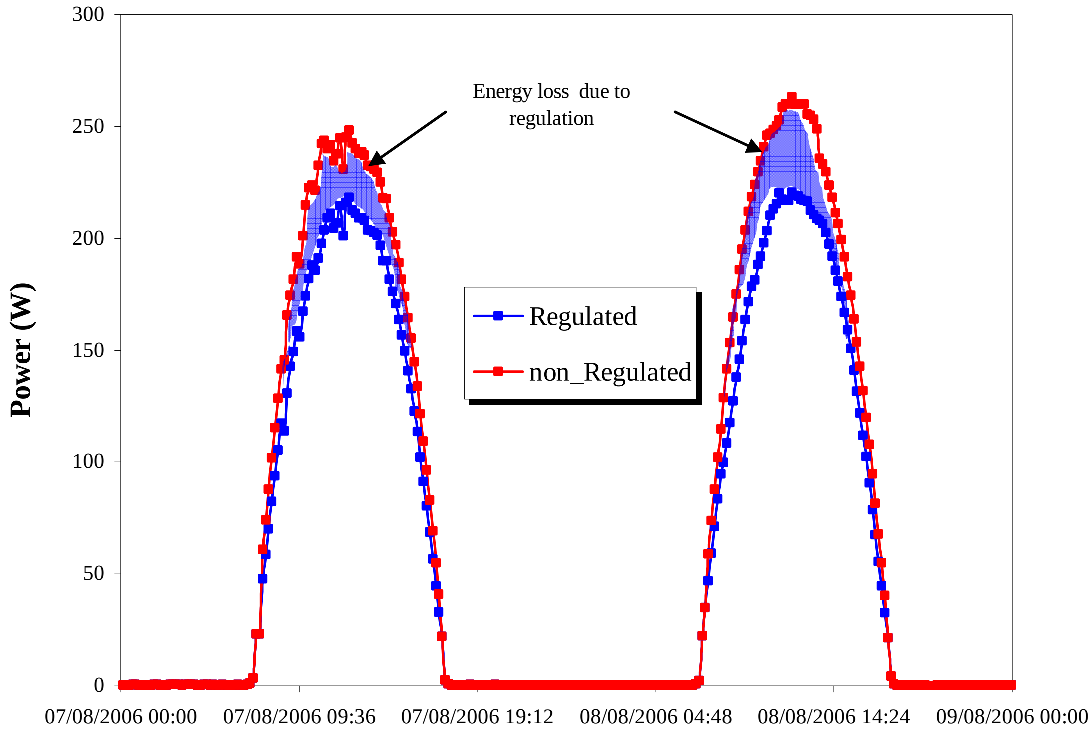

Figure 5.9: Recorded module daily power output under regulation and the expected profile in the absence of regulation

5.6 RESULTS AND DISCUSSIONS

5.6.1 Efficiency

Figures 5.10(a)-(d) compare efficiency of the PV array in response to instantaneous solar irradiation, ambient temperature and cell temperature on four randomly selected days.

It is evident from all the figures that efficiency generally will first increase with increase in irradiance. This phenomenon can be explained in terms of ambient temperature and irradiance increase. Increase in irradiance causes an increase in efficiency while increase in temperature results in a drop in efficiency (refer to sections 5.3 and 5.4). Initially (morning to mid-morning period), increase in efficiency due to irradiance is more than the decrease due to the rising temperature, hence the net effect will be an increase of efficiency. As the day temperature rises, its effect on efficiency becomes more significant, which explains the rate of increase of efficiency that is slowing down as time approaches mid-morning. Between mid-morning and mid-day, the effect of temperature on efficiency is more than that of irradiance, hence there is an overall decline in efficiency. As temperature starts to drop after mid-day, efficiency will slowly begin to rise as well.

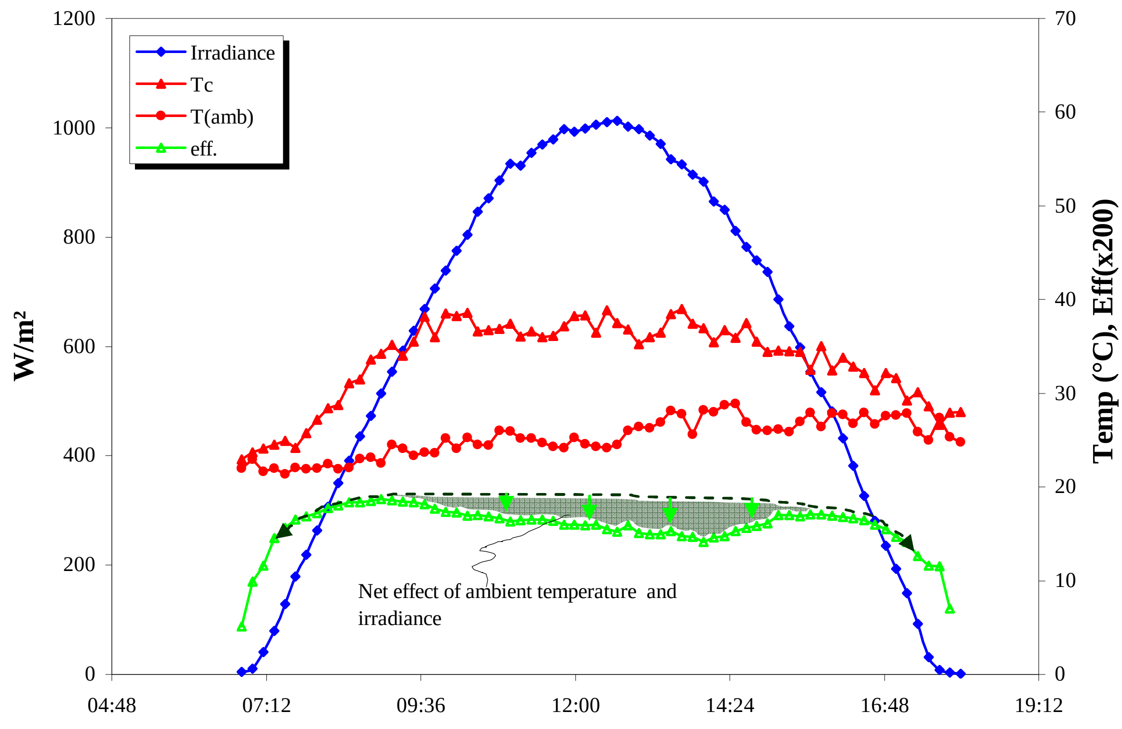

Figure 5.10 (a): Efficiency, irradiation and temperature vs. time on August 11, 2006

During this time, irradiance begins to fall resulting in a decline in efficiency. Initially this decline is less significant than the increase caused by the temperature but it becomes more significant as irradiance continues to fall. As a result efficiency continues to rise at a slowing down rate until such point when effect of irradiance matches that of temperature. Beyond this point efficiency generally drops with falling irradiance.

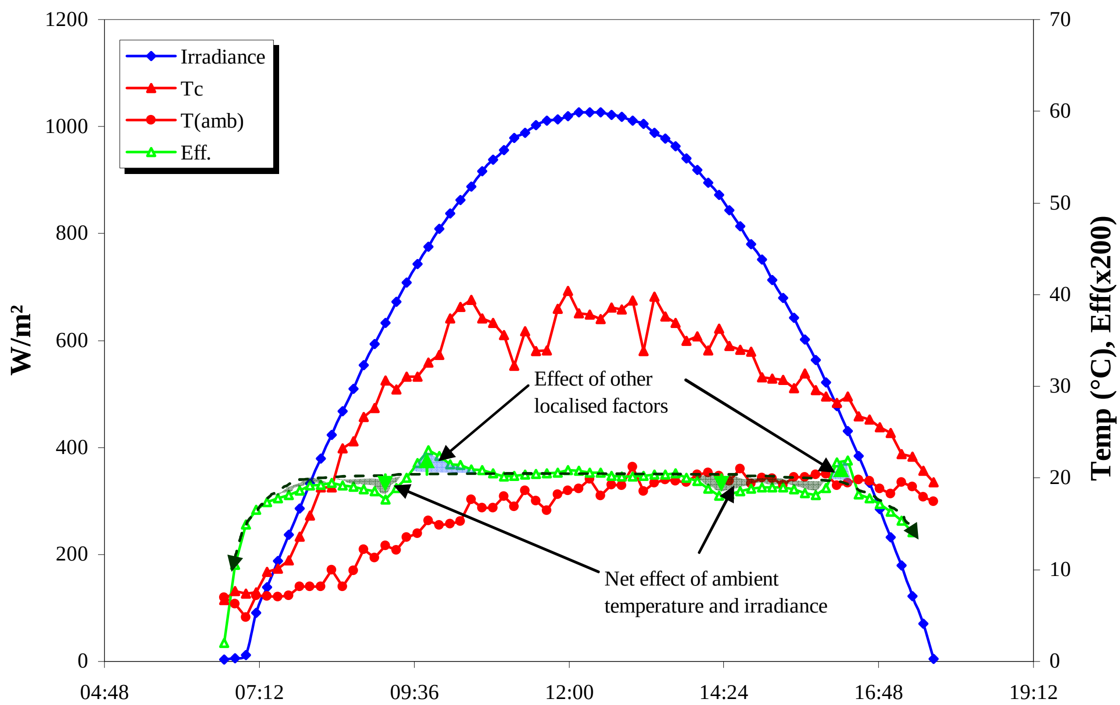

Figure 5.10 (b): Efficiency, irradiation and temperature vs. time on August 13, 2006

Figures 5.10 (c) and (d) show efficiency not gradually rising with rise in irradiance after sun-rise, instead efficiency slightly fluctuates at a low value as irradiance rises. A sudden increase to a high value close to its morning peak is then observed. Upon further investigation, it revealed that the jump in efficiency was caused by the seasonal shift in position of sun-rise. The days in figures 5.10 (c) and (d) fall under winter when the solar position of sun-rise is more northerly and with the modules facing north, the sun shines directly on the modules at the same time as it shines on the pyranometer. In comparison, the days in figures 5.10 (a) and (b) coincide with the beginning of summer when the position of sun-rise has shifted southwards resulting in early morning frame shading.

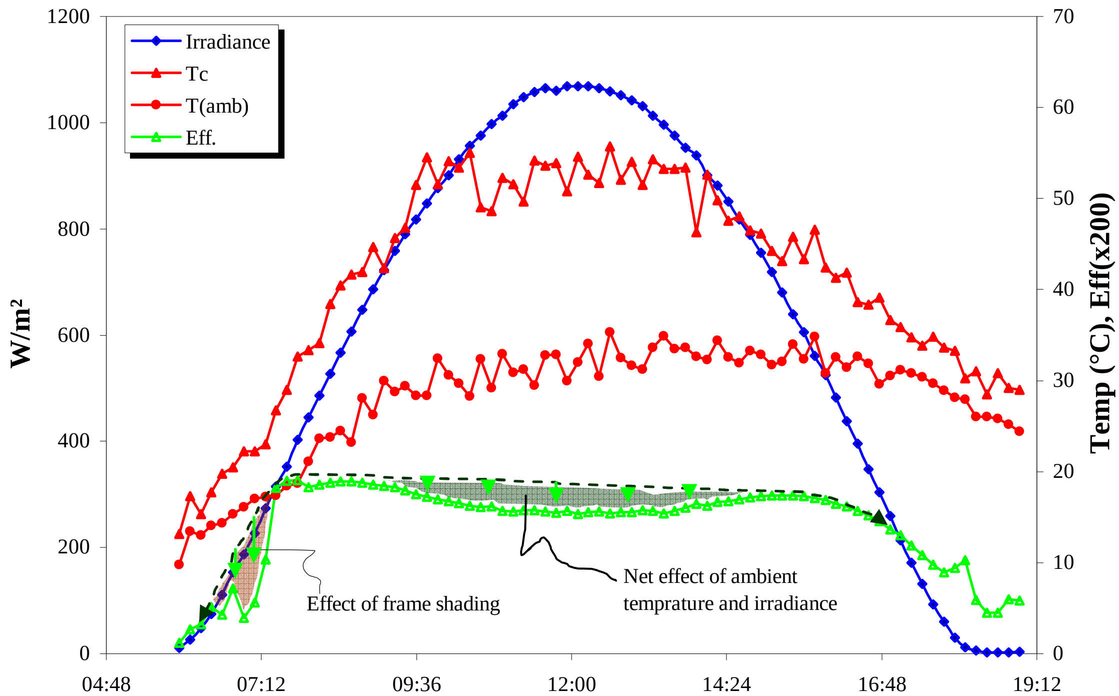

Figure 5.10 (c): Efficiency, irradiation and temperature vs. time on September 28, 2006

The effect of this frame shading is discussed in section 5.6.4. Data collection is done at ten minutes intervals which are long enough for a considerable change in the position of the sun in the sky, hence the sudden jump.

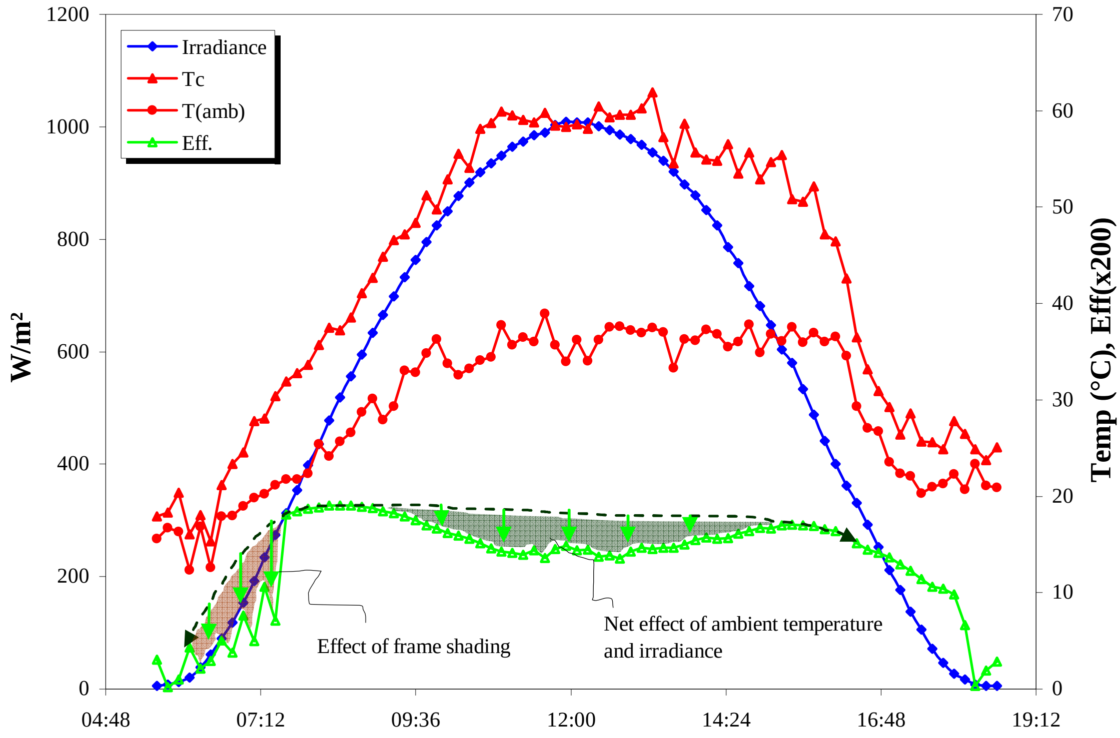

Figure 5.10 (d): Efficiency, irradiation and temperature vs. time on September 29, 2006

Table 5.4: Total irradiation, average ambient temperature and efficiency for each of the four days portrayed in figure 5.10

Day	Date	Total Irradiation (Wh/m^2)	Average Ambient Temperature (°C)	Average Efficiency (%)
1	11/08/2006	6720.9	25.2	8.1
2	13/08/2006	7182.4	16.0	9.9
3	28/09/2006	7834.3	28.1	8.1
4	29/09/2006	7204.2	29.3	7.7

Day 3 received 16.7% more irradiation than day 1 but on both days modules recorded equal average efficiency levels of 8.1%. This attributed mainly to frame shading losses experienced on day 3. Due to frame shading in the morning of day 3, module efficiency is kept at unnecessarily low levels while irradiance level is rising. These low efficiency values will bring the daily average efficiency down.

Days 2 and 4 received almost equal total irradiation, but, day 2 recorded higher efficiency than day 4. This was primarily due to the large temperature difference between the two days. Day 2 was favorably cooler than day 4, hence the modules were able to convert most of the incoming energy from the sun.

5.6.2 Total energy production

Figure 5.11 shows the relationship between two of the outdoor environment factors (ambient temperature and irradiance) on total energy produced by the module. Even though there is a 21.8 Wh/m^2 irradiation difference between day 2 and 4, the difference in output is almost eight times larger that the irradiation difference. This is a direct contribution of low day temperatures on day 2. Average temperature on day 4 was over 80% more than that of day 2. It is generally apparent from figure 5.11 that modules perform better during clear, sunny and cool days than clear, sunny and hot days.

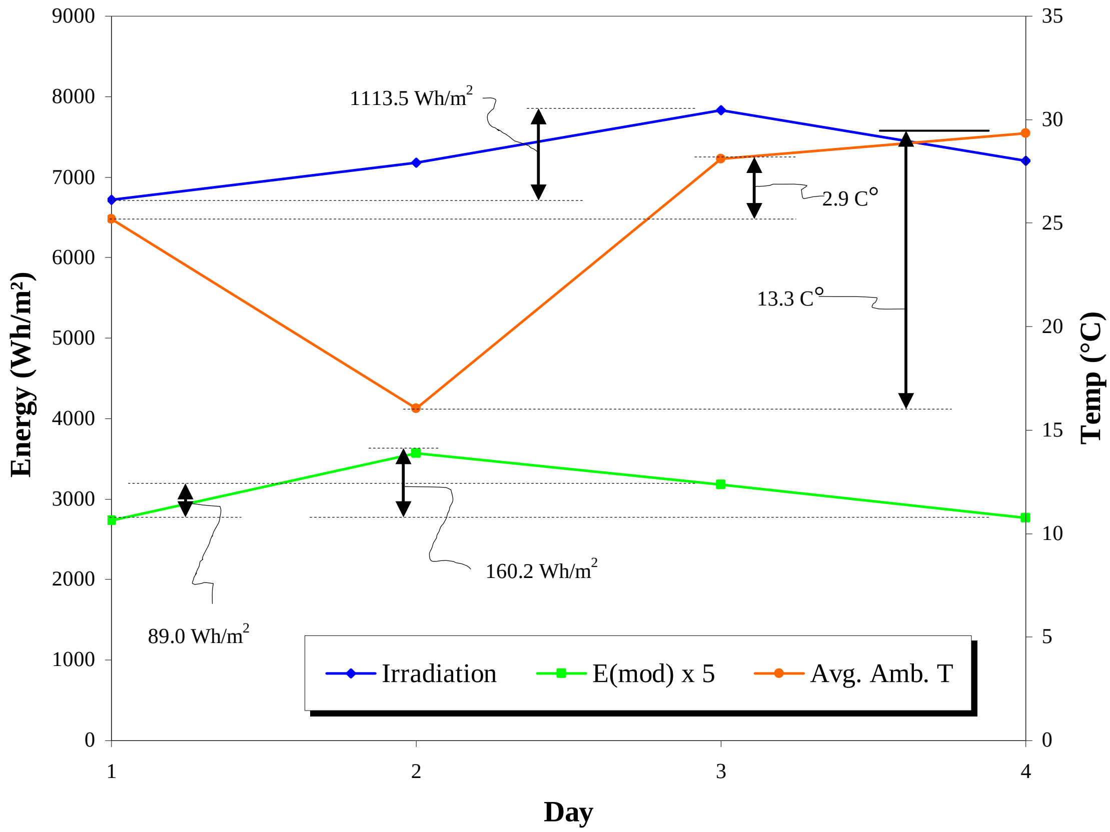

Figure 5.11: Relationship between daily irradiation, average ambient temperature and total daily energy yield

5.6.3 Effect of regulation

Figure 5.12 shows the total regulated (measured) energy yield and the corresponding approximate yield for the non-regulated case on 27 randomly sampled days. Percentage ΔE given in figure 5.11 was calculated as follows:

$$\%Difference = \frac{E_{non-regulated} - E_{regulated}}{E_{non-regulated}} \times 100\% \qquad (5.15)$$

It was found that on average the regulation process resulted in 15% loss of energy. As such regulation losses become more severe and costly during cool sunny days when the modules tend to perform better.

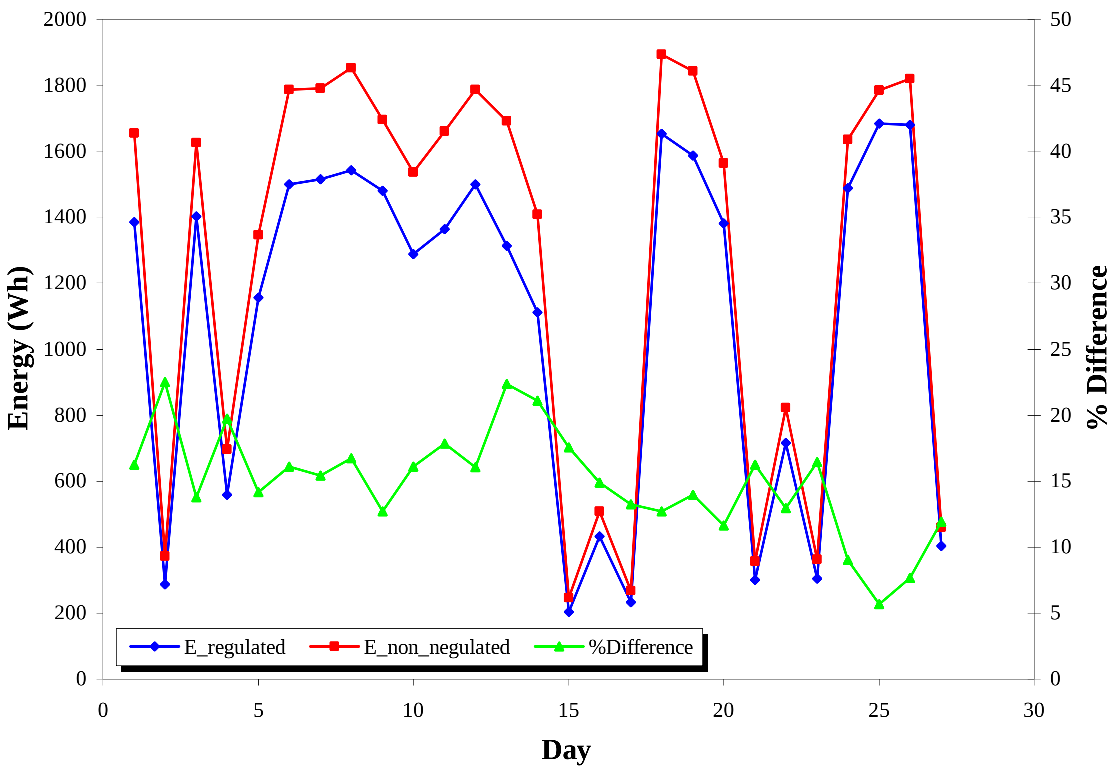

Figure 5.12: Regulated and non-regulated energy yield on 26 randomly selected days

5.6.4 Effect of frame shading

Figure 5.13 shows the array power profile on September 28, 2006. Shaded cells do not generate power; instead they behave like resistors and sink current (dissipate power). As a result module output will be lower than what it should be. The effect of shading is to degrade module performance [Simon, 2005; 97]. Figure 5.14 shows a photograph taken on the morning of September 28, 2006 at 05h33. Module frame shading can be observed in the photograph.

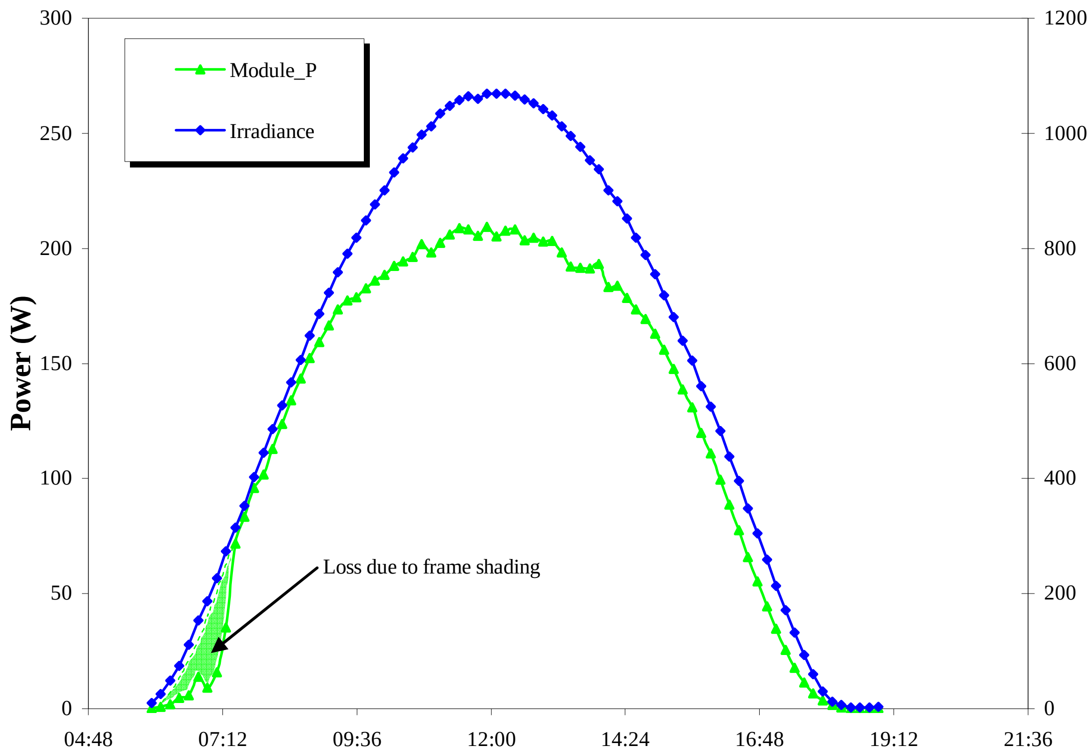

Figure 5.13: Effect of frame shading on module production

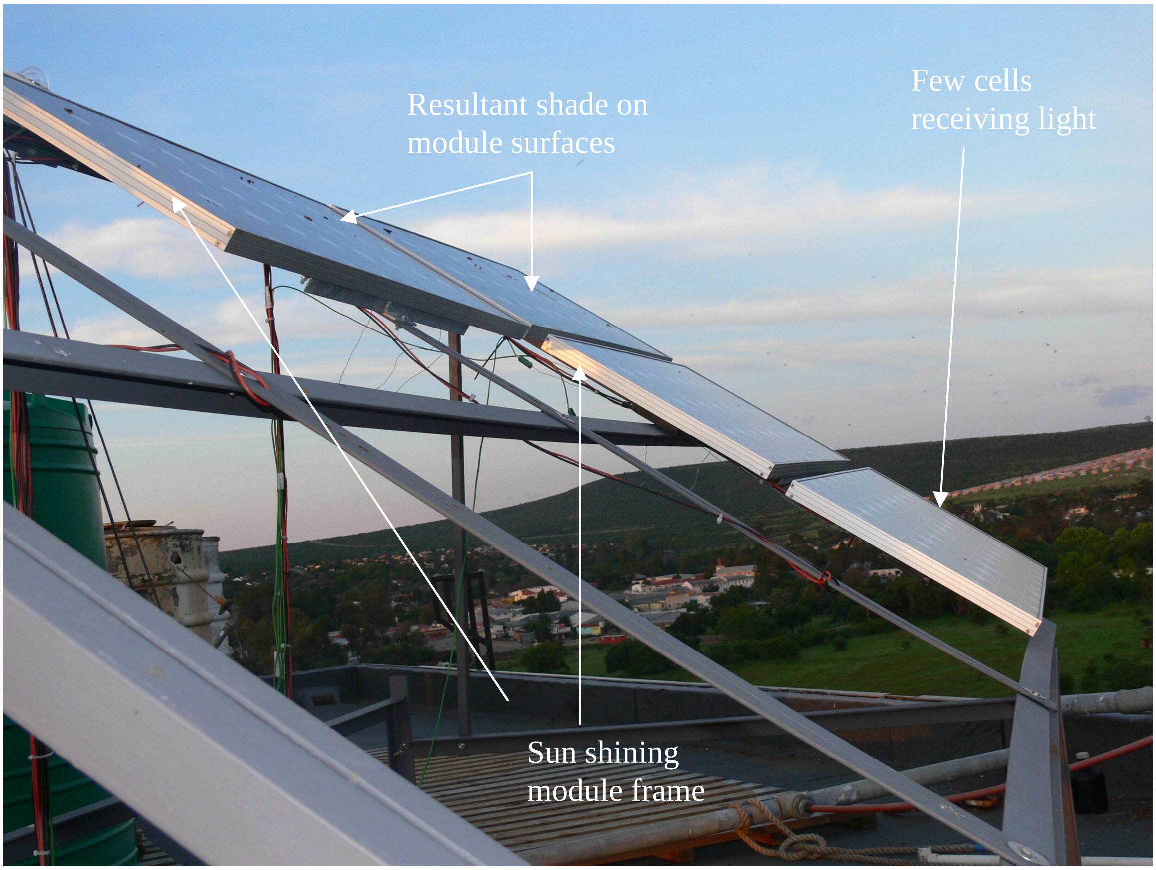

Figure 5.14: Evidence of module frame shading on the morning of September 28, 2006 as a result of the seasonal solar path migration

5.6.5 Effect of Bird Droppings

Bird droppings on surfaces of outdoor-mounted modules may cover the entire cell area or just parts of the PV cells in the module. As a result the covered cell will produce less power. Cells producing less power will be forced to sink current and as a result they heat up forming hot spots on the module. Module power output ultimately decrease as cells obscured by bird droppings will be inefficient.

Figure 5.15 shows the photograph of one of the modules, used in this study, while operating outdoors. Bird dropping can be seen from this photograph. An Infrared Thermography of the same module is shown in figures 5.16 (a) and (b). In figure 5.16 (a) cell areas covered by bird droppings are clearly hotter than the rest. This is supported by the temperature profile, shown in figure 5.16 (b), taken along line 1 (Li1) in figure 5.16 (a).

Figure 5.15: Bird droppings on module surface

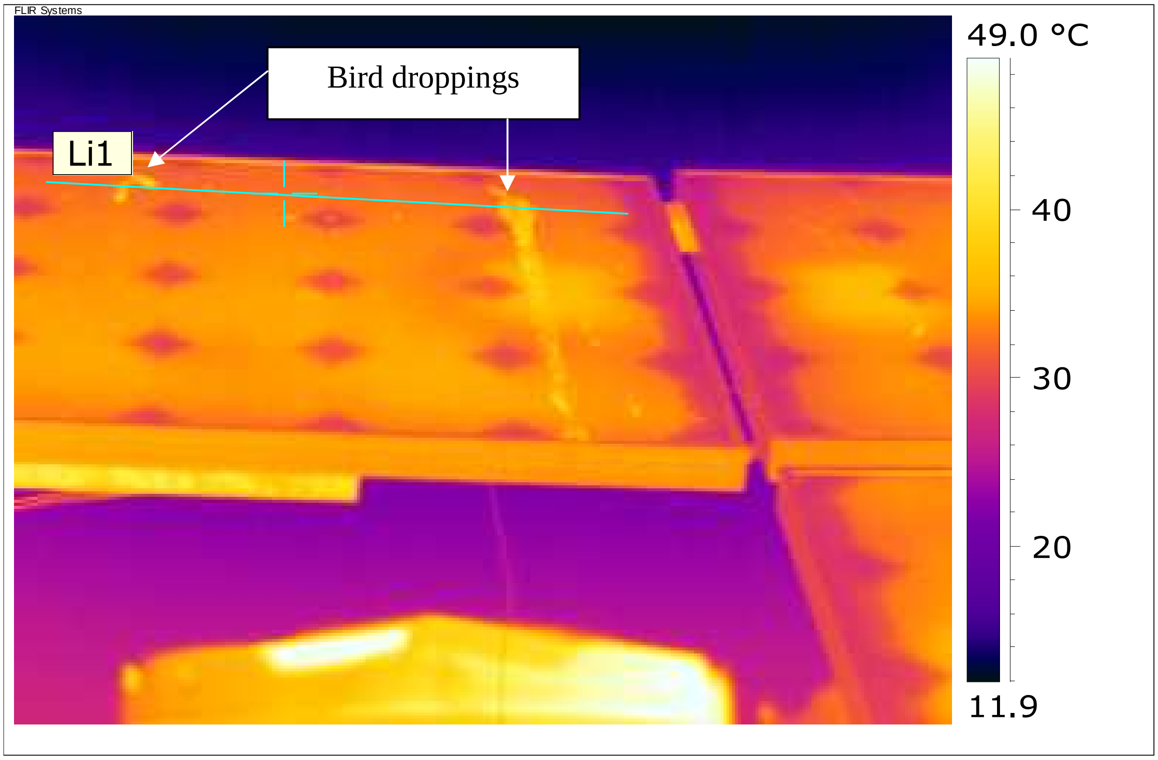

(a)

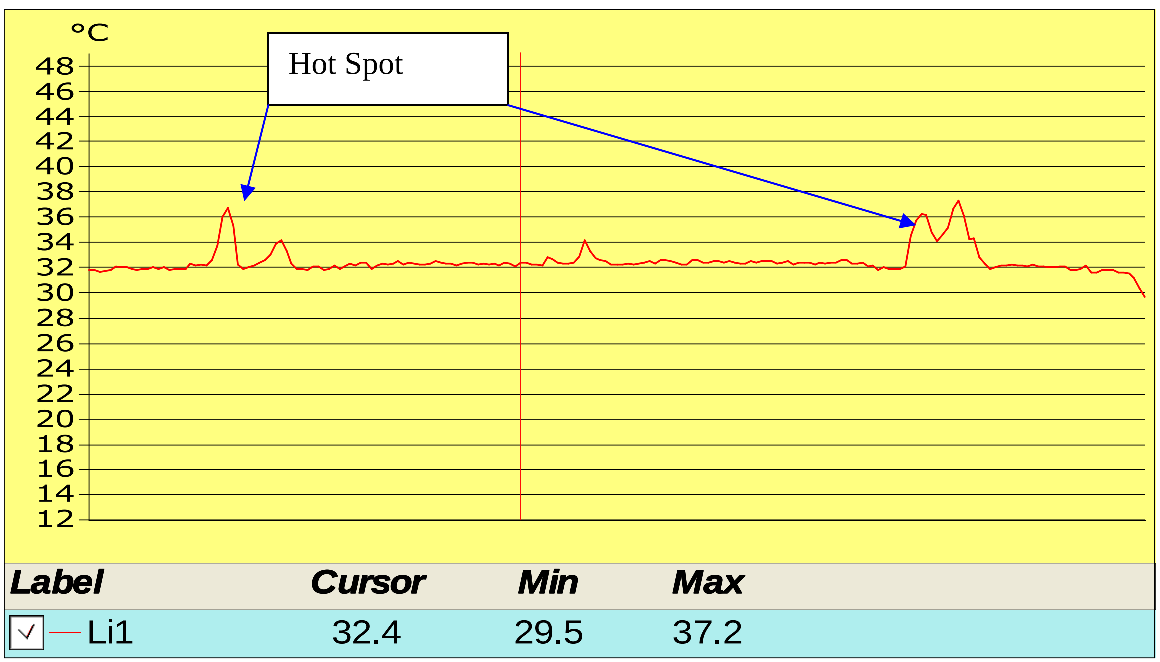

(b)

Figure 5.16: (a) Image of module in figure 5.15 showing hot spots due bird droppings, (b) Temperature profile along line 1 (Li1) in figure 5.16 (a)

5.7 SUMMARY AND CONCLUSIONS

It has been shown that modules mounted outdoors are exposed to more adverse conditions than STC conditions used to rate them. Module outdoor performance in response to concurrent change in irradiance and cell temperature has been presented and discussed. Total daily energy output is directly proportional to total daily solar input and inversely proportional to the average ambient temperature. This means for the same number of sunshine hours per day, total output is more on cooler sunnier days than hot less sunny days. However, this is by no means, a *rule of thumb* since it was also shown in this chapter that days with lower solar yield may in turn yield more output than days with high solar yield, owing this to their favourably low ambient temperature. In that regard, the chapter has proved the need for module performance outdoor modeling that takes into consideration all concurrently changing outdoor environment variables.

It was also shown that regulation does have an effect on the output of the modules regardless of how advanced the regulation technology being applied is. This is derived from the mere fact that regulators force modules to operate at lower regulated voltages than the modules' voltages at maximum power operation. However this subject requires further probing as there are plenty of regulation technologies available commercially. Modules operating outdoors should be maintained as clean as possible in order to prevent bird droppings from accumulating on surfaces resulting in hot spot formation and overall degradation of the PV modules.

5.8 REFERENCES

Bücher K., G. Kleiss, and D. Bätzner (1998), "Photovoltaic Modules in Buildings: Performance and Safety", Renewable Energy Journal; **15**; 545-551.

Crompton T. R. (1990), “Battery reference book”, Butterworths, London.

Fahrenbruch A. L. and R. H. Bube (1983), “Fundamentals of solar cells, Photovoltaic solar energy conversion”, Academic Press, New York.

Lesnier F, T. G. Ang (1990), “Photovoltaic engineering handbook”, Adam Hilger, New York.

Linden D. (1984), “Handbook of batteries and fuel cells”, McGraw-Hill, New York.

Messenger R., J. Ventre (2000), “Photovoltaic system engineering”, CRC Press, London.

Meyer E. L. (2002), *On the Reliability, Degradation and Failure of Photovoltaic Modules*, PhD-thesis, University of Port Elizabeth.

Meyer E. L. and B. Mapuranga (2005), “The Effect of Temperature on the Performance of Photovoltaic Modules at Regulated Voltage”, 15th PVSE Conference, Shanghai, China.

Meyer E. L. and E. E. van Dyk (2000). Development of energy model based on total daily irradiation and maximum ambient temperature. Renewable Energy Journal; **21**; 37-47.

van Dyk EE, E.L. Meyer, F. J. Vorster and A. W. R. Leitch (2002), “Long-term monitoring of photovoltaic devices”, Renewable Energy Journal, **25**; 183-197.

Simon M. (2005), *Design and Implementation of an Automated Photovoltaic Module Current-Voltage Tester Employing a Variable Power Supply Unit*, MSc dissertation, UFH.

Scott B. J. (1998), *Evalution of Photovoltaic Modules and Systems,* MSc dissertation, UPE.

Green M. A. (1992), “Solar Cells: Operating principles, technology and System application”, University of New South Wales; **In**: **Scott** B. J. (1998), *Evalution of Photovoltaic Modules and Systems,* MSc dissertation, UPE.

Duncan T. (1983), “Success in Electronics”, John Murray (Publishers) Ltd, London.

CHAPTER 6

FUNDAMENTALS OF GENERAL PACKET RADIO SERVICES AND INTERNET PROTOCOL NETWORKS

6.1 INTRODUCTION

The term GPRS stands for General Packet Radio Service which is fundamentally the superimposition of a packet-based air interface on an existing circuit switched GSM (Global System for Mobile Communication) network. In essence GPRS is an improvement of the 2G (Second Generation) GSM network. It involves converting GSM networks into dual networks that allow co-existence of the two different data technologies, which are, CSD (Circuit Switched Data) and PSD (Packet Switched Data). The origins of GPRS are characterized by a huge demand for long distance mobile data services on the conventional GSM platform. It is expected that, in the near future, demand for Internet access using wireless networks will be greater than that for access via wired communication systems [Lee, 2004]. Truly the future that Lee and his colleagues meant is now! Mobile subscribers have recently developed quite huge need for wireless access to remote data terminals thereby providing them with remote access to co-operate data, electronic mail, and web information including remote security, control and data acquisition systems. The starting point in trying to provide a solution to these demands was to look at the possibility of integrating PSD services into GSM networks, efforts of which eventually gave birth to GPRS.

Originally 2G GSM was solely based on CSD which proves to be, among other things, slower than its PSD counterpart in terms of data transfer rates. As an example GSM 1800 offers up to 14.4 Kbps and GSM 900 gives up to 9.6 Kbps while on the other hand PSD used in GPRS offers, theoretical data rates, up to 170 Kbps. In practice, however

GPRS rates are below 170 Kbps with a minimum of 32 Kbps which still is higher than what 2G GSM is offering. With the advent of GPRS, GSM networks became 2.5 G which is closer to 3G (3rd Generation) mobile networks. Key features of a 3G mobile network include high data rates (up to 2Mbps), video calling and downloads, web browsing and email, some if not most of which suddenly became a reality with GPRS. Similarly, Internet Protocol (IP) networks for instance the Internet, are based on PSD technology and currently can offer very high speeds in the order of Mbps. An example is the Gigabit Ethernet which gives several hundreds of Mbps in speed. For the mere fact that IP networking and GPRS use a common and fundamental technology, PSD, GPRS enabled devices can be IP networked.

This chapter is dedicated to the detailed discussion of the underlying concepts of GSM and GPRS networks, which will form the basis of the discussions in later chapters. Issues be covered in this chapter include the integration of GPRS in GSM networks, data transmission, radio resource management principles for multiple access and the harmonization of GPRS and IP networks for various mobile data services.

6.2 TRANSMISSION MODES

In every successful communication process there is always a source system and a destination system. It is at the source that the communicated information is created, encoded and sent out to the intended destination system whose job is to receive the information, decode and interpret it normally according to a set of pre-programmed or predetermined rules or protocols. In some cases the process of communication is unidirectional with a fixed source and destination for the entire duration of the communication process, and thus the process is *simplex.* Systems that can only handle simplex communication are sometimes known as either *receive only* or *transmit only systems*. *Half duplex* is a two-way service and is defined as transmission over a circuit capable of transmitting in either direction, but only one direction at a time [Freeman, 2004; 9]. Each one of communicating hosts can be, instantaneously, either source or destination, but not both. The third and final type of communication is known as *full duplex*, or simply *duplex*. By definition it is a simultaneous two-way independent transmission on a circuit in both directions [Freeman, 2004; 9]. Mobile devices like cellular phones are duplex systems that allow independent simultaneous flow of data in both directions. On the contrary, old communication radios like the famous walkie-talkie are half duplex systems allowing independent flow of data in both directions but not simultaneously. Home television and radio systems are good examples of simplex systems and more specifically *receive only* systems.

6.3 CIRCUIT, MESSAGE, AND PACKET SWITCHING

6.3.1 Circuit Switching

Circuit switching requires a call to be established first and the time taken to establish a call is called *setup time (setup delay)*. When a call has been successfully established, network switches transparently interconnect forming complete and dedicated links (circuits) for the entire transmission specifically for that call only (no circuit sharing between different calls). The connections are transparent in the sense that circuit switches merely transfer data from source to destination without modifying it. Information transfer in that case is real time transfer (r.t.t.). Circuits and switching paths will only be released upon termination of the call. So if there are no free circuits and switching paths available *call blocking* occurs whereby calls are unable to complete (indicated by a network busy signal). Systems involved in circuit switched data (CSD) exchange should maintain high levels of synchronization throughout the call period and should be compatible (in data formats, communication protocol sets and so on). Examples of such circuit switching systems include public land telephone systems.

6.3.2 Message Switching

This is a form of store-and-forward interconnection within which every switch has some message storage capabilities. What it means is that a message switch can intercept data, store it (*store delay*) and only put it back on the network or pass it on when it is convenient to do so. So data transfer is non-real time. The store-and-forward concept eliminates *blocking* while the need for compatibility is also eliminated by the fact that information on the network can be converted by message switches to a transmission-specific format and back to compatible format at the receiving end. Unlike circuit switches, message switches are *transactional* switches in that they do more than simple data transfer from source to destination. Examples of such switching are Fax transmission, video-on-demand, electronic mail (E-mail), Telex forwarding and the Unix to Unix CoPy (UUCP).

6.3.3 Packet Switching

Packet switching involves breaking down data to be sent into smaller segments called data packets through a process called data segmentation at the source prior to transmission. Each packet can take a different path from source to destination and thus packets do not necessarily arrive at the same time or in the correct order of transmission. At the receiving end arriving packets are rearranged or reassembled based on the packet number (assigned at segmentation device) to form the original message. Lost packets will not be acknowledged by the destination and the source will have to re-send all those unacknowledged packets. Since packets are held in packet switches for shorter periods than in message switches, packet switched networks are sometimes known as hold-and-forward networks thus data transfer is near real time and without *blocking.* A packet switch is also a *transactional* switch. Examples of PSD services are VoIP, multimedia and so on.

6.4 GSM NETWORK ARCHITECTURE

A GSM public land mobile network (PLMN) consists of a number of critical nodes which will now be discussed in this section. GSM networks are structured hierarchically. A GSM mobile station could be a cellular phone, laptop computer or any other such mobile device and will be denoted as MS. Mobile stations are serviced by their nearest base transceiver station (BTS) with their assigned base station controller (BSC). The mobile switching center (MSC) is responsible for mobile traffic routing within the PLMN. A dedicated gateway mobile switching center (GMSC) forms the interface between the PLMN and the fixed network (e.g. PSTN, ISDN, etc).

The maximum radio coverage of a BTS forms an ‘active’ area of mobile access which is known as a *cell*. A *base station subsystem* (BSS) constitutes of a BSC and all the BTSs under its supervision. Considering all the BTSs assigned to a BSC as a group of cells under the management of the BSC then a *location area* (LA) could be defined as a group of BSSs. An *administrative region* (AR) is made up of at least one LA. Fig 6.1 shows the GSM PLMN system architecture with the most essential components.

Several databases are available for call control and network management: the home location register (HLR), visited location register (VLR), authentication center (AUC), and equipment identity register (EIR) [Bettstetter et al., 1999]. The HLR stores both permanent and temporary data for all users with the network operator. Permanent data is fixed data that is unaffected by the user’s mobility and an example of such data is the user’s profile.

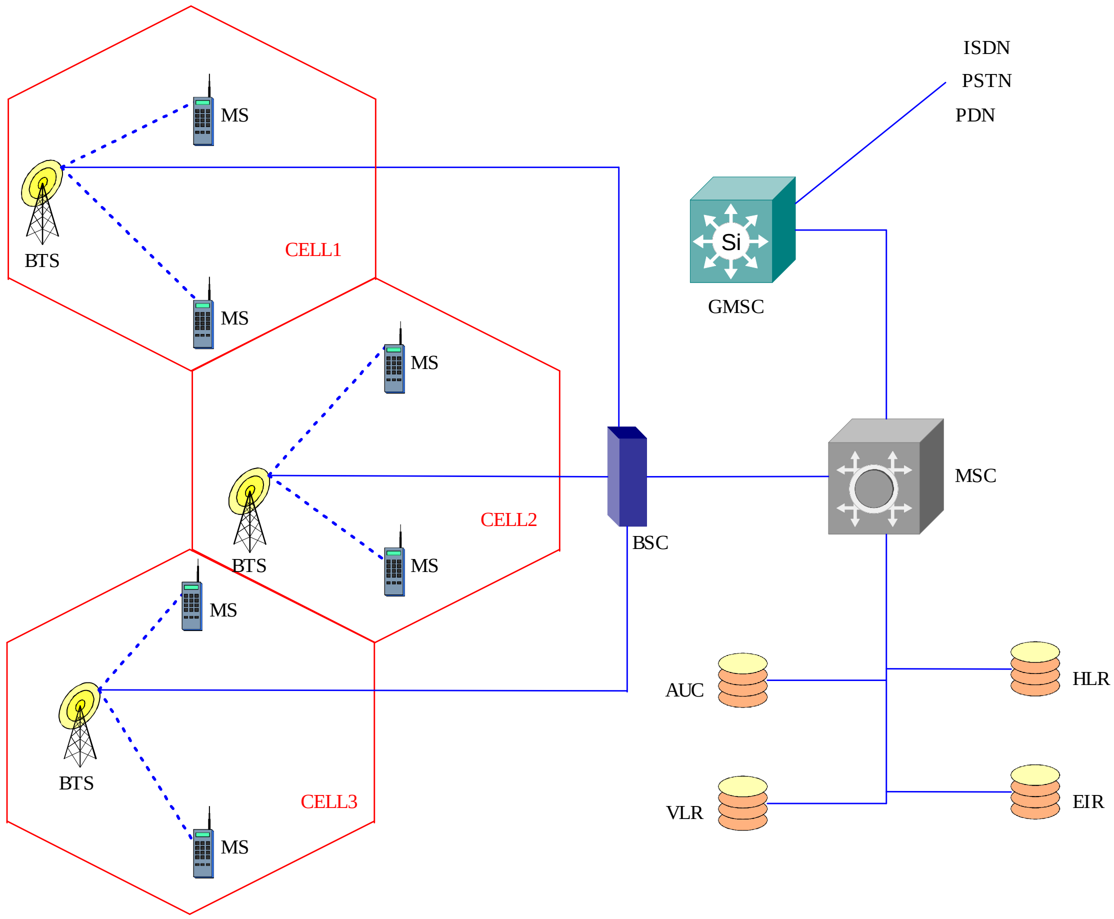

Figure 6.1: Conventional GSM system architecture [Adapted from Bettstetter et al., 1999]

On the other hand temporary data is not fixed and changes as the user moves from one cell to another, one LA to another, and one AR to another. An example of temporary data is the user's current location. While the HLR is for the entire network, the VLR is for bounded section of the network, usually a group of LA's. It keeps data of those users who are currently within its area of responsibility. The data that is kept in the VLR includes parts of the permanent user data that has been transmitted from HLR to VLR for faster access. But VLR may also assign and store local data such as a temporary identification.

Security related data such as encryption keys, authentication keys (pin codes and security codes) is stored in the AUC. EIR acts as the network's inventory that stores data related to the equipment (e.g. Mobile device) and not user data.

6.5 GPRS over GSM

GPRS is integrated into the existing GSM network through the introduction of GPRS capable network nodes known as GPRS support nodes (GSNs). In essence these support nodes are packet data routers with mobility management capabilities. As has been pointed out earlier, the aim of introducing GSNs is to allow PSD communication over a traditionally CSD network. As it were, the traditional GSM network nodes did not have any packet data handling capabilities. Figure 6.2 shows the GPRS system architecture. Two major system changes to the conventional GSM can be noted, that is, the replacement of the MSC with a serving GPRS support node (SGSN) and the GMSC with the gateway GPRS support node (GGSN).

The SGSN is tasked to process and facilitate packet data movements within its service area. Some of its duties include:

- Delivery of packets to and from MSs within its service area
- Routing and transferring of packets
- Mobility management (GPRS attach/detach and location management)
- Logical link management
- Authentication
- Charging (Billing)

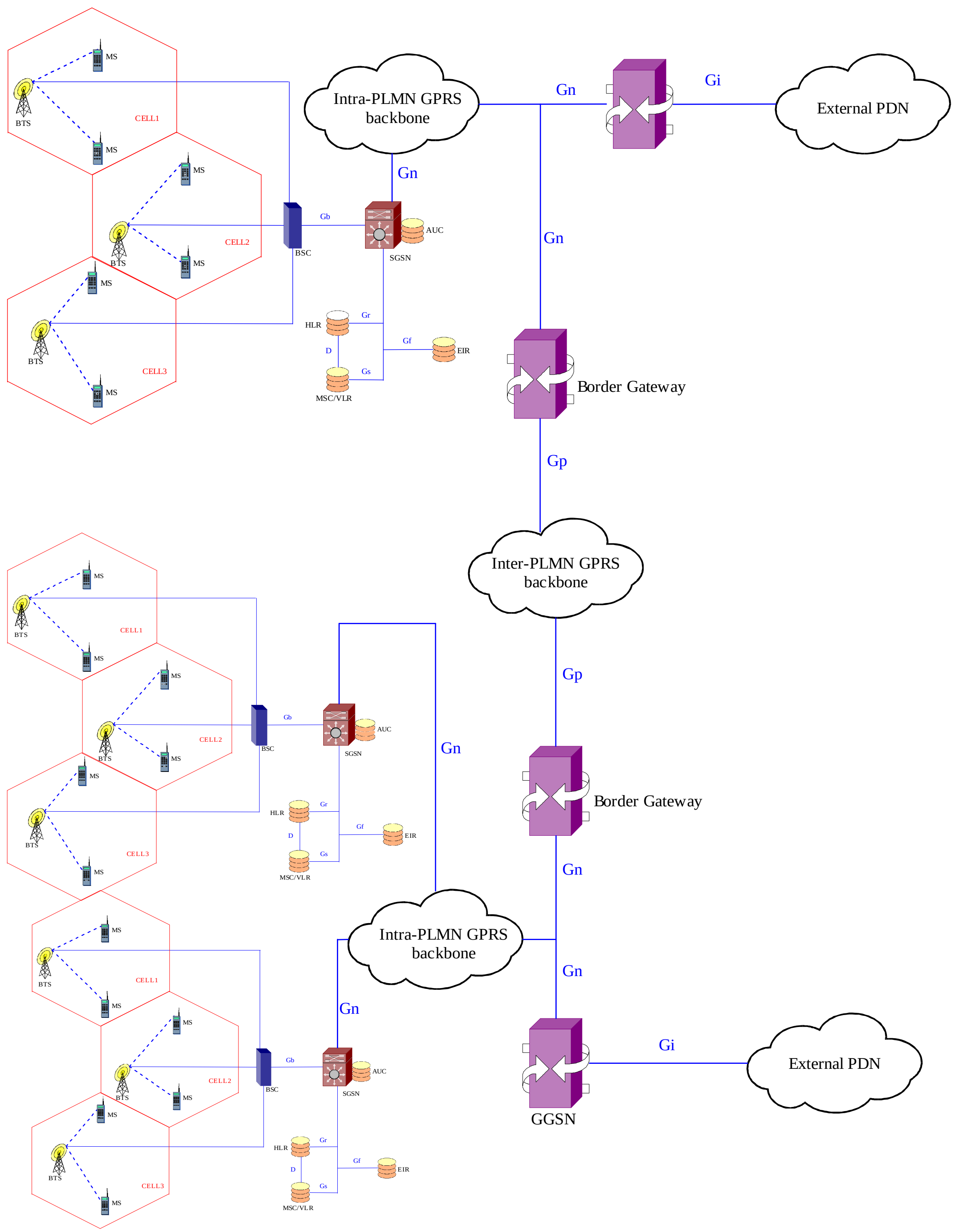

Figure 6.2: GPRS system architecture [Adapted from Bettstetter et al., 1999]

All SGSNs of the same PLMN are interconnected to form an IP-based GPRS intranet known as intra-PLMN GPRS backbone. The idea, among other things, is to facilitate simplified packet data routing and transfer within the PLMN.

A gateway GPRS support node (GGSN) forms the interface between the PLMN and other external packet data networks for example the Internet. Some of its responsibilities include:

- Proper packet data protocol (PDP) formatting of packet data network (PDN) bound data;
- GSM-PDP address resolution;
- Dynamic allocation of IP addresses to PLMN hosts;
- Authentication;
- Charging.

Where roaming agreements have been established between any two GPRS network providers, each one of them will install a border gateway (BG) to act as the interface point of his PLMN to the other provider's PLMN. Connecting these BGs results in an inter-PLMN GPRS backbone, with the BGs as the firewalls that perform security as well as authentication functions to protect their respective private intra-PLMN GPRS backbones against network poachers and attackers.

There is not much change to the network storage system, except for the VLR that transforms to MSC/VLR simply because it now stores extra information and its responsibilities are extended with functions as well as register entries that allow efficient coordination between packet switched (GPRS) and circuit switched (conventional GSM) services. The HLR, in addition to storing the user profile, keeps current SGSN address and PDP address(es) for each GPRS user in the PLMN.

6.6 GPRS SERVICES

6.6.1 Bearer Services

GPRS offers two kinds of bearer services primarily aimed at end-to-end PSD transfer, namely point-to-point (PTP) service and point-to-multipoint (PTM) service.

PTP as the name implies, offers PSD transfer between two users in either of the two modes that exist. The two modes are PTP connection-oriented (PTP-CONS) and PTP connectionless (PTP-CLNS) network services. The main difference between these two modes is in the transport protocols used, where now PTP-CONS uses a reliable connection-oriented transport protocol, the transport control protocol (TCP), e.g. for X.25, while on the other hand PTP-CLNS uses a less reliable, connectionless transport protocol, the user datagram protocol (UDP), e.g. for IP.

Similarly, two implementations of the PTM exist and these are PTM multicast (PTM-M) and PTM group call (PTM-G) service. In PTM-M all the intended users have to be in the same geographical area as the packets are just broadcasted in that area. Sometimes a group identifier is added to the packets simply to emphasize that the broadcasted packets are meant only for the specified group of users. However in PTM-G all users do not necessarily have to be in the same geographical area. A PTM-G packet is addressed to multiple users and it is the network's duty to find the current location of all those intended users before sending the packets through.

6.6.2 Supplementary Services

These are extra services that are brought along with the main services cited in the preceding section and they include the following:

- SMS message over GPRS

- Call forwarding unconditional (CFU)
- Call forwarding on mobile subscriber not reachable (CFNRc)
- Closed user group (CUG)

6.7 QUALITY OF SERVICE (QoS)

In the foregoing section various GPRS bearer services for end-to-end PSD transfer have been presented and this section discusses the associated services. A number of key factors affect the quality of a GPRS service and they are as follows:

Service Precedence

It is sometimes called service priority in relation to other services and determines the urgency of a service in the network. If for example a service of high priority is pooled with services of lower priority in a limited resource network, then network resource allocation is done such that the high priority service gets the resources first before the rest of the services. One example of such high priority service is one that involves live video streaming over GPRS. Three levels of priority do exist in GPRS: high, normal, and low.

Reliability

Reliability concerns itself with data safety, integrity and security during transmission. Three reliability classes are defined, which guarantee certain maximum values for the probability of loss, duplication, mis-sequencing, and corruption (undetected error) [Bettstetter et al., 1999]. Table 6.1 gives these reliability classes.

Table 6.1: A summary of the reliability classes [Adapted from Bettstetter et al., 1999]

Class	**128 byte packet**		**1024 byte packet**	
	Lost	**Duplicated**	**Out of sequence**	**Corrupted**
1	10^{9}	10^{9}	10^{9}	10^{9}
2	10^{4}	10^{5}	10^{5}	10^{6}
3	10^{2}	10^{5}	10^{5}	10^{2}

Delay

It is an estimate of end-to end transfer setback measured in seconds and is given as either mean delay or 95-percentile delay (95pd). 95pd represents the maximum delay guaranteed in 95 percent of all transfers. The delay value is a cumulative total of all delays starting with delay in the request and allocation of resources (access delay), followed by in-network data delay (transit delay), but excluding delay outside the GPRS network, that is in the external PDP network (external transit delay). Table 6.2 shows all the delay classes in GPRS.

Table 6.2: A summary of the delay classes [Adapted from Bettstetter et al., 1999]

Class	**128 byte packet**		**1024 byte packet**	
	Mean delay	**95% delay**	**Mean delay**	
1	<0.5s	<1.5s	<2s	<7s
2	<5s	<25s	<15s	<75s
3	<50s	<250s	<75s	<375s
4	Best effort	Best effort	Best effort	Best effort

Throughput

It stipulates the maximum and mean data transfer rates (DR) in other words, the peak bit rate and mean bit rate.

Based on these QoS classes, QoS profiles can be negotiated between the mobile user and the network for each session, subject, of course, to the QoS demanded and currently available network resources. As a result three factors now contribute to the service billing structure and these are: volume of data transmitted, the type of service, and the negotiated QoS. It is pure logic that with all other things held constant the better the QoS the higher the bill.

6.8 GPRS ATTACHMENT AND DETACHMENT PROCEDURE

GPRS attach is a process that begins immediately after a GPRS enabled MS has indicated its intention to use GPRS network services. Firstly the MS should register with the SGSN. The registration process involves the MS sending both its IMEI and IMSI to the GSGN which then verifies the two identities. If valid the network copies the user's profile from the HLR into some form of 'cache' memory in the SGSN. Finally the SGSN assigns a packet temporary mobile subscriber identity (P-TMSI) [Bettstetter et al., 1999]. This completes the GPRS attachment process, and from then on, the registered MS is free to access any available GPRS bearer services.

GPRS detach is simply the disconnection of an MS from the GPRS network. This process involves the SGSN deregistering the MS from the network by de-allocating the P-TMSI and moving the user's profile back into the HLR. Detachment process can either be *network initiated* (initiated by the SGSN) or *subscriber initiated* (initiated by the MS).

6.9 PDP CONTEXT SWITCHING

An active PDP context is a context in which successful packet data exchange is possible between external PDN and a mobile station. The process of establishing such a context is known as *PDP context switching*.

After an MS has been successfully registered, it can now access the available GPRS bearer services so as to exchange packets with external PDNs. Firstly the MS should have a known IP address and to obtain it, the MS should send a request for PDP address to the SGSN. The request, called *active PDP context request*, consists of basically four parameters which are:

- PDP type
- PDP address
- QoS preferred
- Access point

The MS supplies the value for the PDP type it intends to use, either X.25 or IP, as well as the QoS parameters it prefers. That will form the basis of QoS negotiations between the MS and the network. The PDP address is known to the MS if the network provider uses *static mobile host configuration (SMHC)*, but in *a dynamic mobile host configuration (DMHC)*, the PDP address is not known at this stage and thus will be left blank. In other words the PDP address is dynamically assigned. Similarly, the network service access point, NSAP is not known to the MS yet, and this parameter is unassigned or left blank.

Upon receiving the request the SGSN performs the necessary user authentication and security functions before sending a *create PDP context request* to the GGSN. Since the SGSN does not interface the MS directly to external PDN, the request can only be handled by the GGSN. So the SGSN simply passes a *create PDP context request* to the GGSN, which then processes this request. The responsible GGSN decides on the QoS to render, subject to the currently available network resources. In a DMHC situation, the GGSN will have to assign the PDP address to the MS which is interpreted as the MS's host ID on the IP-based network which makes the MS visible for the external PDN during active PDP context. Every packet destined for the external PDN should be routed via a GGSN which serves as the access point. For that reason there is need for the access point address parameter in the request which helps in establishing the gateway for all the packets that will be exchanged between the MS and external PDN during the active PDP context. After all the parameters have been assigned, the GGSN creates a new entry in the PDP context table for data routing purposes before sending a *create PDP context response* to the respective SGSN containing all the parameters and their values. The SGSN also enters this data in its PDP context table after which it sends an *active PDP context accept* message to the MS. Figure 6.3 shows process of PDP context activation. The numbers 1 to 5 indicate the order in which events occur during PDP context switching.

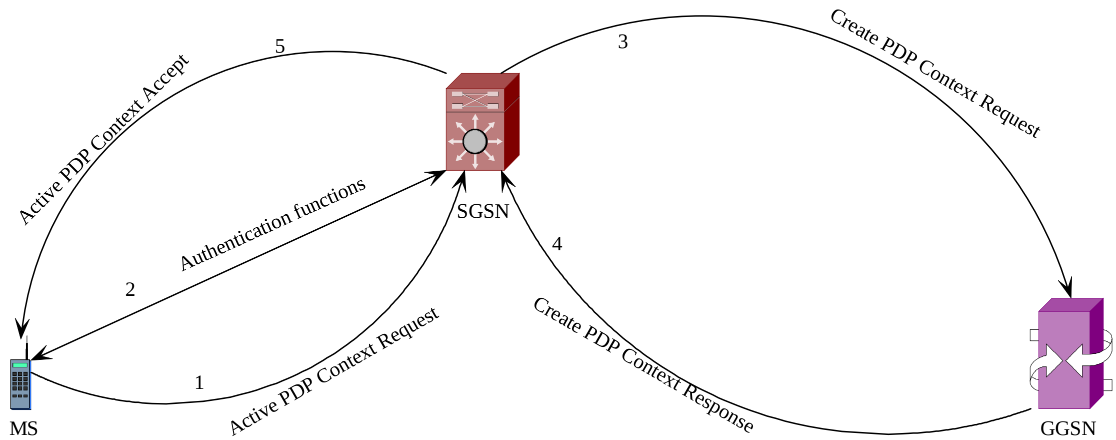

Fig 6.3: PDP context activation

6.10 MULTIPLE ACCESS TECHNIQUES, RADIO RESOURCE MANAGEMENT PRINCIPLES AND PHYSICAL CHANNELS

Two multiple access techniques exist on the physical layer for GSM and of course GPRS. The two, *frequency division multiple access* (FDMA) and *time division multiple access* (TDMA), blend so well as to allow a co-existence of GSM CSD with GPRS PSD.

FDMA involves subdividing the available bandwidth into smaller sections or carrier frequency bands forming multiple carrier channels. In GSM there are two main frequency bands that form the total network bandwidth. Uplink (from MS) transmission uses 890 to 915 MHz while downlink (from BTS) uses 935 to 960 MHz [Bettstetter et al., 1999]. Each of these bands, through FDMA is divided into 124 single carrier channels of 200 kHz width out of which a certain number of channels are allocated to a BTS in a process known as *cell allocation*.

In TDMA, each of the 200 kHz channels is divided into eight time slots forming eight TDMA channels within each FDMA channel. The eight TDMA slots in a channel form what is called a TDMA frame with each time slot lasting for duration of 156.25 bit times equivalent to 576.9 μs. A TDMA time slot can be used to transfer a data burst. The recurrence of one particular time slot defines a *physical channel*.

An enhanced form of Code Division Multiplexing could also be used which employ special algorithms developed for channel-aware priority-based groupwise packet scheduling for non-real time data service with burst-switching Direct Sequence CDMA systems [Kim, 2004].

Conventional GSM allocates, permanently, a channel for a particular user during the entire call period regardless of whether data is transmitted or not. On the other hand, using *capacity on demand principle*, GPRS allocates packet data channels (PDCH) when data packets are sent or received and they are released immediately at the end of transmission. The PDCHs are taken from the pool of all channels available to a cell after cell allocation.

6.11 LOGICAL CHANNELS

Logical channels can be thought of as “software channels” and are defined to perform a number of functions. These functions are user packet data transfer and *network calibration and control*.

Network calibration and control channels represent all those channels used for monitoring and regulating all proceedings on the communications network. Table 6.3 lists all the packet data logical channels defined in GPRS in their categories as well as their functionality on the network.

Table 6.3: Logical channels in GPRS

<table>
<tr><th>Group</th><th>Channel</th><th>Function</th><th>Direction</th></tr>
<tr><td>Packet data traffic channel</td><td>PDTCH</td><td>Broadcast control</td><td>MS ←BSS</td></tr>
<tr><td>Packet data traffic channel</td><td>PBCCH</td><td>Random access</td><td>MS →BSS</td></tr>
<tr><td rowspan="4">Packet common control channel (PCCCH)</td><td>PRACH</td><td>Access grant</td><td>MS ←BSS</td></tr>
<tr><td>PAGCH</td><td>Paging</td><td>MS ←BSS</td></tr>
<tr><td>PPCH</td><td>Notification</td><td>MS ←BSS</td></tr>
<tr><td>PNCH</td><td>Associated control</td><td>MS ↔BSS</td></tr>
<tr><td>Packet dedicated control channels</td><td>PTCCH</td><td>Timing advance control</td><td>MS ↔BSS</td></tr>
</table>

To ensure successful communication, there should be continuous and correct mapping of these packet data logical channels on to the available physical channels. Unfortunately this chapter will not discuss the specifics of the logical to physical channel mapping as well as channel coding schemes. Instead fundamentals of the Internet are discussed next, followed by an illustration of a possible GPRS-Internet network architecture with its most important components.

6.12 IP NETWORKING (based on IPv4 and IPv6 routing/addressing protocols)

Various network components and hierarchical structures can be identified in Internet and will now be discussed.

Router

More precisely we can call it an *internal router* and its function is to route traffic within a given network or within and between subnets of the same network.

Gateway or *external router*

It directs traffic to external networks. It is the interface between any two given independent networks (intranets) or between an intranet and the Internet. *Servers* are network storage facilities and/or control points.

Internet Service Providers (ISPs)

They represent a group of intermediary companies whose business is to connect users to the Internet backbone. The commercialization of the Internet by the Clinton and Gore administration (1992) in the U.S. created this new ISP business [Bates and Gregory, 2001; 404]

Local Area Network (LAN)

Is a communication network that is usually owned by a business customer and normally extending for distances of up to 2 km; for example within an office building, a university campus, an industrial park, or a hospital. Within a LAN, many independent peripheral devices, such as data terminals, are linked to a network through which they can share expensive central processing units, memory banks and a variety of other resources [Nellist, 2002; 213]

6.13 INTERNET OVER GPRS

The intra-GPRS backbone is IP based which means it is capable of routing and transferring IP packets used in the Internet. As a result the last move in trying to provide Internet over GPRS networks would be to simply connect the GGSN of the PLMN operator to the IP gateway of the ISP. Fig 6.4 shows such an interconnection that will enable internet service access for mobile subscribers via GPRS. A firewall is installed by the PLMN operator so as to protect his private IP network from unauthorized external users and attackers. The DHCP (Dynamic Host Configuration Protocol) server is used by the operator for dynamic allocation of IP addresses to mobile stations during PDP context switching. A DNS (Domain Name Service) is used to convert the normal language names, used to name nodes in the Internet, into IP names [Bates and Gregory, 2001; 421]. An example of such English language names is www.ufh.ac.za.

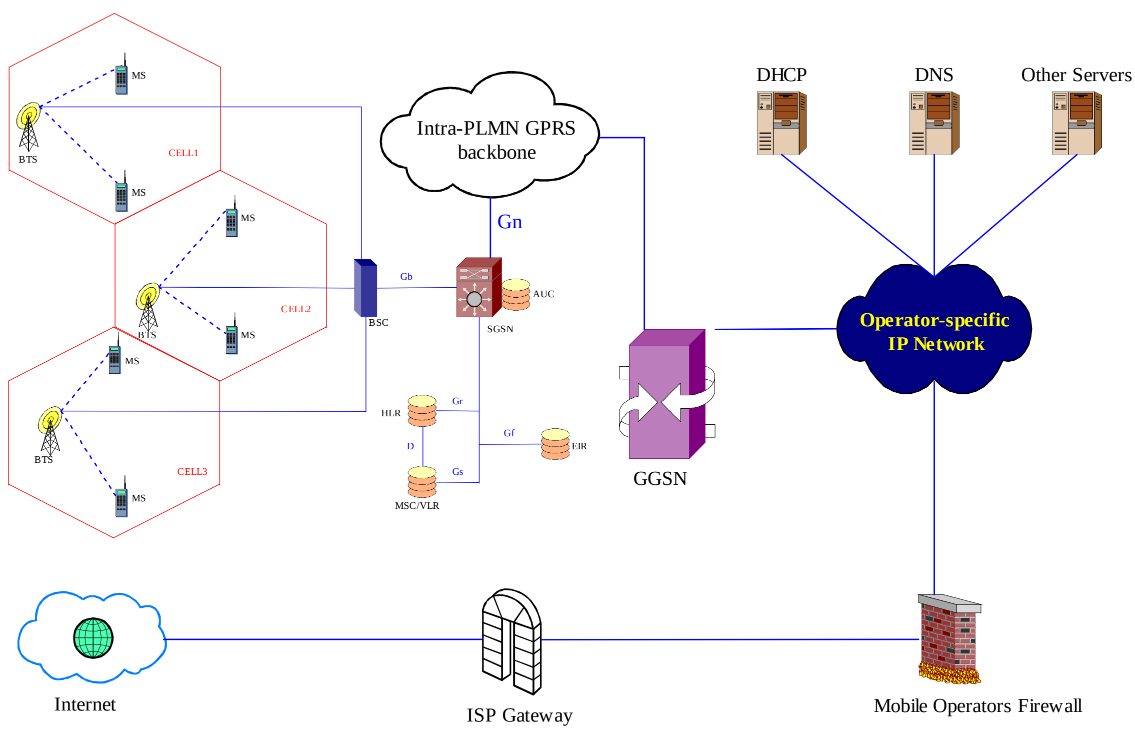

Fig 6.4: Internet over GPRS

6.14 SUMMARY

In summary, GSM has come a long way in a short space of time, which saw it grow in terms of the both user base and technology base. The growth of a user base led to an increased demand for more network resources and better bearer services. Demand for access to packet data services by mobile users resulted in the introduction of GPRS, which even made Internet access possible for mobile users. To integrate GPRS services in a conventional GSM network, a few network nodes are introduced to replace some GSM nodes that do not have packet data handling capabilities. The rest of the GSM nodes only require software upgrading so as to perform packet data processing.

GPRS has proven its potential as a solution for remote Internet connectivity. Remote ICT systems, given the proper interfacing hardware, can indeed be connected to the Information Superhighway (Internet) through GPRS networks. Intended beneficiaries of such a development are the remote and inaccessible rural schools that are lagging behind their urban counterparts in terms of technology. Connecting these schools to the Internet would immensely help in bridging the digital divide, raise the standards of education delivery and above all improve both pass rates and quality of students produced in these schools. However a lot of research is needed before Internet connectivity of this kind can be recommended for such poor schools. Critical issues to look at include affordability, reliability and sustainability. In this regard, a mobile Internet device was designed, installed and used to monitor the performance of GPRS in a multi-user network as part of this research. Chapter 7 explains the design of such a device and discusses its main features. Chapter 8 will follow up with a detailed presentation of the observed performance of GPRS in a multi-user environment.

6.15 REFERENCES

Bettstetter C., H. J. Vogel, and J. Eberspacher (1999), “GSM Phase 2+ General Packet Radio Services GPRS: Architecture, Protocols, and Air Interface”, IEE Communications Surveys, The Electronic Magazine of Original Peer-Reviewed Survey Articles.

Bates R. J. (Bud) and D. W. Gregor (2001), “Voice and Data Communications Handbook”, 4th Edition, McGraw-Hill.

Nellist J. G. (2002), “Understanding Telecommunications and Lightwave Systems”, 3rd Edition, IEEE Press and John-Willey and Sons.

Kim M., A. Ahmad and S. W. Kim (2004), “ Channel-aware priority-based groupwise packet scheduling for non-real time data service with burst-switching DS/CDMA system”, International Journal of Electronics and Communications (AEU), 59 (2005), 432-439.

Lee J. W, H. Lee, and D. H. Cho (2004), “ Effect of dormant registration on performance of mobility management based on IP paging in wireless data networks”, International Journal of Electronics and Communications (AEU), 59 (2005), 319-323.

Freeman R. L. (2004), “Fundamentals of Telecommunications”, John-Willey and Sons.

Tektronix (2005), “GPRS Protocol Testing in the Wireless World”, accessible from www.tektronix.com/commtest ,last viewed 12/11/2005.

CHAPTER 7

DESIGN AND TESTING OF A MOBILE INTERNET DEVICE (MIDevice)

7.1 INTRODUCTION

Wireless Internet Access (WIA) is a relatively new but rapidly growing field in mobile data communications industry. WIA came into being as a direct result of modern business trends that needed portability of work and hence placed huge demand on Wireless Internet provision as opposed to Fixed Internet provision. Such demand was further fueled by the booming of the mobile device industry that saw the release of a multitude of fancy portable Personal Communications (PC) devices with more processing power than the conventional non-portable desktop machines.

To ordinary civilians, WIA and PC device industries present unnecessary luxury goods and service. However, only those who are in business can attest to the reality of being able to conduct business and do all day-to-day office work while traveling, thanks to WIA and PC industries. It is therefore not difficult to comprehend why WIA confined itself more to a small but financially elite niche market.

At the onset of WIA, hot spots were set up at exclusive points in urban areas by Internet Service Providers (ISPs). Such exclusive sites include airports, holiday and recreation sites and so on. Due to the nature of Internet access these ISPs were now referred to as wireless Internet Service Providers (WISP) [WISPA, 2006]. Recently a new form of WIA was introduced to use the Global System for Mobile Communications (GSM) network platforms and thus can be referred to as Mobile Internet Access (MIA).

Since WIA mainly targets urban areas, it therefore contributes toward widening of the digital divide. On the contrary, MIA though introduced as a more extended option to WIA, presents vast potential in bridging the digital divide. Potential of MIA is derived from the reality that most mobile telecommunications operators manage to extend their coverage into remote and inaccessible rural areas that lie outside the cable network of fixed ISPs. As such MIA can be used to connect these rural schools to the Global Information Superhighway (Internet).

A Mobile Internet Device (MIDevice) was designed for connecting rural schools in South Africa to the Internet via GPRS using any of the country's three mobile operators, which are Vodacom, MTN and Cell C. This chapter therefore describes the design and operation of the MIDevice, highlighting some of its exclusive features. Initial test results are presented and briefly discussed as well before the chapter is summarized and concluded.

7.2 MIDevice SYSTEM

7.2.1 Architecture

Figure 7.1 shows the schematic layout of the MIDevice system. The entire system consists of interconnected subsystems each performing a specific task. These subsystems are represented by rectangles in the figure.

Radio frequency (RF) section represents the full duplex radio frequency transceiver subsystem, which means that it handles both sending and receiving data. In order to function as expected, the RF subsystem include an RF power amplifier for boosting transmission signals, front-end circuitry for up-and down-conversion and an antenna for capturing and radiating high frequency electromagnetic waves [Siemens, 2003].

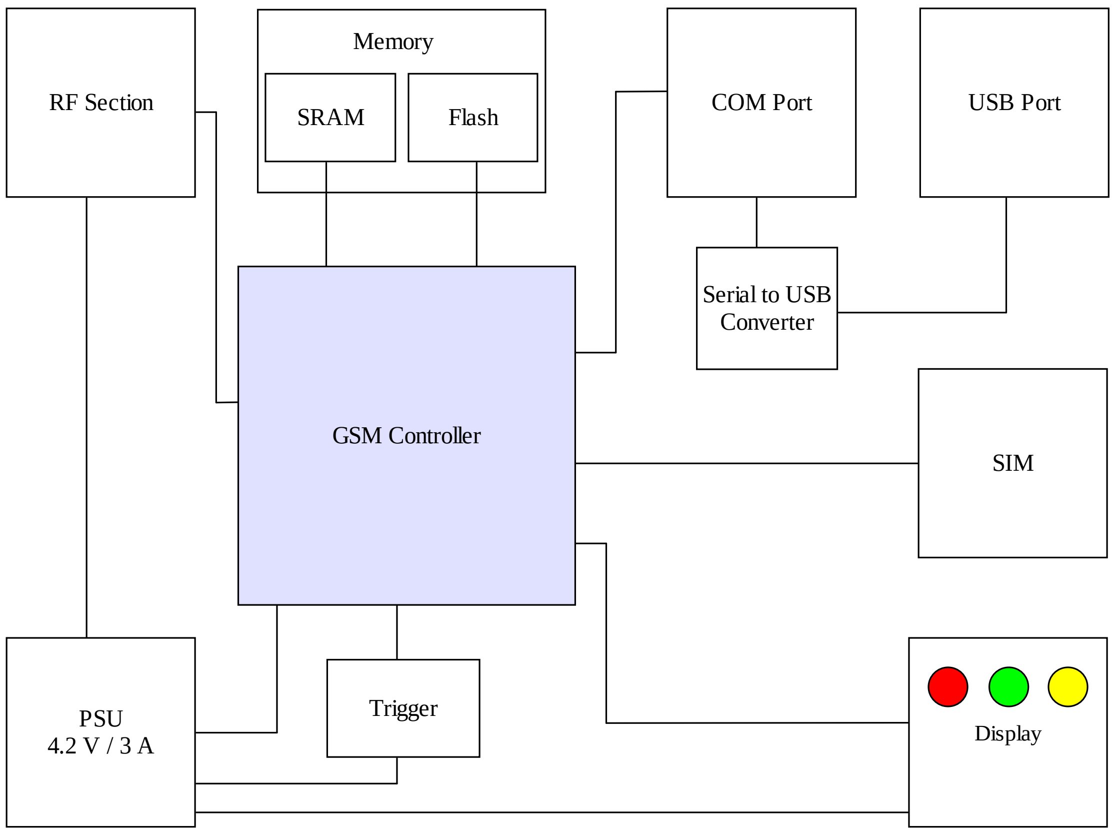

Figure 7.1: Schematic showing layout of the MIDevice

Two kinds of storage facilities exist for the GSM controller. Flash memory keeps important software for the controller owing this to its non-volatility as well as fast read/write property. Part of the critical software stored in the flash memory includes the Basic Input Output System (BIOS). On the other hand, Static Random Access Memory (SRAM) is reserved for additional memory demand during controller operation. Unlike flash memory, it will lose its contents when modem power is switched off [Siemens, 2003].

Figure 7.2 illustrates the MIDevice showing some of the electronic components used in the circuitry. Some of the mentioned subsystems were identified and labeled.

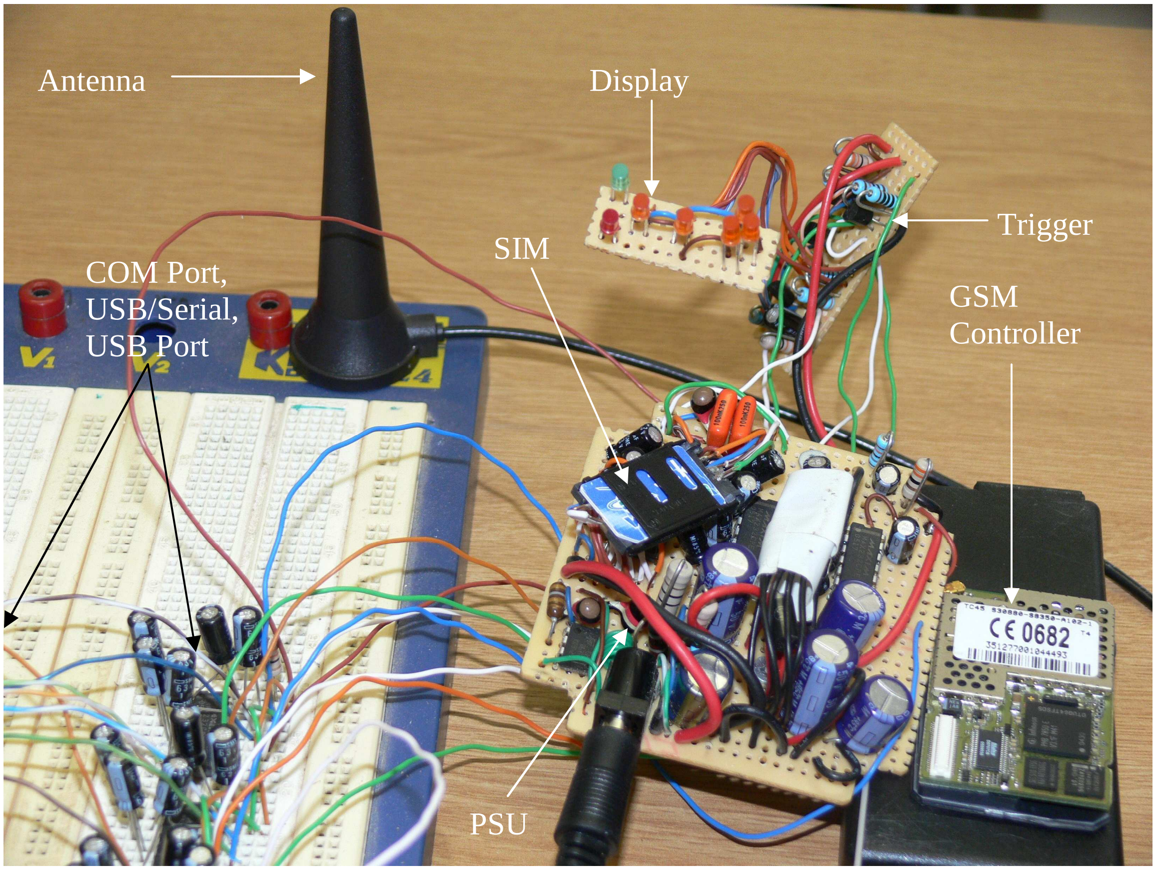

Figure 7.2: Exploded picture of the MIDevice

The power supply unit (PSU) is responsible for processing input power signal. Such processing entails converting the high voltage mains AC signal (240 V rms) to DC levels acceptable for the normal operation of the modem's various microelectronic circuits. In summary, the high voltage AC signal is stepped down, rectified, smoothened and stabilized, accordingly, with the help of specialized electronic chips and various off-chip components.

User-triggered power control signals are all supplied from the trigger circuit. This circuit contains switches for the manual switching on and emergency shutting down of the modem.

The display uses low power light emitting diodes (LEDs) to indicate power, modem and network status. Power LED is on for as long as power is supplied to the modem. The modem LED only turns on when the modem is actually on, otherwise is off. On the other hand the network LED indicates activity on the network by way of blinking at different frequency that depends on the network activity. Network activities include network searching and login, user authentication, monitoring network control channels and user interaction, and GPRS data transfer.

SIM represents standard subscriber identity module (SIM) card interface, card holder and the actual SIM card all of which are in compliance with ISO 7816 Smart Card standard as well as the GSM 11.11 recommendation [ETSI, 1995].

7.2.2 Description of MIDevice Features

The MIDevice houses quite a number of features but only the most important ones will be discussed here. As a mobile station, the MIDevice falls under class B of mobile stations. Mobile stations in this class are able to attach to both GPRS network and conventional GSM networks for packet data and voice call services, respectively. However, it can only use one service at a time, with voice call and SMS services taking precedence over GPRS services. What it means is that any GPRS active context will be suspended to process incoming voice or SMS calls and will be automatically resumed upon termination of the voice and SMS calls.

Also the device uses multislot GPRS class 8 (4+1, 5), that is; it uses up to four time slots (channels) for downloading and only one for uploading. This seems to be well suited for a school set-up where it is expected that there would be more downloading of educational material than sending, for instance, of mails laden with non-educational attachments.

Provision of the Universal Serial Bus (USB) port means that the MIDevice can be used with modern desktop and laptop computer systems. Most of these modern computer systems seem to be phasing out the slower serial (RS232 COM port) in favor of the faster USB port.

The modem is also network independent and can be used in any operator’s network as long as the following conditions are satisfied:

- Operator’s network supports GPRS services;
- The modem is configured according to the requirements of the operator’s network;
- A valid SIM card is used for intended network operator.

7.3 CONFIGURING THE MODEM

Configuring the MIDevice and setting it up for Internet access is fairly simple as the flow chart in figure 7.3 shows. Since a Serial-to-USB converter is implemented, a virtual COM port driver is required in order to create a pseudo COM port from the available USB port. The MIDevice will then communicate with the host via this virtual port. However, while everything else remains the same when configuring the MIDevice for any other mobile network the blue variables should be obtained from the network operator concerned.

Once the MIDevice has been successfully installed and set up as a standard modem, a dial-up connection needs to be set up through which all Internet requests will channeled. In fact this dial-up connection is the computer’s own gateway to the Internet. Figure 7.4 shows a flow chart for setting up and configuring a new dial-up connection for the modem. In both figures 7.3 and 7.4, the variables in blue are operator-specific and should be obtained from the operator concerned. The given values in this case are only valid to Vodacom South Africa.

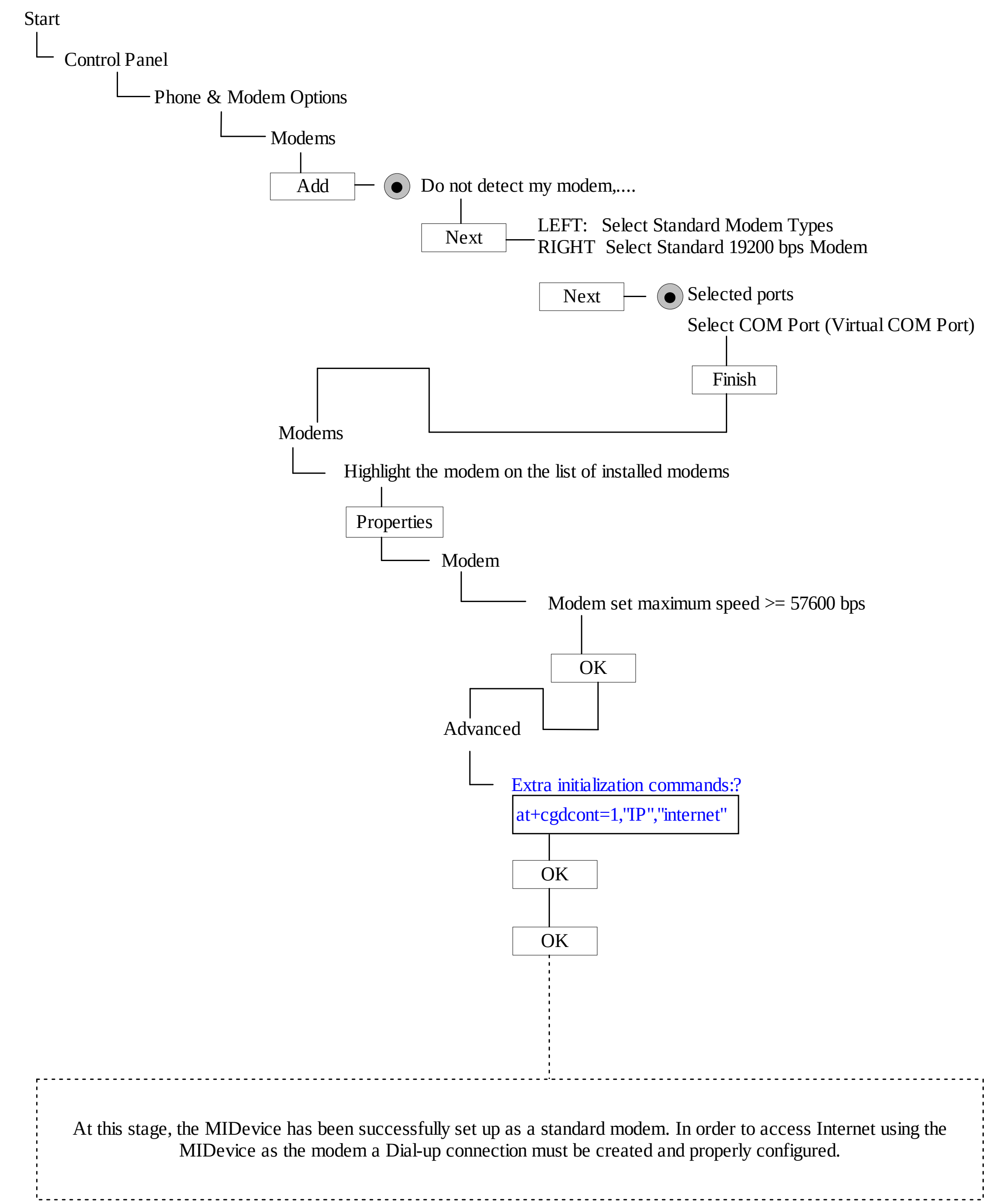

Figure 7.3: Configuring the MIDevice as a modem

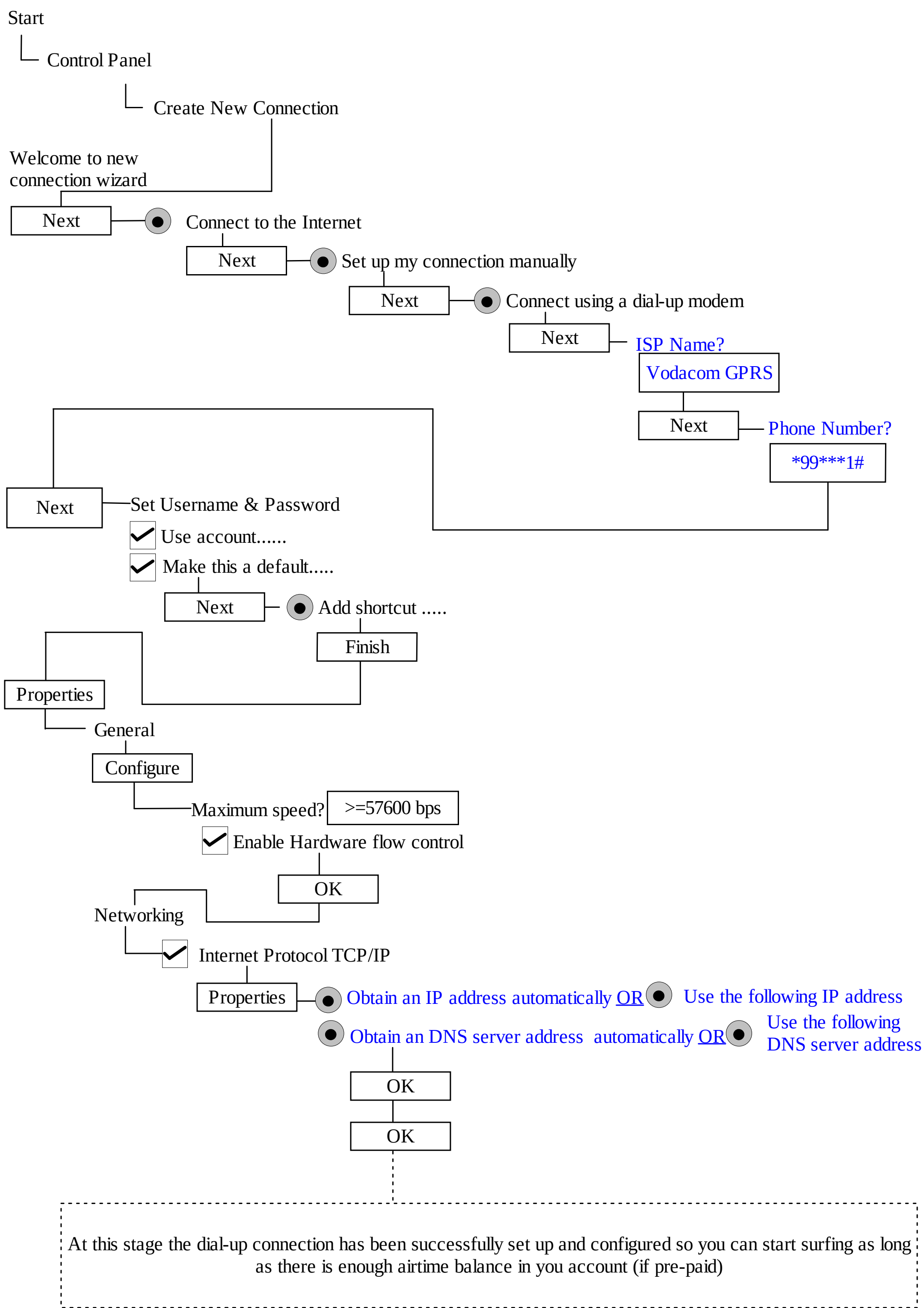

Figure 7.4: Setting up a dial-up connection

7.4 INITIAL TEST RESULTS AND DISCUSSIONS

The MIDevice was successfully tested as shown by figures 7.5 and 7.6. Figure 7.5 reiterates the simplicity of the MIDevice as it only needs to be configured as a standard modem without any special requirements. COM5 in figure 7.5 is virtual and allows the host computer to interact with the modem as if it was connected on the COM port yet it is actually connected on a USB port. For configuration purposes on Windows the modem is treated as a standard 19000 bps modem. It is known that speed of the uploading speed for GPRS multislot class 8 is between 8 and 12 Kbps while the downloading rates are 32 to 40 Kbps [GSM World, 2006]. However the term standard 19000 bps is only used to represent the type of modem and does not give the maximum modem speed. In fact Windows allows you to specify the maximum speed of the modem and this case 115000 bps was selected as the maximum speed.

In figure 7.6, a visiting colleague in the department of Computer Science at the university, Dr Rao, put the downloading capability of the MIDevice to test by downloading a 1.2MB publication from the website shown. What is interesting in the network status shown in the figure is not only the fact that the modem successfully proved its downloading capabilities, but the ratio of uploaded to downloaded data. Of total data packets in the excess of 1.2MB exchanged between network and the modem, uploading accounts for as little as 7% compared with 93% of downloaded packets. It is important here to note that the speed shown in the network status window is not the actual data rate (DR), instead it is the maximum speed of the dial-up connection that was set during configuration.

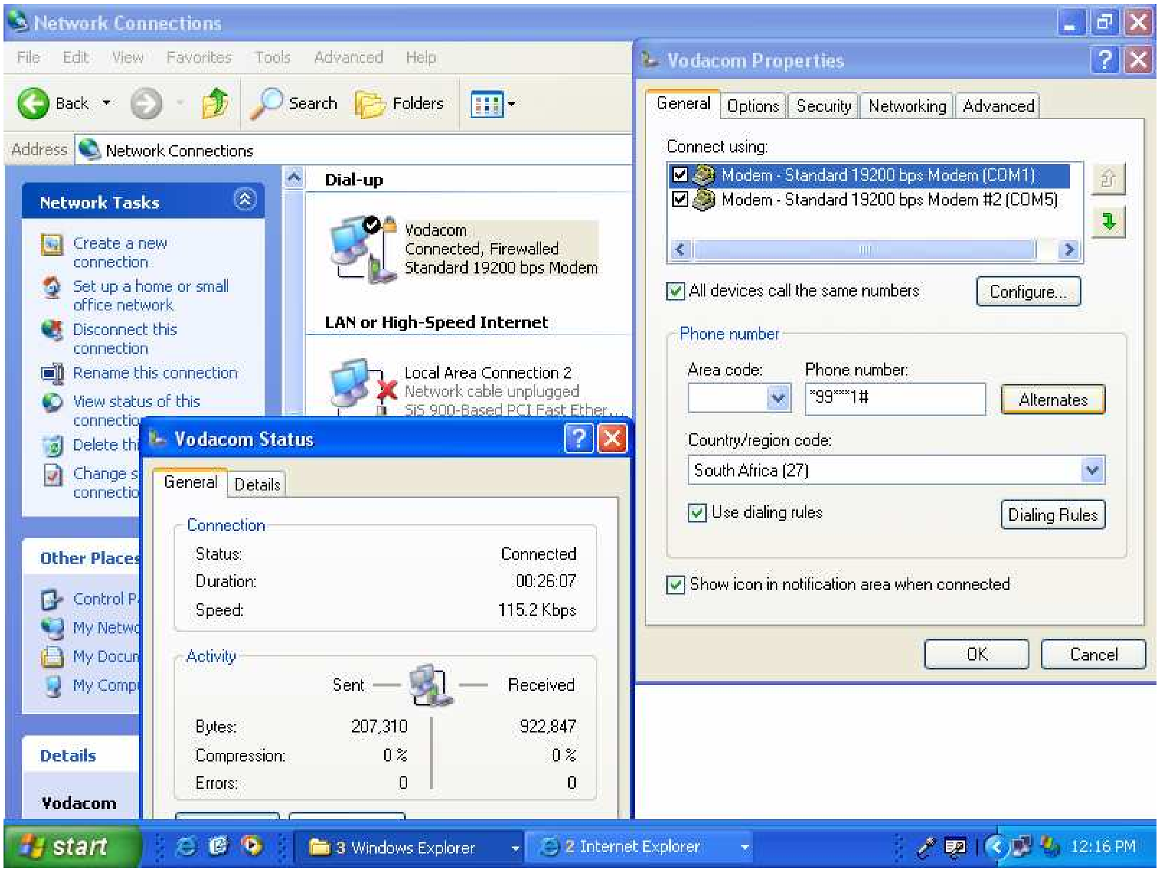

Figure 7.5: the MIDevice configured as a standard modem and a dial-up connection to be used for Internet access created

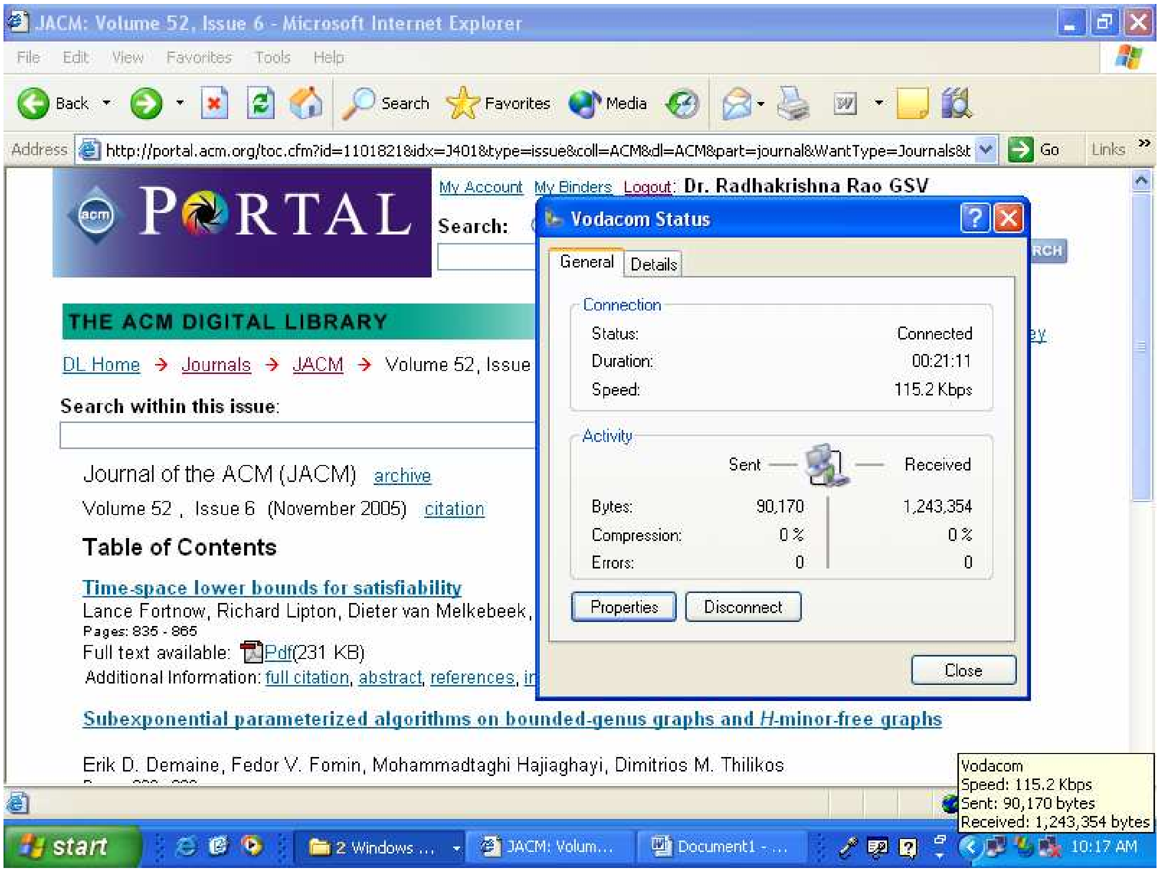

Figure 7.6: Testing downloading capabilities of the MIDevice

7.4 SUMMARY AND CONCLUSSIONS

The design and operation of the MIDevice was presented and discussed. The MIDevice has demonstrated huge potential to provide the much needed Internet connectivity solution to remote rural schools using already existing mobile networks. From a user's perspective, the modem gave impressive access and downloading speeds. The MIDevice was only tested on one of South Africa's three mobile operator's network, Vodacom. However another operator, MTN, has an equally established GPRS network hence the device was simply envisaged to also function well on that network. At the time of tests, Cell C was in the process of upgrading its network for packet data services.

7.5 REFERENCES

ETSI (1995), “Digital Cellular Telecommunications Systems (Phase 2+); specifications of Subscriber Identity Module-Mobile Equipment (SIM-ME) interface – v. 5.0.0”, Accessible from http://www.ttfn.net/techno/smartcards/gsm11-11.pdf ; last viewed 01/12/2006

GSM World (2006), “GPRS Class Types”; accessible from http://www.gsmworld.com/technology/gprs/class.shtml , last viewed 30/11/2006.

Siemens Mobile (2003), TC45 Cellular Engine Hardware Interface Description; In: **TDC** (2006), Telecom Design Communications Ltd, “tc45_hd_v0001_1060586”, TC45 SDK & Documentation.

WISPA (2006), Wireless Internet Service Providers Association, accessible from www.wispa.org; last viewed 30/11/2006

CHAPTER 8

PERFORMANCE OF GENERAL PACKET RADIO SERVICES (GPRS) IN A MULTI-USER ENVIRONMENT

8.1 INTRODUCTION

As mentioned in the previous chapter the Mobile Internet Device (MIDevice) uses a GPRS multislot class 8 (4+1) with uploading speed between 8-12 kilo-bits per second (kbps) and downloading speed of 32-40 kbps. Of course the downloading speed of 40 kbps is achievable when all four downloading timeslots are used. Unfortunately it has already been mentioned in chapter 6 that GPRS physical channels are allocated dynamically based on demand as well as availability of channels. This means that the mobile station (MS) in this case the MIDevice, may not get all four channels for downloading, thus actual data rates will be lower. In this regard, it is valid to suggest that any GPRS-based MS in general would be as fast as the current network status permits. It certainly becomes crucial to observe the general performance of GPRS in terms of the quality of service (QoS) parameters, which are reliability, delay and throughput. This chapter evaluates performance of GPRS-based mobile Internet connections in a multiple user environments. Critical QoS issues are also presented and discussed in detail. Furthermore, the chapter suggests measures for enhancing future mobile Internet solutions.

8.2 BACKGROUND

QoS parameters in any network environment are categorized into performance-oriented and non-performance-oriented quality parameters [Irvine and Harle, 2002; 70-71]. Performance-oriented parameters include all kinds of delays (access, transit, release etc.), throughput (maximum and mean data rates) and reliability (possibility of failure or data error rate). On the other hand, non-performance-oriented QoS parameters do not directly affect network transactions but are concerned with related matters. Such parameters include level of service (deterministic, predictive or best effort), cost of service quality and priority (high or low). In other network environments there are pre-set classes of service CoS from which users of the network clients can choose [Hull, 2002; 17]. GPRS offers pre-determined performance and non-performance-oriented QoS parameters like delay, throughput, reliability and service precedence [ETSI-1, 2000]. These parameters are negotiated between the network and the mobile station for a specific Packet Data Protocol (PDP) context during switching. As such, performance of GPRS is not static and will vary from one PDP context to another. If network resource allocation in GPRS is dynamic and based on resource availability, then it should generally hold that in instances of low mobile traffic, GPRS will offer better service. In other words, the less congested the network is, the better the service delivered. Throughout a given PDP context QoS should remain relatively steady until higher precedence services such as incoming voice and SMS calls cause de-allocation of some packet data channels (PDCHs).

8.3 EXPERIMENTAL SET-UP

In order to determine performance of GPRS in a multi-user environment, a client/server network consisting of four clients, a Linux-based proxy server, a Windows gateway and the MIDevice was set-up as shown in figure 8.1.

All four clients run on dual Windows/Linux platform. In addition all clients randomly and independently generate Internet traffic through the Linux proxy server.

A 10Base-T hub was implemented as a low cost switch that allowed the four clients to share the single connection (interface (1)) to the Linux proxy server. By definition, a 10Base-T hub offers maximum data rates of 10Mbps using baseband transmission. Baseband transmission implies that only one non-modulated digital Ethernet signal is present on the send and receive pair at any point during communication.

The Linux proxy server processes requests from the clients. When a user tries to access a website, the user's computer (client) creates a *web request* and it sends it to the proxy server via the hub on interface (1). The server then creates and sends a web request to the external packet data network (PDN) on behalf of the client via interface (2). The external PDN will then respond with the requested web content. Upon receiving the web content, the proxy server relays it to its rightful client while keeping a copy of the content in its memory (a process referred to as caching). Apart from caching web content, the proxy server was configured to block clients from certain websites like unwanted pornography sites and other non-educational sites. An Open-Source-based server was used in this study mainly for cost reasons. Open Source server platforms are available free of charge and so are the network applications that run on then. It therefore makes economic sense to use open-source codes especially during development stage.

The proxy server uses IP Cop Linux firewall. IP Cop is not only a firewall but it is also a router, gateway and Dynamic Host Configuration Protocol (DHCP) server to the four clients. It is a router in the sense that it directs Internet traffic to and from the clients. From a client's perspective, all Internet traffic should be channeled through the IP Cop Linux server, which therefore makes it a gateway to the external PDN. Also IP Cop renders DHCP services to the clients. Using DHCP, the server automatically/dynamically allocates local and secure IP addresses to clients attached to it in order to facilitate client-network packet data exchange.

Web requests and PDN responses are channeled via a Windows gateway. The Windows gateway was included in the experimental set-up only because the MIDevice could not be detected by the Linux proxy server. Thus in essence, the gateway merely interfaces the server to the MIDevice.

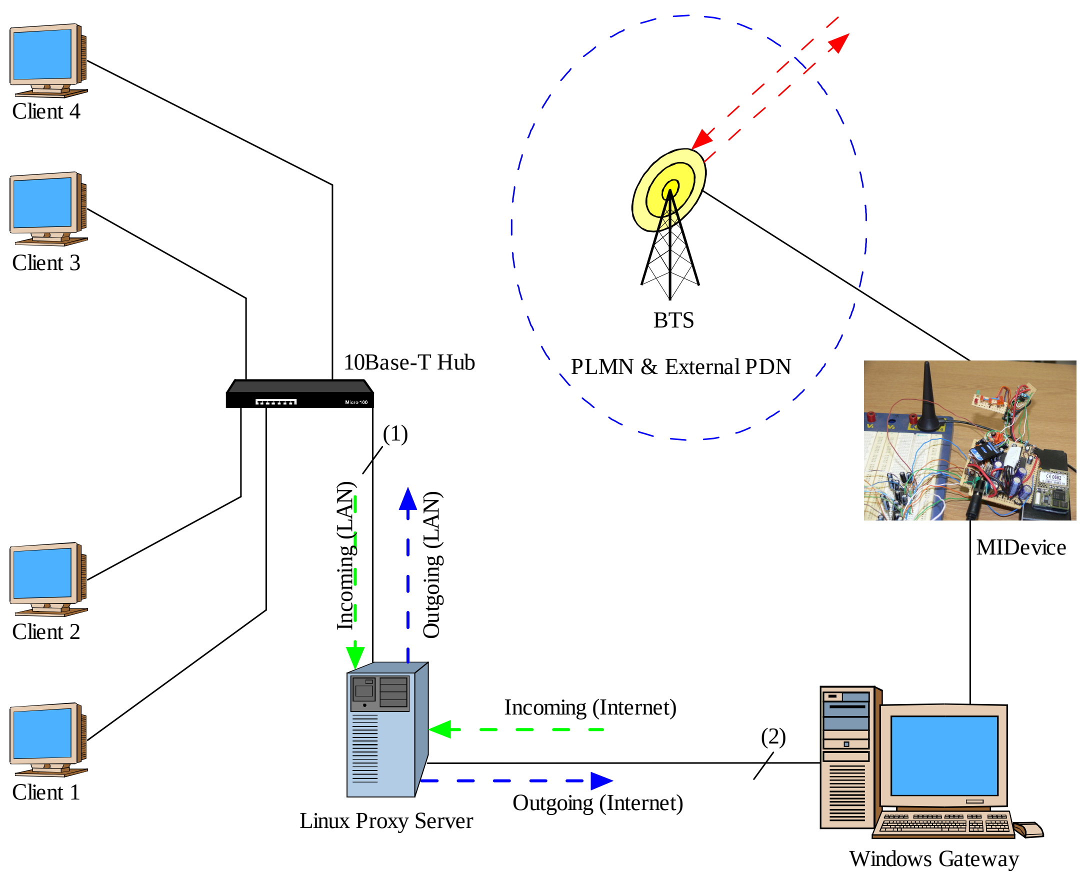

Figure 8.1: Experimental set-up for monitoring performance of GPRS in a multi-user environment.

8.4 RESULTS AND DISCUSSION

In figure 8.1, LAN traffic results from the interaction between the Linux Proxy Server and the four clients attached to it on interface (1). Traffic on interface (1) is shown by figures 8.2 and 8.3. The Linux Proxy Server detects the Windows Gateway and the modem as part of the Internet. As such, Internet traffic results from data transactions between the Proxy Server and Gateway on interface (2) and is shown in figures 8.4 and 8.5. Figures 8.2 and 8.4 show poor GPRS QoS and can be attributed to congestion on the operator's network resulting in the least number of PDCHs being allocated, longest delays and highest probability of loss of packets being offered to the MIDevice during QoS negotiations at PDP context switching. On the other hand, figure 8.3 and 8.5 show better GPRS QoS, which may be attributed to less congestion on the operator's network resulting in the maximum possible number of PDCHs being allocated, shortest delays and the least probability of packet loss being offered to the MIDevice by the network during QoS negotiation at PDP context switching stage. For discussion purposes we refer to figures 8.2 and 8.4 as representing the worst-case and figure 8.3 and 8.5 as representing the ideal-case

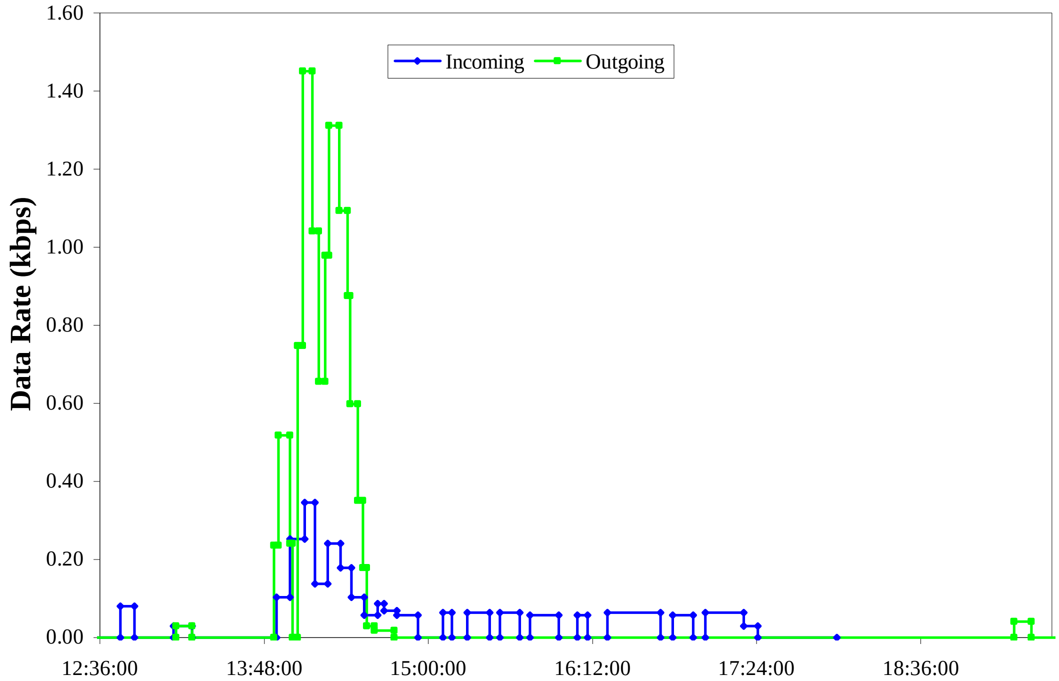

Figure 8.2: LAN traffic (Worst-case) on interface (1)

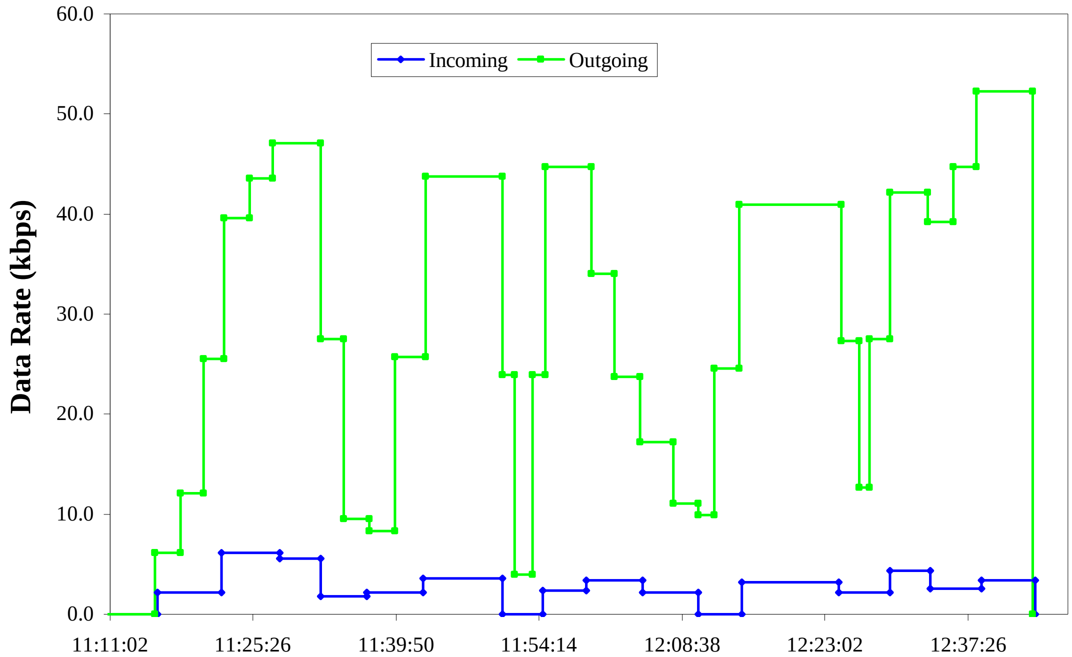

Figure 8.3: LAN traffic (Ideal-case) on interface (1)

Both figures 8.2 and 8.3 show less uploading (outgoing) than downloading (incoming) by LAN clients. During the worst case scenario, clients downloaded 40% more data than they actually uploaded, while in the ideal case scenario total downloads were more than 9 times the total uploads. This is quite understandable if one considers that traffic generated by LAN clients is mainly web requests and acknowledgements. Web requests and acknowledgements are normally small chunks of data of a few bytes in size hence client-to-server traffic is very low. On the other hand, server-to-client traffic consists of the requested web content, which is normally graphics-laden and thus results in higher traffic. Such large ratio of downloads to uploads is expected in a rural school set-up where learners are mainly downloading content from the web with very limited uploading. During the worst-case LAN scenario, maximum downloading rates from the client's point of view were approximately 13.33 kilo-bit per second (kbps) while during the ideal case LAN scenario rates were almost 4 times higher at 52.25 kbps. On a standard Internet modem, a speed of 13 kbps is too slow while 52 kbps gives a feeling of fast connection to the users surfing the Internet.

It is important at this point to mention that traffic in Figure 8.2 and 8.3 is strictly LAN traffic and that it has nothing to do with GPRS. This is due to the fact that the Proxy Server decouples Internet traffic from LAN traffic by buffering and catching slowly arriving packets from the Internet before sending them to their intended LAN clients at higher speeds. This is particularly clear if a comparison is made between LAN and Internet worst case scenarios shown in figures 8.2 and 8.4, respectively. Worst case maximum transfer rate on the Internet link was 1.05 kbps, which is more than 13 times slower than the speed with which server transferred these Internet packets to their intended clients.

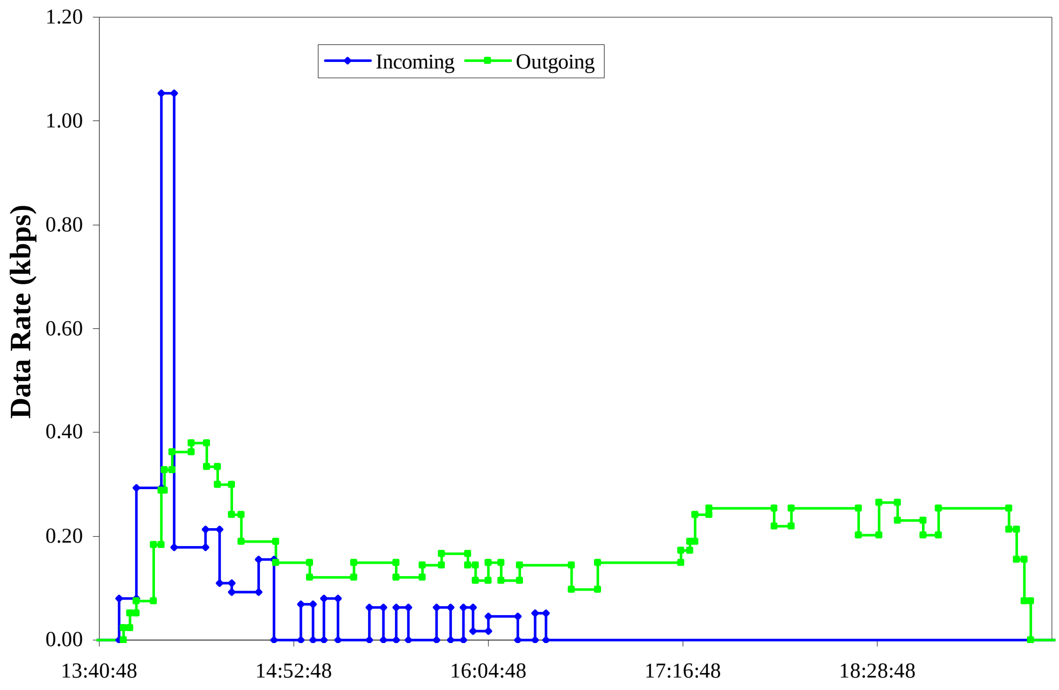

Figure 8.4: Internet traffic (Worst case) on interface (2)

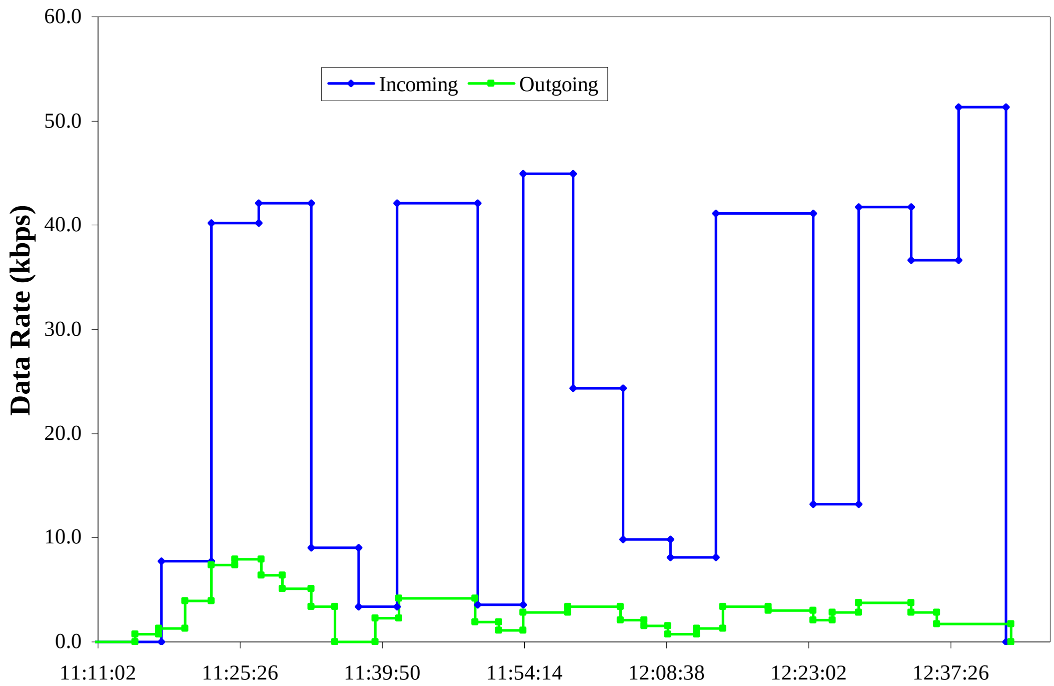

Figure 8.5: Internet traffic (Ideal case) on interface (2)

Figure 8.5 also shows a desirable ratio of downloads to uploads. Total uploads constituted merely 10% of total volume of data transactions that took place between the Internet and the LAN. However, figure 8.4 shows an unfortunate opposite phenomenon in which there were more uploads than downloads. Downloads constituted only 27% of the total volume of data exchanged between the Internet and the LAN. Such a state of affairs is a true reflection of the bad QoS offered to the mobile device by the GPRS operator's network. Poor GPRS QoS is characterized by inadequate number of PDCH channels, long delays and a high probability of packet losses. When the server sends web requests, it awaits acknowledgments as well as the packets. However, due to very long delays and loss of packets, most of acknowledgments and packets either fail to make it to the server or are delayed longer than necessary. As a result the server will resend the requests again thus generating more traffic in the uploading direction.

8.5 GPRS ACCESS – PROBLEMS AND RECOMENDATIONS

It was observed that the firewall (Linux Proxy Server) had a tendency to delay traffic. This was due to the many security functions that it needed to perform with very limited processing power. As a result it induced unnecessary transit delays. In order to rectify this problem, it is proposed that an extremely fast machine with enough processing power be employed for the Proxy Server.

Another problem was inadequate cache memory. This meant that the Proxy Server only stored limited Web content in its cache folder [Schneider and Evans, 2004; 53]. During the ideal case scenario, there were 95% cache misses. As a result most of the Web requests from clients directly resulted in Internet traffic. Having a large cache memory has the advantage that most common Web pages are downloaded only once and stored in the Proxy Server's cache folder. If any client requests the same page at a later stage the Server will reload the page from its own cache memory without having to re-download from the remote site via the GPRS network. Web content in cache folders is reloaded much faster than if it were to be downloaded from a remote Web server. Apart from improving access speed and data rates, caching improves the cost of using GPRS. This is due to the fact that GPRS billing structure is based on the volume of data sent and received through the GPRS network. Since caching results in reduced sending and receiving on the GPRS network, the cost of using GPRS is also reduced. Cost advantage of caching in GPRS Internet access are further enhanced in less diversified client base, for instance controlled learners at a school who are likely to visit similar sites throughout their stay online.

Pop-up messages are usually graphics-rich commercial messages that are automatically downloaded from remote Web servers. Such messages, for instance car, medicine and drug advertisements are undesirable especially in a school set-up and they increase the volume of data downloads that will be charged to the client. Apart from blocking video and audio downloads, the Proxy server should be configured to block all pop-up messages.

8.6 SUMMARY AND CONCLUSIONS

A LAN network was set up in order to monitor performance of GPRS in a multi-user environment employing MIDevice. A Linux Proxy Servers was used for reasons that include cost, ease of use, security and availability of support. IP Cop firewall was implemented in monitoring traffic on the two interfaces on the Linux Proxy Server. It was shown that performance of GPRS is dynamic and to a greater extent, depends on the state of traffic on the mobile operator's network. In less congested scenarios, GPRS is likely to perform better that in congested scenarios. A number of issues were identified that are likely to dent the performance of GPRS on the part of the client. These issues include the client's hardware processing power, caching and unwanted pop-up messages. Solutions to these problems were also suggested and discussed. GPRS proved its potential in providing Internet connectivity solutions to remote rural schools. Continual work will be done to improve performance of the MIDevice in order to take advantage of state-of-the-art technologies in mobile communications with the intention of bringing live video and audio streaming of educational programs to the remote sites. These technologies include Enhanced Data Rates for GSM Evolution (EDGE) and High Speed Downlink Packet Access (HSDPA). These are faster generations of mobile data communications and so would allow real-time audio and video streaming.

8.7 REFERENCES

ETSI-1 (2000), European Telecommunications Standards Institute, “Digital Cellular Telecommunications (Phase 2+); General Packet Radio Services (GPRS) Service Description Stage 1”.

Hull S. (2002), “Content Delivery Networks- Web Switching for Security, Availability and Speed”, McGraw-Hill/Osborne, New York.

Irvine J. and D Harle (2002), “Data Communications and Networks an Engineering Approach”, John Willey and Sons, New York.

Schneider G. P. and J. Evans (2004) “New Perspectives on the Internet”, Thomson Course Technology, USA.

CHAPTER 9

CONCLUSIONS

In general the objective of this study was to develop and implement PV-powered ICT solutions to rural schools. Such work was to involve the development, implementation and evaluation of mobile Internet connectivity solutions.

Specifically, a customized and network-independent GPRS-enabled mobile Internet device (MIDevice) that universally allows computer systems to be connected to the Internet via the existing mobile networks was to be developed. Installation and monitoring of the device was to be done in order to ascertain performance of mobile data services in solving Internet connectivity quagmire. Also a PV power system specifically for powering ICT equipment (personal computers and the MIDevice) was to be sized, installed and monitored. Both objectives were successfully achieved and in this chapter the various conclusions drawn from a number of observations throughout the course the study will be presented.

Performance of PV systems needs to be regarded under two categories, which are cost and service performance. Cost performance assessment will ascertain the viability of a capital investment in a PV power source as opposed to the national utility grid. Service performance assessment establishes whether the PV system is delivering as stipulated in the design or not.

PV system loads that are based on switched-mode power supply units (SMPSUs) can be operated at low AC voltages (as low as 100 VAC). The SMPUs will ensure proper functioning of the devices at those low voltages thus making it a more economical option than powering the same devices at voltages as high as 240 VAC.

The use of shallow discharge batteries requires larger storage spaces than would be needed when deep cycle batteries are employed. However, shallow discharge batteries support more rapid rates of discharge and charging than deep cycle batteries. Regulation losses depend on the type of regulation technology used. In this study, a pulse width modulation regulator was used and resulted in minimum losses. This was made possible by the fact that the regulator switches the battery bank into standby mode under float charge while it channels excess generation from the PV array directly to the load.

Ambient temperature has a more significant impact on module efficiency than irradiance from mid-morning to just after mid-day. As a result efficiency generally drops during this period. In general, modules tend to produce more energy on cool sunny days than hot sunny days.

The MIDevice is a universal and network-independent device. Universal, in the sense that unlike other PC mobile Internet cards that require special card holders found on laptop computers, the MIDevice uses the universal serial bus (USB) interface found on any modern computer (desktop or laptop). It is also designed to work on any mobile communications network as long as a Subscriber Identity Module (SIM) valid to the intended mobile operator is used, which makes the device network-independent.

General Packet Radio Services (GPRS) and mobile Internet services in general rely mainly on the current state of traffic on the operator's network. GPRS Quality of service (QoS) was very poor when there was congestion in the network. Also on a congested network, most IP packets are lost or they are delayed for longer periods than necessary. As a result the bulk of data transactions between the user and the mobile network will constitute duplicated transmissions that are also charged on the user's account. This has a negative impact on the cost performance of mobile Internet services. In a non-congested network, GPRS delivered high quality data services in terms of both response time and throughput. However, mobile Internet services are most likely to greatly improve when more advanced access technologies than GPRS are employed. For instance, the use of Enhance Data Rates for GSM Evolution (EDGE), which gives theoretical data rates of up to 384 kilo-bits per second (kbps) or High Speed Downlink Packet Access (HSDPA), which gives up to 10 Mega-bits per second (Mbps), will surely give far improved results.

APPENDIX A

THE LOAD'S DC CONSUMPTION

A1. INTRODUCTION

The characteristic system load used in this research consisted of three devices, which are; a single Pentium 4 (P4) central processing unit (CPU), a cathode ray tube (CRT) monitor and the mobile internet device (MIDevice). In order to properly size the photovoltaic (PV) power system, all three devices were connected to the domestic electricity mains line. The domestic mains line in South Africa carries 240 Volts root mean square (rms), at 50 Hz [Eskom, 2006]. A Fluke 177 true root mean square (rms) current and voltage meter was used to measure current and voltage of each of the three devices on the mains. The results obtained using the Fluke were later verified by a Hewlett Packard 971 multimeter. The product of a device's average current and voltage became that device's average AC demand while the product of the average demand and daily operational hours gave the daily energy consumption for the device. Total demand and daily energy consumption for the entire load was therefore the sum of the individual average demands and daily energy consumptions, respectively. Of course it was assumed that the reactive part in the load was negligible such that true power was equivalent to the apparent power. This assumption was substantiated by an excellent power factor of 0.99.

System sizing was accordingly done, based on the obtained total demand and energy consumption and following the methodology described in chapters 3 and 4. However, it was observed that the load consumed practically half of the anticipated DC consumption that was used in the sizing of the system. In other words the system's capacity utility rate was at 50%. This definitely was a serious cause for concern and demanded immediate investigations. This appendix therefore contains the results of further investigations that were carried out in order to explain the causes and implications of the difference in the actual and anticipated load demand and consumption. This appendix will further give recommendations on the design of cost effective stand-alone PV power systems.

A2. ENERGY FLOW AND CONVERSIONS

Initially energy in photovoltaic (PV) systems comes in the form of photon energy contained in light photons from the sun. p-n junction solar cells absorb this photon energy and convert it to electrical energy. A series of these solar cells are connected together to form PV modules. The PV modules are themselves connected in parallel and in series to form PV arrays. Electrical energy from the solar cells is transferred on conducting wires to the external circuit, which in this case consists of the battery bank, the system load and other components such as the regulator and inverter. Figure B1 shows the flow of energy in its different forms from the PV array to the system load. Our discussion will focus mainly on the inverter and the system load. Every load device incorporates a switched mode power supply unit (SMPU) whose main function is to break down the input high voltage AC signal into the various low DC voltage signals that are needed by its internal circuitry.

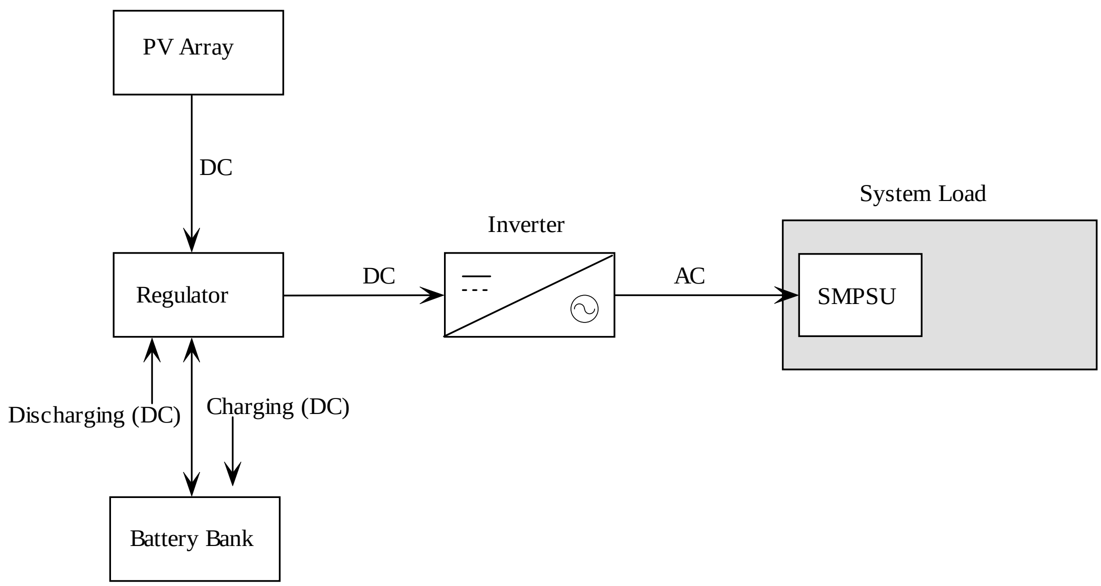

Figure B1: PV power system energy flow diagram

A3. THE INVERTER

In a PV system, the inverter is used to convert (more precisely invert) power from a direct current (DC) to an alternate current (AC) form. The PV array and the battery bank both operate on a DC level while the system load was entirely AC. As a result, an inverter was employed between the regulator and the system load. The inverter used in this research was a Cotek S600-series Pure Sine Wave Inverter with a 600 W capacity. Figure B2 shows a photograph of the inverter used.

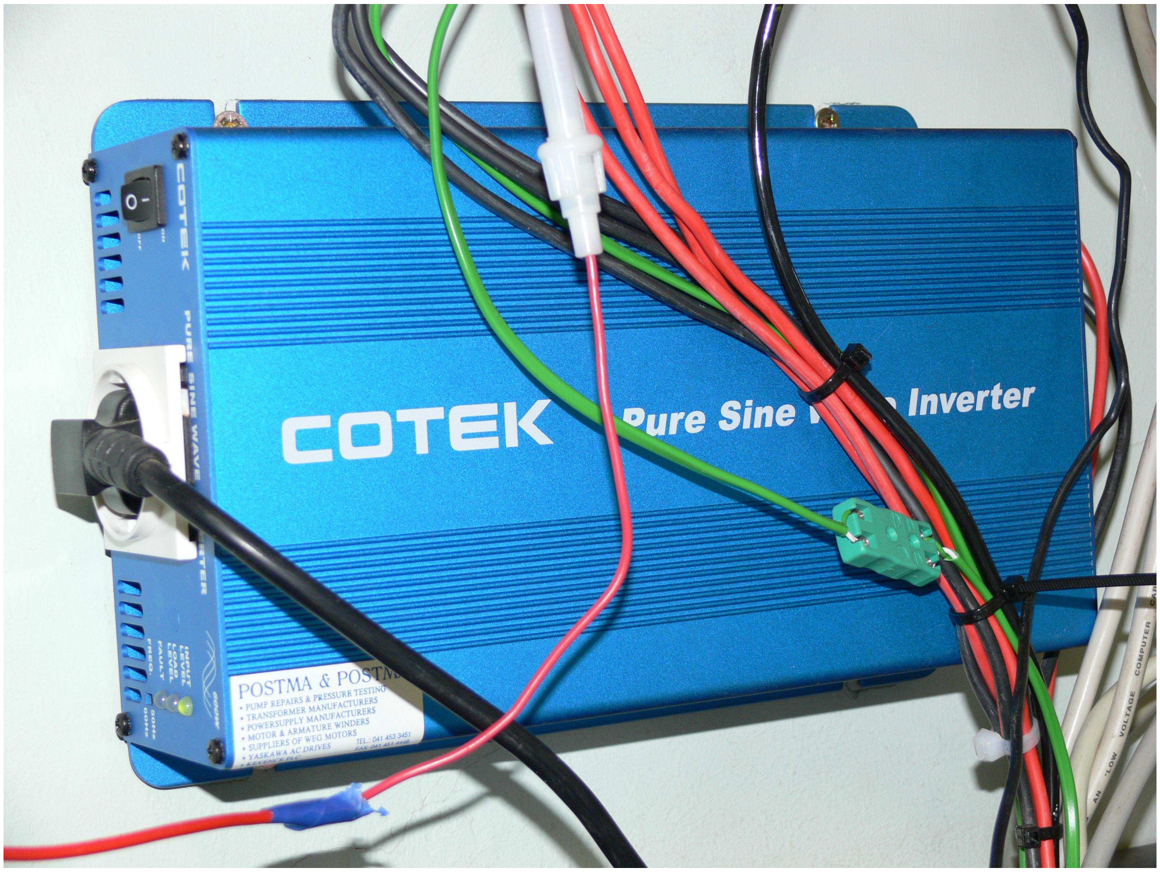

Figure B2: The Cotek Pure Sine Wave Inverter

This inverter is capable of stepping up a 12V DC source to a 220/240 V true sine wave AC signal at 50Hz [Cotek, 2006]. That means the load could operate at almost the anticipated level. However, this was not the case as output from the inverter turned out to be running at a peak AC voltage of 150 V, which translates to 106 V_{rms}. Intuitively one would expect the load not properly function under such supply conditions. However, due to the SMPSUs in the load devices, the system load functioned properly. Operation of the SMPUs will be discussed in brief in the next section.

A4. SWITCHED MODE POWER SUPPLIES

Contrary to the linear power supplies that employ stepping transformers, SMPUs use switching regulators. These switching regulators are primarily internal control circuits that switch power transistors (such as MOSFETS) rapidly on and off in order to stabilize the output voltage or current [Wikipedia, 2006]. Every SMPU design needs to conform to the ATX12V standard for power supply design. It is required that every ATX12V power supply be able to supply full rated power over two input voltage ranges rated 100-127 VAC and 200-240 VAC and must be able to start up under peak loading at 90 VAC [ATX12V, 2005]. As highlighted earlier, the inverter's output was at 106 V_{rms}, which was sufficient for the normal operation of the devices. The excellent regulation of SMPUs can be tested using a variac and a TV set where the variac varies the voltage input from as low as 40 VAC (note: the SMPU needs 90 VAC to start before the voltage can be lowered to this level) to as high as 260 VAC and the image will show absolutely no alterations [Wikipedia, 2006].

A5. SUMMARY AND CONCLUSSIONS

It has been mentioned as a fact that operating a TV set using a SMPU over a voltage range from as low as 40 VAC to as high as 260 VAC would cause no alterations. In this research it was observed that all three devices functioned as well on the PV system (106 V_{rms}) as they do on the mains (240 V rms). It becomes apparent that the actual microelectronic circuits inside these devices are operated at stabilized (almost constant) low DC voltages and that the SMPU needs to have internal power dissipating circuitry. This internal power dissipation capability allows the SMPU to be operated at high voltages and still be able to supply the right amount of power to the microelectronic circuits. The higher the input voltage, the more power dissipated in the SMPU. On the other hand the lower the voltage, the less power dissipated in the SMPU. For the characteristic load for the system designed in this study, only three 70W modules and five shallow discharges lead acid batteries could have been sufficient. In view of this, it is reasonable to suggest that it is cost-effective to size stand-alone PV systems (for powering SMPU-based devices) using low AC voltages.

A6. REFERENCES

ATX12V Version 2.2 (2005); Accessible from www.formfactors.org/developer/specs/**ATX12V**_PSDG_2_2_public_br2.pdf, last viewed 26/01/2007.

Eskom (2006), South Africa's National Utility Company, "Eskom Tariffs and Charges 2006/7", accessible at: www.eskom.co.za , last viewed: August 20, 2006.

Foutz J. (2006), "Switched mode power supply design tutorial"; Accessible from www.smpstech.com/tutorial/t00con.htm, last viewed 26/01/2007.

Watkins S. (1998), "History and Development of Switched Mode Power Supplies", Accessible from www.steve-w.dircon.co.uk/fleadh/mphil/history.htm, last viewed 26/01/2007.

Wikipedia (2007), "Switched-mode power supply"; Accessible from http://en.wikipedia.org/wiki/Switched-mode_power_supply, last visited 07/01/2007.

APPENDIX B

RESEARCH OUTPUTS

Research outputs associated with this study constitute papers presented on international and national conferences, papers submitted for publication in internationally recognized journals and seminars presented at the University of Fort Hare.

B1. INTERNATIONAL CONFERENCES

R. Kaseke and E.L. Meyer, "Photovoltaic-powered Wireless Communication System for Rural Schools outside National Utility Grid", *IEEE PES 2005 Inaugural Conference and Exposition in Africa*, Durban, South Africa. (11/07/2005 – 15/07/2005).♣

R. Kaseke and E.L. Meyer, "PV power system sizing for information and communication devices in schools outside the utility grid", *World Renewable Energy Congress IX*, Florence, Italy. (19/08/2006 – 25/08/2006).

R. Kaseke, E.L. Meyer, M. Simon and X.T. Fadana, "Combined Effect of Ambient Temperature and Irradiance on Outdoor Module Efficiency and Energy Production", Submitted for the *22nd European Photovoltaic Solar Energy Conference and Exhibition*, Fiera Milano, Milan, Italy. (3/09/2007 – 7/09/2007).

♣ Awarded prize for the Best IEEE Power Engineering Society Student Paper.

M. Simon, E.L. Meyer, R. Kaseke, and X.T. Fadana, "The Effect of Spectral Distribution on Photovoltaic Module Performance in South Africa", Submitted for the *22nd European Photovoltaic Solar Energy Conference and Exhibition*, Fiera Milano, Milan, Italy. (3/09/2007 – 7/09/2007).

E.L. Meyer, M. Simon, R. Kaseke and X.T. Fadana, "Infrared Thermography as a Diagnostic Tool for Photovoltaic Cells and Modules", Submitted for the *22nd European Photovoltaic Solar Energy Conference and Exhibition*, Fiera Milano, Milan, Italy. (3/09/2007 – 7/09/2007).

B2. NATIONAL CONFERENCES

R. Kaseke and E.L. Meyer, " Photovoltaic System Sizing for ICT Solutions for Schools in the Rural Eastern Cape, south Africa", *51st South African Institute of Physics Conference,* UWC, South Africa (3/07/2006 - 7/07/2006).

R. Kaseke and E.L. Meyer, " Photovoltaic-powered wireless communications network in rural schools not connected to the national utility grid", *50th South African Institute of Physics Conference,* University of Pretoria, South Africa (5/07/2005 - 7/07/2005).

B3. GENERAL PRESENTATIONS

R. Kaseke and E.L. Meyer, "Cost Performance of Photovoltaic Power System",
University of Fort Hare, Telkom CoE Seminar series No. 1 (2006).

R. Kaseke and E.L. Meyer, “The design and Testing of a Mobile Internet Device (MIDevice)”, Fort Hare Institute of Technology seminar series No.1 (2006).

R. Kaseke and E.L. Meyer, “Design, Installation and Monitoring of a Stand-Alone Photovoltaic Power System”, Fort Hare Institute of Technology seminar series No.2 (2006).

B4. PUBLICATIONS

R. Kaseke and E.L. Meyer, “Net response of outdoor mounted modules to continuously changing ambient temperature and irradiance”, Submitted for publication in the Renewable Energy Journal.

R. Kaseke and E.L. Meyer, “Stand-alone systems for powering ICT equipment in remote rural schools in South Africa”, Submitted for publication in the South African Journal of Science.

R. Kaseke and E.L. Meyer, “Mobile Internet connectivity in remote rural schools: Problems and Solutions”, Submitted for publication in the International Journal of Communication Systems.